Politecnico di Milano

PhD thesis in Materials Engineering, Cycle XXX°

Development and Life Cycle Assessment of Polymeric Materials from Renewable Sources

Maria Nelly García González

Politecnico di Milano

Department of Chemistry, Materials and Chemical Engineering
"Giulio Natta"

PhD thesis in Materials Engineering, Cycle XXX°

Development and Life Cycle Assessment of Polymeric Materials from Renewable Sources.

Author:
Maria Nelly García González

Supervisor:
Prof. Stefano Turri

Tutor:
Prof.ssa Marinella Levi

>>
Abstract

The general aim of the present thesis was focused on the study of different polymer systems obtained from renewable sources and its manufacturing through various technologies related to the coating industry. This concept was based on the principles of green engineering, green chemistry and sustainability (especially LCA studies) for materials such as lignin, polyurethanes and polyesters.

One of the emerging topics in modern polyurethane (PU) technology is the exploitation of monomers and macromers from renewable resources to improve the environmental sustainability while preserving their excellent technical performances. Based on this concept, the main objective of the first part of the present thesis was related to a new class of polyester binder based on FDCA suitable as precursor of PU coating materials. The new 100% bio-based structure was re-designed and obtained through the selection and copolymerization of four different monomers, all available from modern biorefinery downstreams such as glycerine (Gly), 1,3-propanediol (1,3-PD), 2,5-furandicarboxylic acid (FDCA) and succinic acid (SA). The selection of all monomers was according to their functional role and available data from literature for the environmental study. Moreover, this new structure was benchmarked against a partially bio-based (75% renewable carbon) and two fossil-based polyester binders. Successively, the corresponding four PU coatings were obtained by crosslinking of a conventional polyisocyanate and the polyesters synthesized on lab-scale. Their technological performances were evaluated, especially for the new precursor of PU coating. The results obtained in the technological evaluation showed a stiffer PU1 coating (based on FDCA) and a more hydrophilic character leading not only to a better adhesion but also to a more moisture-sensitive surface compared to the other

coatings. With these characteristics, a possible application is in the field of coil coating and automotive as intermediate layers or primers where a high adhesion of the material and recoatability are required.

The evaluation of the total impact of greenhouse gas emissions (GHG) and the total non-renewable energy use (NREU) of all polyesters by the Life Cycle Assessment (LCA) were included on the basis of a cradle-to-gate approach separating the contributions due to the monomer mixture composition and those related to the copolymerization process, and considering an FDCA production process starting from sugar beet (primary data). Specifically, a finer analysis of the impact of marine eutrophication and freshwater eutrophication was developed, providing relevant information about the environmental implication of the production of a chemical derived by biomass (sugar beet). The latter part was developed at Lund University during my PhD internship. The results obtained in this environmental impact assessment showed that the introduction of bio-monomers may significantly reduce the total GHG emissions and the total NREU.

The second objective of the research was related to the improvement of filler/matrix compatibility by introducing nanometer/sized particles of lignin, expecting to obtain a more efficient interaction with the polymer matrix (polyurethane and epoxidized natural rubber, ENR). The preparation of nanolignin (NL) particles was carried out by ultrasonication treatment and after 6h of treatment, 10 nm – 50 nm dimensions were obtained. An excellent water-dispersion stability of the ultrasonically treated NL-based system for over 15 months was observed and an increase of polarity on NL compared to pristine lignin was obtained. Successively, the obtained NL particles were initially incorporated at varying concentrations into a rubber matrix (10 and

40%) and the vulcanization process parameters and mechanical properties of the resulting (nano)composite materials were evaluated. The results testified that the reduction of the micro-particles to nano-particles in the lignin was not enough to reduce the big polarity existing between the filler and the rubber matrix. In particular, the use of nanosized lignin particles allowed to improve the stiffness of the rubber matrix material without affecting its elongation at break, especially for ENR/NL-10. Nevertheless, a decrease of toughness was observed at increasing filler loading. The vulcanization process indicated that the retardant vulcanization effect with the introduction of pristine lignin (IND) was weaker than the effect found with the incorporation of NL.

Finally, the obtained NL particles were also incorporated at varying concentrations into a thermoplastic PU matrix (5, 10 and 20%) and the morphological, thermal and mechanical properties of the resulting (nano)composite materials were assessed. The results attested that there was an excellent level of dispersion and distribution of NL particles into the PU matrix and an ability of NL to establish effective non-covalent interactions with the polymer matrix. In the case of tensile tests on the (nano)composites at increasing filler loading, there was a remarkable development in the mechanical properties of the systems incorporating NL particles compared to pristine lignin in terms of elastic modulus, ultimate tensile strength and elongation at break, especially for 20% of filler.

>>

Table of contents

1.
Sustainability in polymer industry

1.1 GENERAL INTRODUCTION

The bioplastics industry is a young, innovative sector with an enormous economic and ecological potential for a low-carbon, circular bioeconomy that uses resources more efficiently. The European Union has started to acknowledge the many benefits of the bio-based economy and it is now allocating funds and resources to research and development in this sector. The global market for bioplastics is predicted to grow continuously over the next years. According to the latest market data compiled by European Bioplastics in collaboration with the nova-Institute, global production capacities of bioplastics are predicted to grow from around 4.16 million tonnes in 2016 to approximately 6.11 million tonnes by 2021 (Figure 1). Bio-based, non-biodegradable plastics, such as bio-based polyester (PE) and bio-based polyurethanes (PUs) are in the lead, while polylactic acid (PLA) will be the major growth driver in the field of biobased and biodegradable plastics[1].

Of all the consumption, 70% corresponds to five different varieties of polymers: vinyl polychloride, high-density polyethylene, low-density polyethylene, polypropylene and polystyrene. The polymeric materials are daily used in numerous situations and contexts, becoming essential in most of the activities. Plastic industry, according to the data offered by the INE, 48% corresponds to packages and wrappings; 19% to mining; 18% to construction; 8 agricultures; 5% to homeware; and 2% to other activities. These kinds of materials are very appreciated for their easiness in moulding, being capable of getting adapted to complex geometries in a very short time, and for their durability in outdoors contexts[2].

Plastics presents a noticeable yielding point at temperatures over 50 °C, being limited in their technical applications. The Engineered Thermoplastics

(polycarbonates, polyamides, copolymer of styrene, and polyesters) are used in the automobile industry; in a generic form, they are used when a dimensional stability up is required for at least 100 °C. They estimate around a 10-15 of the automobiles' total weight, providing security, economy and aesthetics. Polyester and polyamides are also the base material for most of the synthetic fibres used in the textile industry. The thermoset resins are used as adhesives, varnishes and paintings of chemical conversion, which have a total resistance to paint thinners. They are also used as binders in composite materials[3].

- Rubbers (or elastomers) have the singular propriety of getting reversible elastic elongations superior to 500%. This characteristic makes them irreplaceable as pneumatics, sealants, etc.
- Special thermoplastic polymers are used in windows, glazing, toys, etc.
- Polystyrene is used in disposable food containers, air conditioners, medical machines, glasses and disposable liquid recipients.
- Polyethylene is used in cables, pipes, cling film and other types of film, etc.

The main problem that these materials present is their impact in the environment. They have negative effects on soils, oceans, air and living organisms. During the last years there has been a true interest in minimizing the effects of the plastic industry, but it is still pending to concrete some policies oriented to maintain and increase the natural resources for future generations.

The pollution generated by the processes of production, and its consequent impact on the environment, makes necessary the development of polymeric materials with a minimal effect on the natural environment. Therefore, a

sustainable control over the production and use of the polymer materials, as well as the new technologies, have become essential for society in order to minimize the damage on the natural environment.

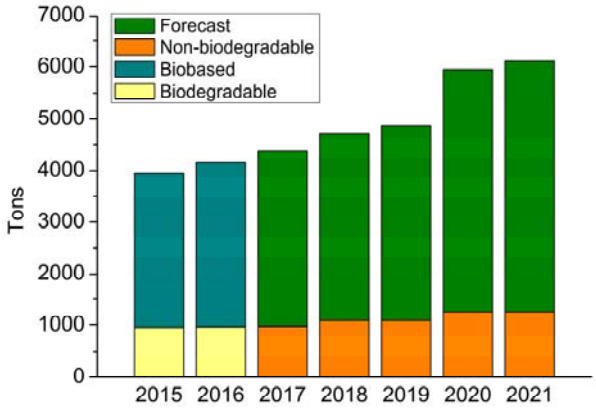

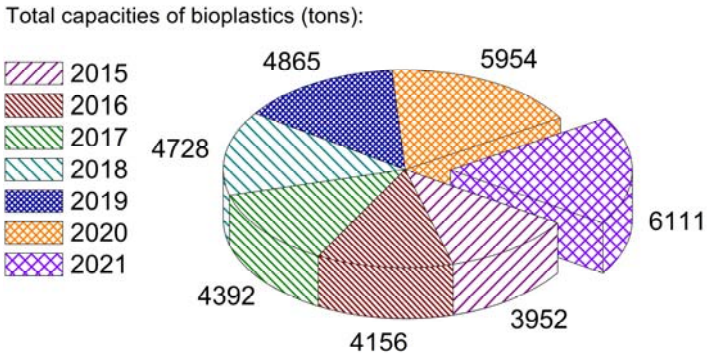

Figure 1. Global production capacity of bioplastics (2016), Source: European Bioplastics, nova-Institute (2016)

1.2 "GREEN" CONCEPT

Green Chemistry and Engineering technologies are "tools" that provide innovative solutions for today and tomorrow in many areas of product and process research and application. Efforts in Green Chemistry and Engineering need to be focused on the major issues for sustainability which include global climate change, sustainable energy production, food production and the associated agricultural practices, depletion of nonrenewable resources, and the dissipation of toxic and hazardous materials in the environment[4]. Although the green chemistry, green engineering and sustainability terms are often used interchangeably, they provide slightly different ideas and encompass different scopes of activities[5]. They are related terms with some superposition as shown in Figure 2.

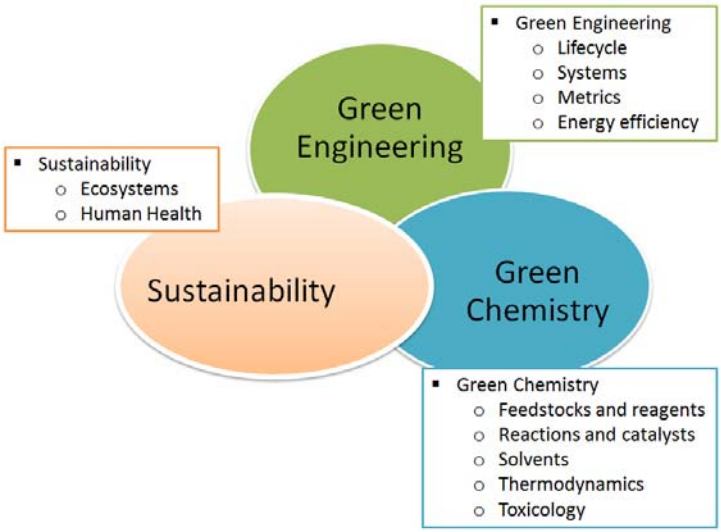

Figure 2. Sustainability, green engineering, and green chemistry.

As to the details, sustainability is focused on the nature of the material, how is it is produced and why is it needed. Green engineering is more oriented

towards the process which is important to identify how the manufactured products (inherently chemical in nature or not) are produced and used. Green chemistry instead is based on the design of chemical products thanks to the fundamental principles of chemistry to reduce or to eliminate their hazard and toxicity (including feedstock, reagents, solvents, products, and byproducts). It also includes the use of sustainable raw material and energy sources for this manufacturing process[4].

1.2.1 "Green" chemistry

In the Green Chemistry: Theory and Practice book published in 1998, green chemistry is defined as "the utilization of a set of principles that reduces or eliminates the use or generation of hazardous substances in the design, manufacture and application of chemical products"[6]. One of the distinct features of this concept is the action to make a chemical product or process inherently less hazardous.

The American Chemistry Institute established green chemistry principles so that scientists and engineers could design and build products, processes, materials, and systems with lower environmental impacts. To demonstrate how green chemistry can be applied, Anastas and Warner have provided some detailed directions in the twelve principles of green chemistry[6]:

1. Prevention
2. Atom economy
3. Less hazardous chemical synthesis
4. Designing safer chemicals
5. Safer solvents and auxiliaries
6. Design for energy efficiency
7. Uses of renewable feedstock

8. Reduce derivatives
9. Use of catalytic reagents
10. Design for degradation
11. Real-time analysis for pollution prevention
12. Inherent safer chemistry

Prevention of waste generation during the manufacturing of the chemicals is better than treating or cleaning up those wastes after they have been created. *Atom economy* guides developers in maximizing and incorporating all materials in the creation of chemicals as a final product. *Chemical syntheses and chemicals less hazardous* should be created minimizing their toxicity to favor the human health and the environment. *Solvents, separation agents, and other auxiliary substances* should be used with moderation or avoided if it is possible. *Energy usage* should be minimized during the chemical processes. *Renewable feedstock* should be the main material source of the chemical substances rather than fossil fuel-based sources whenever they are technically and economically practicable. Obtained *unnecessary derivatives* should be minimized or avoided to reduce chemical waste which can be generated. The *use of catalytic reagents* should be higher than the use of stoichiometric reagents. *Chemical products* should be biodegradable so that they do not persist in the environment and contaminate it. The development of *real-time analysis for pollution prevention* is needed with the creation of analytical methodologies. *Chemical substances and processes* should be able to minimize the potential risks of accidental chemical spills, explosions and fires. The 12 green chemistry definitions described can be grouped into three main areas. Reduction in energy usage, reduction in waste, and reduction in pollution. These three areas are used to define sustainable manufacturing.

1.2.2 "Green" engineering

Green engineering is, according to The Environmental Protection Agency (EPA), "the design, commercialization, and use of processes and products that are feasible and economical while minimizing generation of pollution at the source and risk to human health and the environment"[7]. Engineers apply the risk assessment method to pollution prevention in their strategies, which help to quantify the degree of environmental impact for each chemical product.

Twelve principles of green engineering were proposed by Paul Anastas and Julie Zimmerman[8] and published in Environmental Science and Technology on March 1, 2003 to develop products, processes, or systems with lower environmental impacts as it is described in the definition of green engineering. According to Anastas and Zimmerman, there are two fundamental concepts that designers should integrate in their design: "life cycle considerations" and the "first principle of green engineering, inherency":

1. Inherent rather than circumstantial
2. Prevention instead of treatment
3. Design for separation
4. Maximize efficiency
5. Output-pulled versus input-pushed
6. Conserve complexity
7. Durability rather than immortality
8. Meet need, minimize excess
9. Minimize material diversity
10. Integrate material and energy flows
11. Design for commercial "afterlife"
12. Renewable rather than depleting resources

Some principles are common within the green chemistry principles such as prevention and renewable feedstock since both terms are often related in some points as it is shown above. *Inherent rather than circumstantial* means that all material and energy inputs and outputs should be as inherently nonhazardous as possible. *Design for separation and purification operations* should be created to minimize energy consumption and materials use. *Maximize efficiency* in mass, energy, space, and time for products, processes, and systems, should be *output-pulled rather than input-pushed* through the use of energy and materials. *Conserve complexity* must be viewed as an investment when making design choices on recycling, reusing, or beneficial disposition. The design goal should be product-targeted *durability* rather than product immortality. *Meet need and minimize excess* should be considered as a priority in the design and multicomponent products should be designed to promote disassembly and value retention. *Integration and interconnectivity* with available energy and material flows should be designed into products, processes and systems.

1.2.3 Sustainability

Sustainability is defined as "meeting the needs of the current generation without compromising the ability of future generations to meet their needs" according to the World Commission on Environment and Development in 1987 (WCED 1987). Since then, the thinking of how to achieve goals of sustainability, and what actions to take up has strengthened during the last years through developing a "global view" with respect to our planet's future. Sustainability can be measured by the outcomes of using a material, process, or system on the environment, society, and economy. As it is shown in Figure 3, the three components of sustainability have economic, social, and

environmental aspects, which are related to each other. The evaluation of these three components is analysed with a "Triple Bottom Line" approach which is the key to creating a sustainable organization. The social aspect of sustainability can measure the impacts of products and processes in society. The economic aspect can measure the economic impacts of using a material and manufacturing process to build products. The environmental aspect can measure the environmental impacts of making a product or system in terms of usage of natural resources for raw materials, energy, and real estate land[9]. The latter aspect is measured by the Life Cycle Assessment (LCA) technique, which was used in this study.

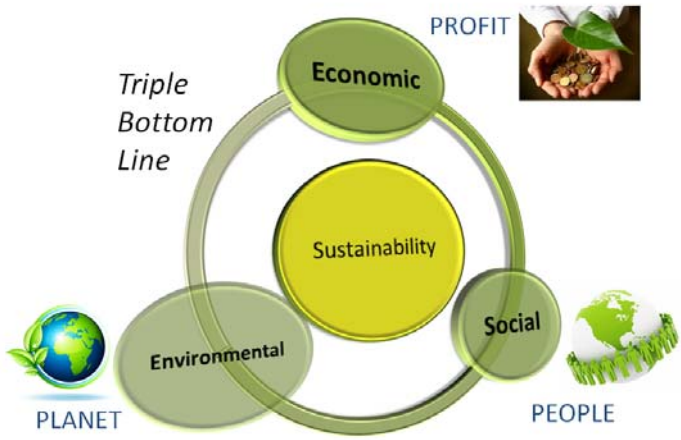

Figure 3. Sustainability definition.

1.3 LIFE CYCLE ASSESSMENT

LCA is a "technique to assess environmental impacts associated with all the stages of a product's life from raw material extraction through material processing, manufacture, distribution, use, repair and maintenance, and disposal or recycling" according to the international standards ISO 14040[10] and ISO 14044[11]. The idea for the LCA was conceived in the 1970s and the methodology was originally developed by the Society of Environmental Toxicology and Chemistry in the early 1990s[12,13]. The general principles and framework for LCA are described in the international standards ISO 14040 and ISO 14044 (ISO, 2006b, c), where the LCA is defined as "compilation and evaluation of the inputs, outputs and the potential environmental impacts of a product system throughout its life cycle". All the materials and energy flow either enter or leave a unit process are composed by inputs and outputs. In a life cycle, the consecutive and interlinked stages of a product system, from raw material acquisition or generation from natural resources to final disposal (i.e. "from cradle to grave") are referred.

1.3.1 LCA framework

The structure of the international standard ISO is represented in Figure 4. The phases of LCA have been renamed, compared to earlier structures, and the following terms are now internationally mandatory[13]: goal and scope definition, life cycle inventory analysis (LCI), life cycle impact assessment (LCIA) and interpretation. Those phases allow an iterative approach that is often necessary during the LCA studies.

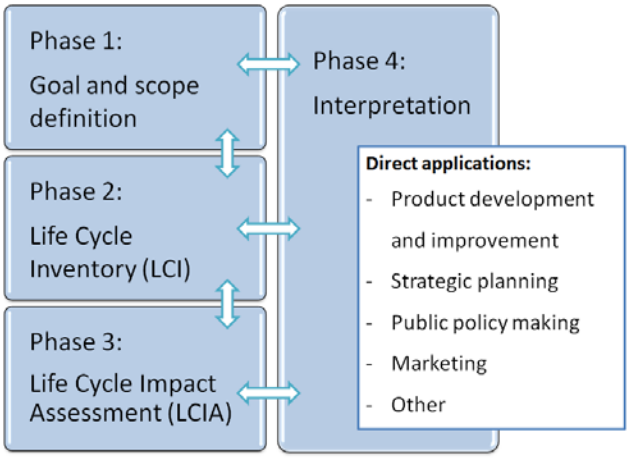

Figure 4. LCA phases according to ISO 14040:1997/2006.

1.3.1.1 Phase 1: Goal and scope definition

The goal of an LCA states the intended application, reasons to carry out the study, intended audience, and determine whether results are intended to be used in a comparative study or in a disclosed one. The scope defines the parameters and the entire study of what is included in and excluded from the analysis. Moreover, it should support the selected goals. It includes some of the most important elements of an LCA study, such as the definition of the functional unit (FU), the system boundary and the allocation procedures. *Functional unit* provides a reference to which the input and output data are normalised. In this sense, FU must be clearly defined, measurable and consistent with the goal of the study. When the goal of the LCA is to compare two systems, the function(s) of the FUs must be equivalent so that each system is defined by an equal amount of product or equivalent service delivered to the consumer. *System boundary* determines the limits of the studied system, always in concordance with the proposed goal and scope. It includes geographical, technological and temporal delimitations and its definition is

critical to determine the amount of work to be done. *Allocation* is the procedure of partitioning the input or output flows of a process or a product system between the product system under study and one or more product systems. According to ISO standards, when dealing with systems involving joint co-production and recycling systems, allocation should be avoided by dividing processes into sub-processes or by expanding the system to include the additional functions related to the co-products (ISO, 2006c). If allocation cannot be avoided, inputs and outputs should be partitioned according to the co-products importance in a way the physical relationships between them are reflected (normally mass or volume). If a physical relationship cannot be established, the inputs should be allocated between the products and functions in a way the other relationships between them are reflected, for example, the economic value of the products. Two distinct goals in LCA studies originate different approaches named "Attributional LCA" (ALCA) and "Consequential LCA" (CLCA). ALCA aims at describing a product system and its environmental exchanges while CLCA aims at describing how the environmental exchanges can be expected to change as a result of actions taken in the system[14] giving different results in the study. If any information regarding system (data, process, material, production scheme…) is assumed, simplified or taken as a value choice, it has to be explained and motivated in the LCA report.

1.3.1.2 Phase 2: Life cycle inventory analysis

Life Cycle Inventory (LCI) represents the second phase of an LCA study and it involves two fundamental aspects that are the compilation and quantification of inputs and outputs of the product system. The key activity in this phase is the data collection (measured, calculated or estimated) as an accuracy study

will depend on the quality of the data collected. The quantitative outcome is a list of environmental exchanges always related to the FU previously defined.

1.3.1.3 Phase 3: Life cycle impact assessment

In the third phase, Life Cycle Impact Assessment (LCIA) evaluates if environmental impacts generated in the process can be considered as significant, taking into account the Life Cycle Inventory analysis data considering the impact categories (e.g. global warming, eutrophication, etc.). These impact categories can be related to inputs of the system (e.g. abiotic depletion, water consumption, etc.) or to outputs (e.g. global warming, eutrophication, etc.). This phase can be an iterative process to review the goal and scope of the LCA study to determine if the objectives of the study have been met, or to modify the goal and scope if they are not possible to achieve. The first and mandatory step of this phase is the *classification*, which consists of connecting the contribution of each input and output connected with the selected impact categories. The *characterisation* is the second mandatory step which consists of the assignation of the obtained data in classification stage to each impact category. Each pollutant or action which causes an impact, has a numerical factor which is multiplied to the output/input amount. This way, each impact category is quantified in comparable units (e.g. Global Warming Potential (GWP) converts each kilogram of emitted greenhouse gas results into kg of carbon dioxide equivalents). These numerical factors depend on the characterization methodology: *mid-point* indicators quantify the environmental damage in an intermediate point between emission point and receiving environment while *end-point* indicators express direct damage to the environment. With non-mandatory character, some elements and information can be introduced in the LCA study depending on the goals and scope:

Normalisation involves the dimensionless results to make all impact categories comparable, obtaining a total impact amount with the idea of understanding better the relative magnitude for each indicator result of the production system under study. *Grouping* sorting, *ranking* of impact categories and *weighting* is the process of converting indicator results of different impact categories by using numerical factors based on value-choices. Transparency is a critical point to the impact assessment to ensure the assumptions are clearly described and reported, since choice, modelling and evaluation can lead to subjectivity (ISO 14040:2006).

1.3.1.4 Phase 4: Interpretation

This fourth phase is the concluding part of the LCA's iterative process and aims to propose the necessary changes to reduce the environmental impact of the processes or activities considered[15]. At this stage, the results of the study are interpreted in order to identify which of the various alternatives applicable to the system ensures maximum efficiency from the environmental and energy points of view. The interpretation must take into account that LCIA's results are based on a relative approach that indicates potential environmental impacts and do not have actual impact on the category endpoints, exceeded safety or risk thresholds (ISO 14040:2006). A useful procedure is to carry out checks of completeness (all relevant information should be considered and justification should not be provided), a sensitivity check (evaluating the reliability of the results, estimating whether and how uncertain data, allocations, category indicators, etc. are reflected in the conclusions) and a consistency check (to determine if the hypotheses, methods and data are consistent with the objective and scope)[16].

1.3.2 LCA in bio-based polymers

Renewable raw polymeric materials may reduce the environmental impacts compared to petroleum based counterparts. These effects can be quantified by the Life Cycle Assessment (LCA) method. There has been a growing use of this method for bio polymers since it is necessary to take measures against global climate change, to become less dependent on petroleum sources. An example is the study of LCA applied to the bio-based polyester polylactic acid (PLA)[17] which was produced with the new lactic acid production process with reduced environmental impacts for the PLA production system. The LCA provides energy and water requirements, greenhouse gas emissions, waste generation, and pollution production[18,19]. In addition, an extensive number of studies have been reported where the assessment on a life-cycle basis of the different impacts of bio-based products has been compared to conventional fossil-derived products[20,21] and to other bio-based products[22].

1.3.3 Database and software Simapro

SimaPro 8.2 software, developed by the Dutch company Pré (Product Ecology) Consultants since 1990, has been used to carry out the life cycle analysis of this study. Ecoinvent database (version 3.2) was also used when generic data were necessary for the research.

1.4 POLYMER INDUSTRY

The increase of plastic presence in daily live is an unstoppable tendency due to the versatility this material presents. For this reason, the innovation of the plastic industry has focused in the development of more sustainable plastic materials, with improved properties, and economically viable that, at the same time, still have the functionality required by the different sectors: to contain, to protect and to keep. Traditional packages protect the products; besides, they are cheap and durable. Precisely, durability is one of the most serious problems for the environment. For this reason, one of the main focuses in research has been developing sustainable materials that kept the characteristics of the traditional ones. In this sense, one of the strategies adopted is the promotion of materials obtained from renewable sources, which are biodegradable and, once their lifespan has expired, have the capability of returning to the natural cycle. "Currently, those materials represent just 1% of the world production, but an increase of the segment in the short time is expected according to the European Bioplastics[1]. Bioplastics' industry is a dynamic sector that it is in constant increase. That has allowed the reduction of the selling price of that kind of materials, and the expectation is for them to reach, in a relatively short period of time, a price that could be similar to the conventional plastics. This aspect has allowed to focus the applied research in the food package sector, where packages based on biodegradable and/or renewable materials are being developed.

1.4.1 Green monomers

As it is mentioned in previous paragraphs, in green economy, it is imperative to reduce the demand for resources and energy, minimize wastes, prevent environmental pollution and hazards, reduce greenhouse gas emissions,

optimize manufacturing processes, and establish effective recycling of wastes. By this definition, "green" is not synonymous with biomaterials and biotechnology. In fact, many existing polymers and polymerization processes meet the demands of green chemistry. Prominent examples of successful sustainable materials are polyolefins such as polyethylene and polypropylene, which represent around half of the global polymer production[25]. In the 1930s, the first industrial process to make polyethylene required temperatures above 150 °C and very high pressures exceeding 1000 bar. Catalytic olefin polymerization was discovered during the 1950s. This enabled olefin polymerization at low pressures below 10 bar and at temperatures below 100 °C. During the 1980s, in the aftermath of the first oil crisis in 1973, the energy-efficient catalytic copolymerization of ethylene and 1-olefins for manufacturing linear low-density polyethylene (LLDPE), used in food packaging, became a million tons business. It is most likely that the marketing efforts by Union Carbide represent the first striking example of how the argument of improved energy effectiveness successfully triggered substantial changes in the market place, with catalytic ethylene copolymerization progressing at the expense of energy-intensive high-pressure ethylene polymerization[6].

Instead of developing new biotechnology routes to biopolymers with rather tedious polymer purification and difficult tuning of processing properties, biotechnology and biorefinery processes are employed to supply renewable monomers, which are polymerized in highly effective conventional melt- or gas-phase polymerization processes. Compared to polymers, monomers are much easier to purify. Moreover, the resulting bio-based polymers combine the advantages of a low carbon footprint, typical for renewable feedstocks, with the recycling capability and high resource- and energy-effectiveness of

solvent-free melt-, and gas-phase polymerization processes. Biofeedstocks such as agricultural and forestry wastes are used preferentially in order to avoid conflicts with food production. Fermentation of glucose, obtained from lignocelluloses and starch, can be used to produce a great variety of bio-based monomers. Selected examples to produce bio-based monomers are presented in Figure 5.

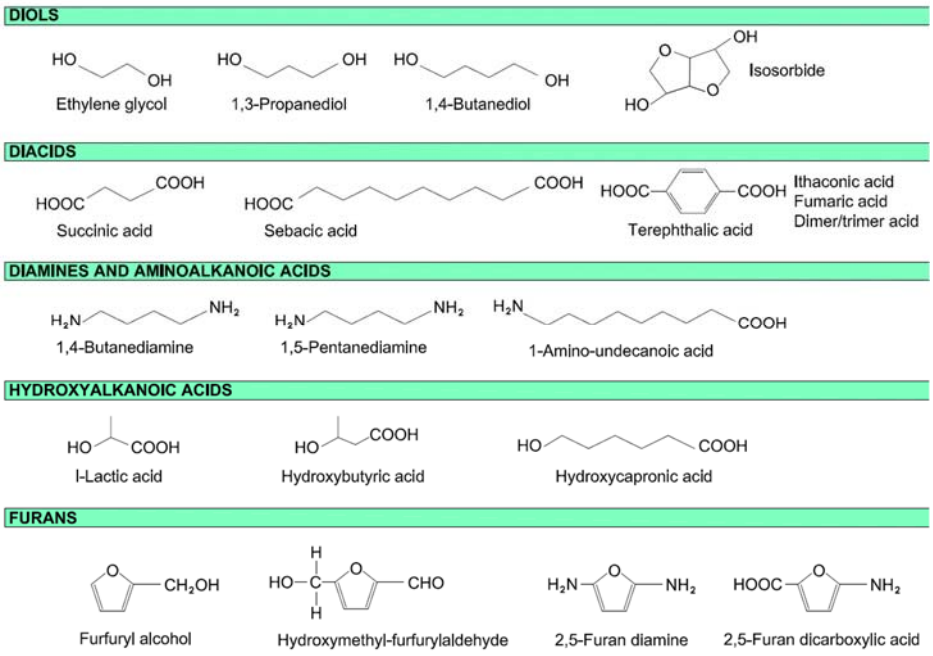

Figure 5. Selected examples of renewable monomers supplied by biotechnology[6].

For example, bioethanol is readily converted into ethylene, propylene, also butadiene that can be used to synthesize bio-based polyolefins and butadiene rubber. Diols, polyols, diacids, hydroxyalkanoic acids, aminoalkanoic acids, and diamines are also available and they can be used in polycondensation reactions which are in a melted state to produce bio-based polyesters, polyamides, polycarbonates, as well as thermoset resins such as unsaturated

polyesters and air-drying finishes. Starting from glucose, it is possible to obtain sorbitol, isosorbide, also a large variety of furans, most of which are not natural products. Furan derivatives offer attractive opportunities to prepare bio-based thermoset and thermoplastic resins from furfuryl alcohol, furfuryl aldehyde, hydroxymethyl furfuryl aldehyde, and 2,5-furandicarboxylic acid. Side-products of biofuel production, such as glycerol, are also attractive bioresources to produce bio-based monomers such as acrylic acids, epichlorohydrine, 1,3-propanediol, and acrolein[6].

1.4.2 Bio-aromatics

Just a few years ago, bio aromatics seemed far away. Aromatic compounds could be so easily extracted from (fossil-based) naphtha, that bio aromatics seemed to be a dream for the future. But in this field, as in many branches of green chemistry, knowledge advances so fast, the company foresees the possibility of commercial production of bio aromatics from lignin in less than ten years time[24]. Lignin is abundantly present in wood, where its acts as a kind of glue that binds together the strains of cellulose and hemicellulose. Its structure is very complex, as it is a three-dimensional conglomerate of various aromatic components tightly linked together. Present chemical know-how is not sufficient to separate lignin into these components. Moreover, nowadays on the market, lignin is considered as a side-product of the well-developed Kraft process for paper production, and it contains too much sulphur for subsequent successful processing due to catalyst inhibition. There are new processes towards producing bio aromatics from lignin that could develop fast in the following years.

Four pathways towards bio aromatics: The first pathway is to feed lignin (after de-oxygenation) to a cracker. This way properties that can be

comparable to crude oil and will produce a kind of naphtha, containing a variety of aromatic compounds are obtained. This process is nearly operational today, although its cost-effectiveness is very much dependent on crude oil prices. The second pathway is to produce BTX (benzene, toluene, xylene) catalytically from biomass or lignin in one step. This process is still in development. In the third pathway, bio aromatics are produced from sugars by the Diels-Alder reaction. With the Diels-Alder reaction, aromatic compounds can be easily produced from furan derivatives (furan is an aromatic hydrocarbon in which the ring structure contains four carbon atoms and one oxygen atom; it and its derivatives can easily be produced from sugars). For instance, dimethylfuran will produce p-xylene when it is treated with ethylene. This is a direct route to get bio aromatics from sugars, that are increasingly available at low prices in the market. The fourth pathway, finally, will produce bio aromatics directly from lignin. A prosperous first achievement in this stage is that finally, researchers have succeeded in producing a replicable quality of pure lignin that can be used as a benchmark. In this fourth step, lignin will be hydrolysed, followed by isolating the components by nanofiltration or pervaporation.

In bio-economy, chemical industry will need a variety of resources for a solid feedstock position. It cannot rely on just one crop. Across Europe, we will need a balanced input of the first and the second-generation of biofuels. If the gap between aliphatic and aromatic chemicals could be easily bridged by the Diels-Alder reaction, this will greatly enhance the flexibility of resources for the chemical industry. In the bio-economy policy makers' minds, 2019 is just around the corner. Time is upon them to study new molecules, highly functionalized, and with new characteristics that will lead to better performing polymers and materials[24].

1.4.2.1 Lignin

Lignin is one of the most abundant polymers in plants. Cellulose and hemicellulose conform a cellular wall in a disposition regulated at a nanostructural level, giving as a result nets of lignin-carbohydrates. The composition or distribution of the components in those nets vary depending on the type of plant considered. In the case of wood composition, the most common ranges are: cellulose 38-50%; hemicellulose 23-32%, and lignin 15-25%[25]. Lignin is present in all the vascular plants and, like many other components of the biomass, it gets formed by a photosynthesis' reaction. Lignin is considered as a renewable and affordable resource with potential in the industrial field. Its production has been estimated in the interval of 5.36 x 108 tones per year. Table 1 shows the percentages of lignin in different plants that are important in a commercial way[26].

Table 1. Percentage of lignin in different types of plants[26].

Plant		Lignin content (%)
Scientific name	**Common name**	
Picea abies	Norway Spruce	28-39
Tsuga canadensis	Canadian Hemlock	31
Panicum virgatum	Switchgrass	33
Pseudotsuga menziesii	Douglas-fir	29
Pinus sylvestris	Scots Pine	28
Pinus radiata	Monterey Pine	27
Prunus amigdalus	Almond tree	26
Eucalyptus grandis	Rose Gum	25
Eucalyptus globulus	Blue Gum	22
Acacia mollisima	Black Wattle	21
Betula verrucosa	Silver Birch	20
Populus tremula	Aspen	19
Olea europea	Olive tree	19
Gossypium hirsutum	Cotton	16
Saccharum species	Sugar Maple	14
Oryza species	Rice straw	6.1

Lignin structural definition has never been as clear as the one for other natural polymers, like cellulose or proteins, due to the complexity that affects its isolation, composition analysis, and structural characterization. The problem for a precise lignin definition is associated with the nature of its multiple structural units, which do not usually get repeated regularly, as the lignin composition and structure vary depending on its origin and the extraction method or isolation used[27]. In Figure 6, there is a representation of one of the chemical structures proposed for lignin[28].

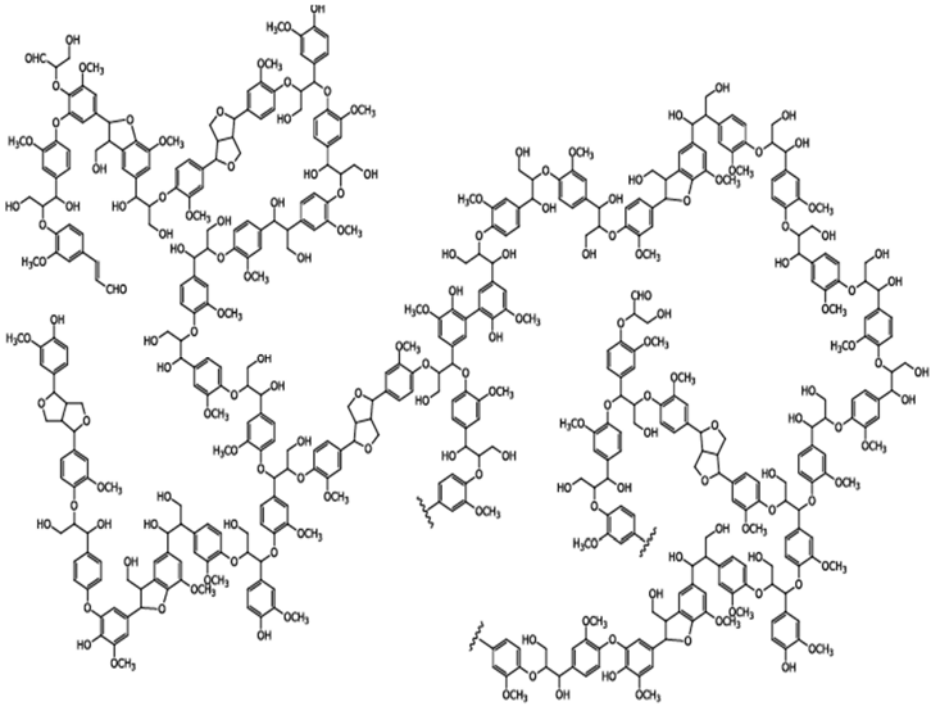

Figure 6. Lignin structural model of sawn timber[28].

Lignin characteristics are:

a) vegetal polymers constructed by units of phenylpropanoids.

b) present most of the methoxyl groups contained in the timber.

c) resistant to acid hydrolysis, easy to oxidize, soluble in bisulphites or warm alkalis, and easy to condensate in phenols or thiols.

d) when in ebullition in a hydrochloric acid ethanolic solution, lignin forms monomers of Hibbert's ketones (a mix of aromatic ketones resulted from the break of the main ether links (β-O-4) between lignin units).

The three main monolignin used to synthesize lignin polymers are formed in the cytoplasm shikimate method, which produces phenylalanine as an intermediate key[29,30], through others that are mediated by the enzyme,

deamination, hydroxylation, reduction and methylation reactions. Lignin precursors are formed as represented in Figure 7.

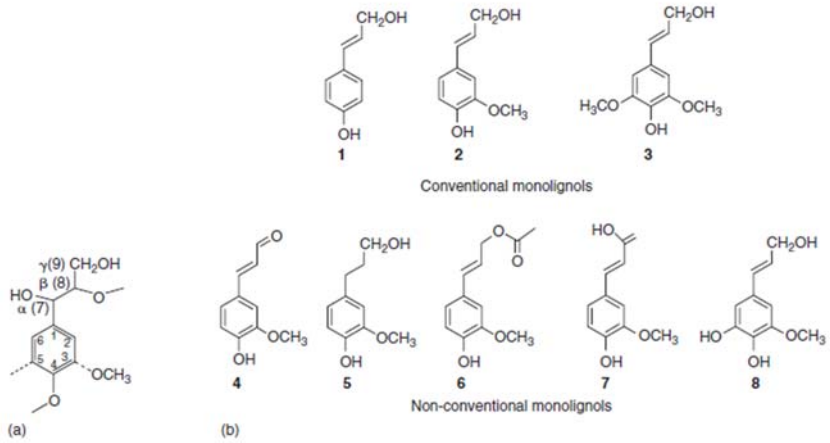

Figure 7. (a) Numbering system in monolignols. (b) Types of monolignols found as building block in lignin. 1= p-coumaryl alochol (H-unit), 2= coniferyl alcohol (G-unit), 3=sinapyl alochol (S-unit), 4=coniferaldehyde, 5=dihydrocofineryl alochol, 6= coniferyl alochol-9-acetate, 7= ferulic acid, 8= 5-hydroxyconiferyl alochol[29].

The monolignin additional reactions in the cellular wall of the plant, in order to form lignin, may occur through an initial phase of the laccase or peroxidase oxidation of the monolignin, having as a result a stabilised phenoxy radical[31,32] as represented in Figure 8. The next step is a coupling reaction. In Table 2, the participation degree of most of the monolignin in different types of plants is shown[26].

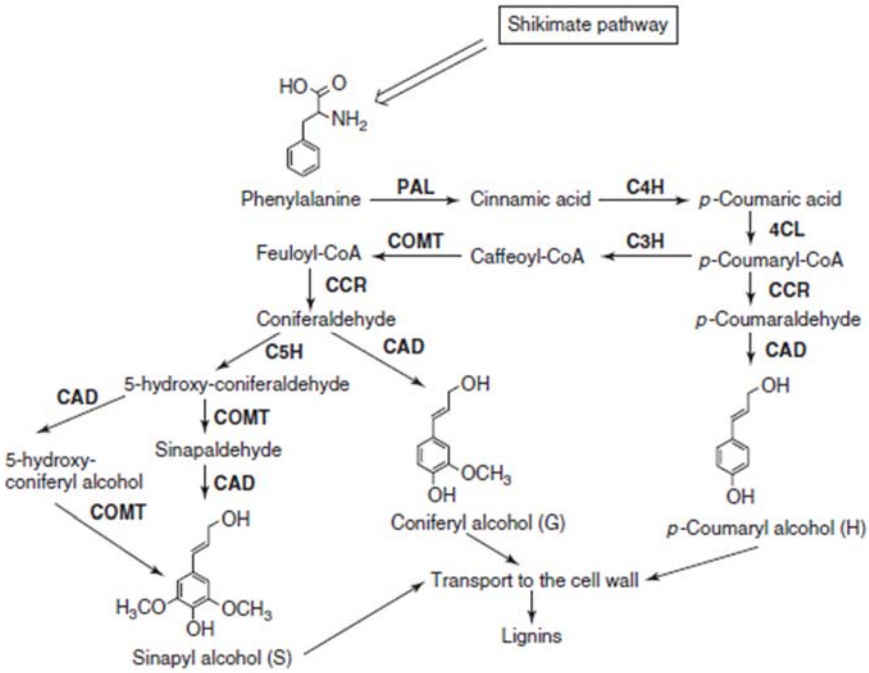

Figure 8. The lignin biosynthesis pathway. Abbreviations of enzymes are: PAL= phenylalanine-ammonia-lyase; C4H=cinnamate 4-hydroxylase; 4CL=hydroxycinnamate: CoA-ligase; C3H=4-hydroxycinnamate3-hydroxylase; COMT=S-adenosyl metionine: caffeate/5-hydroxyferulate-O-methyltransferase; CAD=hydroxycinnamyl-alcohol dehydrogenase; C5H=coniferaldehyde-5-hydroxylase[30].

Table 2. Percentage of different monolignin present in different types of plants[26].

Type of plants		Percentage (%)		
		Paracoumaryl alcohol	Coniferyl alcohol	Sinapyl alcohol
Gymnosperm	Conifers (soft timber)	<5	>95	0
Angiosperms	Eudicots (strong timber)	0-8	25-50	45-75
	Monocotyledon (grasses)	5-35	35-80	20-55

Lignin can be isolated from lignocellulosic material through a range of methods that imply different mechanical and/or chemical processes. Those methods can be split in two main groups. The first group includes methods that liberate the cellulose and hemicellulose through solubilization, leaving the lignin as an insoluble residue. The second group includes methods that imply the lignin dissolution, leaving as insoluble residues the cellulose and the hemicellulose, followed by the lignin recuperation from a liquid phase.

At the moment, due to the heterogenic nature of the raw materials (timber and pulp), there is not any available method to achieve the quantitative isolation of the natural or residual lignin without taking the risk of modifying it structurally during the process. However, the information obtained about the chemical reactivity and the lignin structure isolated is valuable[33]. In Table 3, there are some of the main methods usually used to isolate residual lignin[34].

The interest on renewable energies and chemical products is increasing due to the forecasted decrease of oil and gas sources, and increasing concern about the accumulation of greenhouse gases in the atmosphere. The concept of an Integrated Biorefinery of Forest Products has been developed by different researches. The Integrated Biorefinery is a process in which carbohydrates, oils, lignin and other biomass' materials are extracted in order to turn them into fuels, chemical products with a high added value, and other materials, all with very few residues[3]. Paper pulp and paper factories that produce multiple products from biomass can be classified as biorefineries. Approximately 20% of the dry wood weight contain hemicellulose that gets dissolved in black-liquor and then gets burned by the chemical recuperation systems. Hemicellulose pre-extraction before the kraft paper pulp and the subsequent conversion into chemical products of high added value offer a very interesting economic opportunity for that industry.

Table 3. Different types of lignin isolation[35].

Preparation	Methodology	Observations
Milled Wood Lignin (MWL)	Aqueous extraction with dioxane of the milled wood.	Around 20% of profit obtained from an original lignin.
Milled Wood Enzymatic Lignin (MWEL)	Reside left after the milled wood carbohydrates' hydrolysis.	95% profit, but it contains 10-12% of carbohydrates, it is not completely soluble in common solvents.
Cellulose Enzymatic Lignin (CEL)	Soluble fraction resulted from the MWEL.	Similar to MWL
Braun's Native Lignin	Residual wood ethanolic extract (particle size similar to sawdust).	Lower profits and molecular weights than the ones obtained by MWL.
Kraft type and Sulphite type lignin	Lignin chemical dissolution at elevated pressures and temperatures.	It is not representative of the original lignin, important sub product in paper production.
Soda type lignin	Dissolution in an alkaline environment of non-wood fibres, like straw.	Low molecular weight lignin insoluble in water and with low polluting levels (e.g. sugars and sulphur).
Klason's lignin	Insoluble, condensed residues after polysaccharides hydrolysis with sulphuric acid.	It is not representative of the original lignin.

The kraft process consists in the wood and other biomass delignification to produce kraft pulp. This implies a treatment at a high temperature with an aqueous solution of sodium hydroxide and sodium sulphur. Under these conditions, most of the lignin β-O-4 structures get hydrolysed (95%) and the lignin fragments left get dissolved in the alkaline solution[35]. Some other reactions of the degradative lignin also take place under though conditions within the digester and most of the phenylpropane lateral chains get partially

eliminated. During the process, there is a dissolution of 90-95% of all the lignin present in the original material, due to the acidification of the liquor-pulp. The lignin dissolved can be mostly recovered as a complex mix of phenolic structures with a molecular mass of a range of 150-200.000[36,37].

By dissolvent fractionation, it has been proved that a predominant portion of soft wood kraft lignin has a low molecular mass weight with a low degree of polydispersity, as it is shown in Table 4. The rest, on the contrary, have a high molecular mass and a high polydispersity, presumably because the presence of polysaccharides and condensed lignin structures in those fractions[38]. A similar fractionation technique applied to a kraft lignin of birch provided the results shown in Table 4. Again, with a queue of high molecular weight, a high degree of polydispersity for one of the fractions[39] is obtained as a result.

Table 4. Analytic data of the Kraft lignin after the fragmentation with industrial lignin dissolvent of isolated industrial birch[40]. Fraction 1 = soluble in methylene chloride; Fraction 2 = residue soluble in methanol; Fraction 3 = residue; b = Acetylated lignin fractions.

Fraction No[a]	Yield (%)	M_n[b]	M_w[b]	M_w/M_n	Phenolic OH (mmol/g)	Aliphatic OH (mmol/g)
1	32	650	910	1.4	5.0	1.0
2	38	1320	2110	1.6	4.4	2.2
3	30	3760	87080	23	2.9	3.7

1.4.2.2 Furans: FDCA

Furans are organic compounds that are formed during the food treatment with heat, contributing to the sensorial properties of the product. They are the result of a reaction called Maillard's reaction – between carbohydrates, unsaturated fatty acids and ascorbic acid or derivatives. They have industrial

use, as an intermediator in the tetrahydrofuran production or in lacquers production, as a resin solvent and in the synthesis of chemical products for agriculture (insecticides), stabilisers and pharmaceutical products (fine chemistry). They can also be found in thermally treated foods, like baby food, preserves and foods processed at high temperatures like toasted bread and biscuits.

2,5-Furandicarboxylic acid (FDCA) is one of the 12 main chemical compounds with a highest added value listed by the United States DOE[41] in 2004. The list was updated in 2010 and FDCA was again included, in this occasion being part of a group along with furfural and 5-hydroximethilfurfural (HMF). These three molecules are the main representatives of the furan compounds (furan derivatives), known as the "Sleeping Giants", due to its huge potential on the market. During the last years, the FDCA has been subjected to a rising attention due to its possible applications in different sectors, particularly the possibility of substituting the terephthalic acid (PTA) derived from fossil sources in the synthesis of useful polymers[42-46].

The first work describing the synthesis of FDCA was published by Fittig and Heinzelman in 1876. In this study, the authors reportedly produced FDCA through dehydration of galacturonic acid with fuming hydrobromic acid[47]. A second publication in 1888 by Sohst and Tollens described a similar process, but instead used a saccharide acid isomer for the reaction[48]. The first reported use of HMF and its derivatives to derive FDCA was published in 1899 by Fenton and Gostling[49]. A later publication by Hoehn describes the condensation of glyoxal with dimethyl diglycolate with sodium methoxide[50]. This momentum in research focused on bio-based materials continued into the 1960s as evidenced by the US patent obtained by Atlas Chemical Industries Inc describing the oxidation of HMF to FDCA by reacting HMF with gaseous

oxygen and a platinum or palladium catalyst with a molar excess of an alkali metal hydroxide such as copper or gold oxide[51].

The furan-2,5-dicarboxylic acid (1, FDCA, Figure 9) is a very important chemical substance for its application in polymerization, compensating the construction blocks in the production of polymers that contain an aromatic rest. It is also valuable in pharmacology[52,45].

Furthermore, the furan-2,5-dicarboxylic is an essential and versatile component for the synthesis of interesting organic compounds and biologically active natural products[53,54]. The production of FDCA 1 is generally based on the conversion of hexoses in conditions of strong acid at high temperatures[55,56] or in different furans 2,5- di-substituted oxidative processes, principally 5-(hydroxymethyl) furfural and acid 5-(hydroxymethyl) furoic as C6 substances, compounds that contain 6 atoms of carbon, principally derived from the biomass[57,58].

The most investigated method in the laboratory implies the conversion of the methyl ester of the furan 2-carbolixic acid by chloromethylation – exchange of chlorine-substituent with hydroxyl group – oxidation process along with previous works, treating with the synthesis of furan-2,5-dicarboxylic species[59,60].

The last procedure represents the synthesis of some of the steps provided by FDCA 1 and its derivatives with a low total profit. On the other hand, this allows the possibility of obtaining value of the product FDCA 1 from C5 compounds that can be created from hemicelluloses that contain a range of pentoses[61] using furan-2-carbolyxic acid (2) as intermediate (Figure 9). This strategy was published for the first time by Tao Pan et al., who discovered a new way of converting furfural, a chemical product in bulk based on biomass,

into FDCA, catalytic disproportionation of furoate to furan and 2,5-furandicarboxilate catalysed by zinc chloride[62].

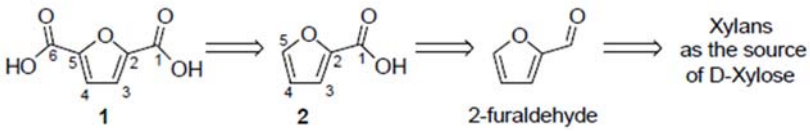

Figure 9. Retrosynthetic analysis of FDCA 1 from C5-compounds.

The main applications for FDCA are on polyesters, polyamides, polyurethanes; plasticisers among others as it is shown in Figure 10. The most important group of transformations that can suffer the FDCA the polymerization one. The monomer FDCA offers big opportunities to create a vast range of polymers: polyesters (bottles, containers and films), polyamides (new nylon) and polyurethanes. The application of the polyurethanes is on insulating products for construction, freezers and fridges, furniture and beds, shoes, automobiles, adhesives among others.

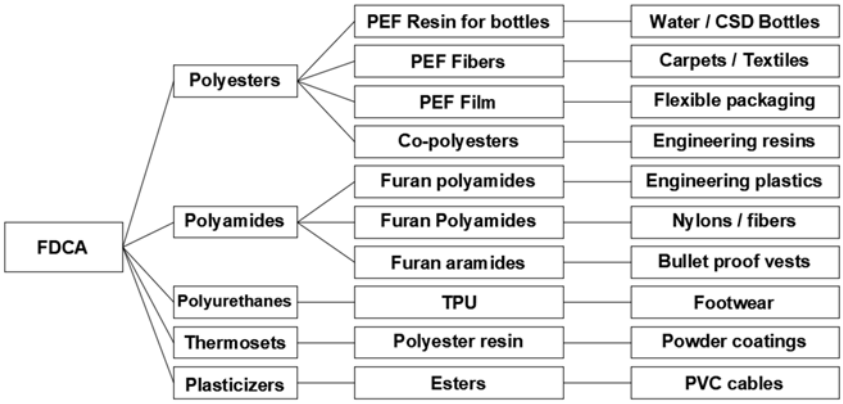

Figure 10. Table of FDCA uses.

In the case of polyesters, FDCA can be polymerized into polyethylene furanoate (PEF) making use of existing polyester infrastructures. PEF gives improved finished product performance, due to better barrier, thermal and mechanical properties when compared to polyethylene terephthalate (PET). At the same time, it improves packaging sustainability, since PEF produced from FDCA is 100% bio-based when bio-based monoethylene glycol (MEG) is used. PEF is intended to replace PET in blow-moulded cold beverage bottles. Furthermore, PEF can be used in fibres, films, and other polyester applications. The primary monomer in PEF is 2,5-furandicarboxylic acid (FDCA), which can be produced from 5-hydroxymethyl furfural (HMF) derived from C6 sugar via chemical catalytic dehydration of sugar to 5-HMF, followed by selective oxidation of 5-HMF to FDCA. 5-HMF can also be produced via thermal pyrolysis. PEF is produced by copolymerizing FDCA dimethyl diester with ethylene glycol via transesterification and polycondensation. Its molecular weight is then increased to approximately 30,000 (required for bottle-grade PET) via solid state (melt phase) thermal polymerization. A parallel effort is made to produce FDCA from 5-HMF via enzyme fermentation, and polymerize it to PEF[63]. The primary uses for conventional PET polymer are to produce bottle-grade resins for cold beverage containers (carbonated beverages and bottled water), and as polyester fibre, which, when it is blended with cotton fibre, produces a wide variety of textile fabrics useful in clothing. Bottle-grade PET resin is also used in industrial fibres. The plastic bottle beverage industry has been under intense pressure from environmentalists over the solid waste generated from discarded conventional PET-based bottles. It is believed that migration from hydrocarbon-based PET to a 100% bio-based plastic PEF bottle resin will relieve some of the environmental pressure; it could also result in lower-cost

resins, given the long-term anticipated price increase in crude oil, which is the fundamental feedstock to produce PET from conventional feedstock PTA (purified terephthalic acid) and monoethylene glycol[63].

The improved properties of PEF compared to PET offer better performance in existing applications, such as in carbonated soft drink bottles. In addition, PEF opens the door to new applications where PET properties do not suffice, like in smaller serving sizes and light-weighting, and to replace other packaging materials like glass and aluminium cans.

1.4.3 Solvents

Due to the big range of applications solvents have at an industrial level, its effect on environment and humans has to be considered, trying for them to be benign. For that reason, the investigation of alternative substances becomes very important. Green chemistry, also known as sustainable chemistry, involves the products, materials and chemical processes that help to reduce the formation of resides or, directly, their elimination as it is previously mentioned. There are alternative solvents that belong to this branch of chemistry. Some of the uses they have in chemical industry are[64]:

- New synthetic routes with a low environmental impact.
- Solvents substitution to eliminate the emissions of volatile organic compounds (VOCs), toxicity and inflammability.
- The use of renewable raw materials.
- The use of safe reactants to reduce the impact on the environment and the human exposition to dangerous chemical products.
- The use of more sustainable technologies.

The use of those technics allows to eliminate or to reduce:

- The use of toxic products persistent in chemical synthesis.
- The number of synthetic phases and isolations to economise the production processes.
- The number of tones of residues per commercialized product.
- The use or generation of solvents and toxic substances in the processes of production and synthesis.

In sectors like Oil Refining, Basic Chemistry, Fine Chemistry, or Formulated Products, the VOC are vastly used. The substitution of this kind of solvents for "green" solvents would avoid the risk of fires in the production plant and during transport, as well as the problems of exposition the factory workers may have.

- Chemical synthesis:
    - Reaction medium in laboratories and at industrial scale.
    - Vastly used for purification (more than as a reaction medium).
- Analytic Chemistry:
    - In spectroscopy as an extraction sample and preparation.
    - Chromatography of mobile phase.
- Crystallization
    - Recrystallization can purify components and preparing crystals adequate for analysis.

Among the application of green solvents there is their use as pesticide. Among the advantages of its use there are:

- They increase the pesticide efficiency.
- The have a low resistance.
- They increase selectivity.

- They have a strong power of solvency.
- They are biodegradable.
- They reduce pollution.
- They reduce the toxicity for warm-blooded animals.
- They are not toxic for fish, worms, or daphnia.
- High Flash Point

There are factors that have influence on the penetration speed when using "green" solvents as pesticide:

- Lipophilic/hydrophilic character and reaction mode.
- Chemical nature (length of the alkyl chain)

Other applications:

- Coatings: paintings, adhesives (solvent usually extracted by evaporation after its application).
- Cleaning: dry cleaners.
- Extraction: coffee's decaffeination (benzene, CH_2Cl_2).

Types of "green" solvents:

- Reactant solvents: solvents that have a low relative volatility, and have the capacity of reacting with other components, getting evaporated (they do not constitute VOCs).
- Benign solvents: solvents that do not harm the environment. Among this kind of solvents there are solvents free of chlorinated compounds.
- Neoteric solvents: it involves the solvents that present a smaller toxicity. They are safer and less contaminants than the traditional solvents. Among them there are new fluids with adjustable properties, and compounds rarely used as solvents but are under investigation due to the potential they present as solvents.

1.4.4 Emission-free

Polymer companies produce a range of basic products, from raw materials to high added value materials. They are fabricated in both, batches and continuous processes, which cover capacities between 10000 and 300000 tons per year. Basic polymers are sold to transformation companies that are providers of a vast variety of final users' markets.

The chemistry used in the polymer production has three basic reactions: polymerization, polycondensation and polyaddition. Therefore, the number of operations/processes used, including the preparation, the reaction between them and the product separation, are kept relatively low. In most of the cases, it is necessary to use heating processes, refrigeration, pressure or the application of vacuum conditions. The inevitable flows of residues are treated in recuperation and/or reduction systems, or are eliminated as residues. The key environmental points in the polymer sector are:

- The emission of volatile organic compounds (VOCs).
- The industrial wastewaters which can have elevated percentages of organic compounds.
- The relatively big quantities of solvents used and the non-recyclable residues.
- The energy consumption.

Due the sector's diversity and the wide range of polymers that are fabricated, this paper does not provide an exhaustive analysis of the emissions of the polymers' sector. However, some data can be observed, regarding emissions and consumption, gathered from a range of industries of the sector that are currently functioning.

The basic characteristics the polymers' sector has to accomplish are:

- Reducing the fugitive emissions by having an advanced designing team that would have to include:
    - The realisation of a measurement and an evaluation regarding the fugitive leaks in order to classify the components according the type, application and conditions of the process to identify the elements with a higher leaking potential.
    - The establishment and maintenance of the team of maintenance management (M&M), and a program of leaking detection and repair (LDAR), with a database of compounds and applications along with the evaluation and measurement of fugitive leaks.
- Reducing dust emissions.
- Minimizing the machinery start/stop processes to avoid emission peaks and reducing the general consumption of, for example, energy or monomers per ton of product.
- Securing the reactors' content in case of an emergency stop.
- Recycling the material or use it as fuel.
- Avoiding water pollution by using pipes with an adequate design and composition.
- Using effluent collection systems.
- Reusing the potential residues that could get produced by the polymer plants[65].

1.5 REFERENCES

1. http://docs.europeanbioplastics.org/publications/EUBP_FAQ_on_bioplasics.pdf, assessed 19/10/2017.

2. Garrido T, Etxabide A, Leceta I, Cabezudo S, De la Caba K, Guerrero P (2014) Valorization of soya by-products for sustainable packaging. J Clean Prod 64:228-233.

3. Shackelford JF (1998) Introducción a la ciencia de materiales para ingenieros. 4ª Edición 373.

4. Anastas PT, Lankey RL (2002) Sustainability through green chemistry and engineering. ACS Syrup Series 823:1-11.

5. Marteel-Parrish AE, Abraham MA (2014) Green Chemistry and Engineering: A Pathway to Sustainability. Chapter 2. Principles of green chemistry and green engineering. John Wiley & Sons, Inc.

6. Anastas PT, Warner JC (1998) Green Chemistry: Theory and Practice. Oxford University Press, New York. 30.

7. http://www.epa.gov/opptintr/greenengineering/, assessed 19/10/2017.

8. Anastas PT, Zimmerman JB (2003) Design through the twelve principles of green engineering. Environ Sci Technol 37:94A-101A.

9. Greene JP (2014) Sustainable Plastics: Environmental Assessments of Biobased, Biodegradable, and Recycled Plastics. John Wiley & Sons, Inc, Hoboken, New Jersey. 1-15.

10. ISO 14040:2006. Environmental management – Life cycle assessment – Principles and framework. Geneva, Switzerland.

11. ISO 14044: 2006. Environmental management – Life cycle assessment – Requirements and guidelines. Geneva, Switzerland.

12. Azapagic A (1999) Life cycle assessment and its application to process selection, design and optimisation. Chem Eng J 73: 1-21.

13. Klöpffer W, Grahl B (2014) Life cycle assessment (LCA): A guide to best practice. John Wiley & Sons, Hoboken, New Jersey, USA.

14. Rebitzer G, Ekvall T, Frischknecht R, Hunkeler D, Norris G, Rydberg T, Schmidt WP, Suh S, Weidema BP, Pennington DW (2004) Life cycle assessment part 1: framework, goal and scope definition, inventory analysis, and applications. Environ Int 30: 701-720.

15. Baldo G, Marino M, Rossi S (2008) Analisi del ciclo di vita LCA - Gli strumenti per la progettazione sostenibile di materiali, prodotti e processi. Edizioni Ambiente.

16. Rigamonti L (2011) Analisi del ciclo di vita: generalità. Dispense del corso di "Complementi di Rifiuti Solidi". Milano, Politecnico di Milano.

17. Vink ETH, Davies S (2015) Life cycle inventory and impact assessment data for 2014 Ingeo polylactide production. Ind biotechnol 11: 167-180.

18. Vink ETH, Davies S, Kolstad JJ (2010) The eco-profile for current Ingeo polylactide production. Ind Biotechnol 6:212–224.

19. Madival S, Auras R, Singh SP, Narayan R (2009) Assessment of the environmental profile of PLA, PET and PS clamshell containers using LCA methodology. J Clean Prod 17:1183-1194.

20. Adom F, Dunn JB, Han J, Sather N (2014) Life-cycle fossil energy consumption and greenhouse gas emissions of bioderived chemicals and their conventional counterparts. Environ Sci Technol 48:14624-14631.

21. Urban RA, Bakshi BR (2009) 1,3-Propanediol from fossils versus biomass: A life cycle evaluation of emissions and ecological resources. Ind Eng Chem Res 48:8068-8082.

22. Cok B, Tsiropoulos I, Roes AL, Patel MK (2014) Succinic acid production derived from carbohydrates: An energy and greenhouse gas assessment of a platform chemical toward a bio-based economy. Biofuels Bioprod Biorefining 8:16-29.

23. White JL, Choi DD (2005) Polyolefins - Processing, structure development, and properties. Hanser Publishers, Munich, Germany.

24. https://www.biobasedpress.eu/2014/12/bio-aromatics/, assessed 19/10/2017.

25. http://www.forestbioenergy.net/training-materials/training-curriculum-notebook/BiomassTrainNotebook.pdf, assessed 19/10/2017.

26. Gellerstedt G, Henrinksson G (2008) Lignins: Major sources, structure and properties. Elsevier 201-224.

27. Grabber JH, Schatz PF, Kim H, Lu F, Ralph J (2010) Identifying new lignin bioengineering targets: 1. Monolignol-substitute impacts on lignin formation and cell wall fermentability. BMC Plant Biology 10:114.

28. Sifontes MS, Domine ME (2013) Lignina, estructura y aplicaciones: métodos de despolimerización para la obtención de derivados aromáticos de interés industrial. Av cien ing 4:15-46.

29. Higuchi T (1990) Lignin biochemistry: Biosynthesis and biodegradation. Wood Sci Technol 24: 23–63.

30. Boudet AM (2000) Lignins and lignification: Selected issues. Plant Physiol Biochem 38:81-96.

31. Freudenberg K, Neish AC (1968) Constitution and biosynthesis of lignin. Springer-Verlag, Berlin-Heidelberg 47-122.

32. Ralph J, Lundquist K, Brunow G, Lu F, Kim H, Schatz PF, Marita JM, Hatfi eld RD, Ralph SA, Christensen JH, Boerjan W (2004) Lignins: Natural polymers from oxidative coupling of 4-hydroxyphenylpropanoids. Phytochem Rev 3:29-60.

33. Bauer S, Sorek H, Mitchell VD, Ibáñez AB, Wemmer DE (2012) characterization of miscanthus giganteus lignin isolated by ethanol organosolv process under reflux condition. J Agric Food Chem 60:8203-8212.

34. Chávez-Sifontes M, Domine ME (2013) Avances en Ciencias e Ingeniería – ISSN: 0718-8706. Av cien ing 4:15-46.

35. Wayman M, Lora JH, Gulbinas E (1979) Material and energy balances in the production of ethanol from wood. ACS Symposium Series 90:183-201.

36. Alonso MV, Rodriguez JJ, Oliet M, Rodriguez F, Garcia J, Gilarranz MA (2001) Characterization and structural modificatión of ammonic lignosulfonate by methylolation. J Appl Polym Sci 82:2661-2668.

37. Alonso MV, Oliet M, Rodriguez F, Garcia J, Gilarranz MAR, Rodriguez JJ (2005) Modification of ammonium lignosulfonate by phenolation for use in phenolic resins. Bioresource Technol 96:1013-1018.

38. Lora JH, Wu CF, Cronlund M, Katzen R (1988) Recovery of lignin. Patent US 4764596 A.

39. Lora JH, Creamer AW, Wu CF, Goyal GC (1993) Industrial scale production of organosolv lignins: characteristics and applications. Repap Technologies Inc 2650. Eisenhower Avenue, Valley Forge, PA 19482, USA. 251-256.

40. Morck R, Yoshida H, Kringstad K (1986) Fractionation of kraft lignin by successive extraction with organic solvents I. Functional Groups. ^{13}C NMR-spectra and Molecular Weight Distributions. Holzforschung 40:51–60.

41. Van Putten RJ, Van Der Waal JC, De Jong E, Rasrendra CB, Heeres HJ, De Vries JG (2013) Hydroxymethylfurfural, a versatile platform chemical made from renewable resources. Chem Rev 113 1499-1597.

42. Lewkowski J (2001) Synthesis, chemistry and applications of 5-hydroxymethyl-furfural and its derivatives. ARKIVOC 2001:17-54.

43. Teong SP, Yi G, Zhang Y (2014) Hydroxymethylfurfural production from bioresources: past, present and future. Green Chem 16:2015-2026.

44. Werpy T, Petersen GR (2004) Top value added chemicals from biomass. Volume 1: Results of Screening for Potential Candidates from Sugar and Systhesis Gas. U.S. Department of Energy, Energy Efficiency and Renewable Energy. 21-26.

45. Bozell JJ, Petersen GR (2010) Technology development for the production of biobased product from biorefinery carbohydrates–the US Department of Energy's Top 10 revisited. Green Chem 12: 539-554.

46. De Jong E, Dam MA, Sipos L, Gruter G-JM (2008) Furandicarboxylic acid (FDCA), a versatile building block for a very interesting class of polyesters. ACS Symposium Series 1105:1-13.

47. Fittig R, Heinzelman H (1876) Berichte der deutschen chemischen Gesellschaft. Eur J Org Chem 1198.

48. Sohst O, Tollens B, (1888) Über krystallisirte Zuckersäure. ustus Liebigs Ann. Chem 245: p 1.

49. Fenton HJH, Gostling M (1899) XLI-Bromomethylfurfuraldehyde. J Chem Soc Trans 75:423-433.

50. Hoehn W (1936) Iowa State Coll. J Sci 11:66.

51. Lew BW (1967) Method of producing dehydromucic acid. Patent US 3326944 A.

52. Gandini A, Belgacem MN (1997) Furans in polymer chemistry. Prog Polym Sci 22: 1203-1379.

53. Schmuck C, Machon U (2006) 2-(Guanidiniocarbonyl)furans as a new class of potential anion hosts: synthesis and first binding studies. Eur J Org Chem 4385-4392.

54. Yin B-L, Yang Z-M, Hu T-S, Wu Y-L (2003) Molecular diversity of tonghaosu: synthesis of lactam-containing tonghaosu analogs. Synthesis 13:1995-2000.

55. Yoichi T, Akihiro O, Hiroshi L (2008) One-step Synthesis of Dibutyl Furandicarboxylates from Galactaric Acid. Chem Lett 37:50-51.

56. Lewkowski, J (2001) Convenient synthesis of furan-2,5-dicarboxylic acid and its derivatives. Pol J Chem 75:1943-1946.

57. Koopman F, Wierckx N, De Winde JH, Ruijssenaars HJ (2010) Efficient whole-cell biotransformation of 5-(hydroxymethyl)furfural into FDCA, 2,5-furandicarboxylic acid. Bioresour Technol 101: 6291-6296.

58. Brasholz M, Von Känel K, Hornung CH, Saubern S, Tsanaktsidis J (2011) Highly efficient dehydration of carbohydrates to 5-(chloromethyl)furfural (CMF), 5-(hydroxymethyl)furfural (HMF) and levulinic acid by biphasic continuous flow processing. Green Chem 13: 1114-1117.

59. Moldenhauer O, Trautmann G, Irion W, Pfluger R, Döser H, Mastaglio D, Marwitz H, Liebigs A (1953) Beiträge zur Furanchemie I. Eur J Org Chem 580:169.

60. Nielek S, Lesiak T (1988) Isocyanates of heterocyclic compounds. I. The Synthesis of 2,5-Diisocyanatofuran. Adv Synth Catal 330:625-629.

61. Feather MS, Harris DW, Nichols SBJ (1972) Wege zur umwandlung von d-xylose, hexuronsaeuren oder l-ascorbinsaeure in 2-furaldehyd. Eur J Org Chem 37:1606.

62. Pan T, Deng J, Xu Q, Zuo Y, Fu Y (2013) catalytic conversion of furfural into a 2,5-furandicarboxylic acid-based polyester with total carbon utilization. ChemSusChem 6:47-50.

63. Pavone A (2016) Bio-Based furan dicarboxylic acid (FDCA) and its polymer polyethylene furanoate (PEF). IHS Chemical 18-20. https://cdn.ihs.com/www/pdf/RP294-toc.pdf

64. http://practica-uno.blogspot.it/2009/04/solventes-verdes.html, assessed 19/10/2017.

65. http://www.prtr-es.es/data/images/PRODUCCI%C3%93N-DE-POL%C3%8DMEROS-1BDCAAE0950F2E40.pdf, assessed 19/10/2017.

2.
Aim of the work

The general aim of the present thesis was focused on the study of different polymer systems obtained from renewable sources and its manufacturing through various technologies, including polyurethanes, polyesters and lignin concerned to the coating industry.

The main objective of the first part of the present research was the development and environmental study of a **new class of polyester binder based on FDCA suitable as precursors of PU coating materials**. The strategy for the new 100% bio-based structure initially involved the **selection and copolymerization of four different monomers**, which were all available **from modern biorefinery downstreams** such as glycerine (Gly), 1,3-propanediol (1,3-PD), 2,5-furandicarboxylic acid (FDCA) and succinic acid (SA). This new structure was developed together with partially 75% bio-based and two fossil-based polyester binders. Successively, the obtained polyesters were **crosslinked with a conventional polyisocyanate to obtain the corresponding PU coatings**. The **evaluation of its technological performances** was present for all of them, and some preliminary experimental tests were included such as pull-off adhesion, indentation hardness, contact angle, and hydrolytic stability tests. In addition, **the evaluation of the total impact of greenhouse gas emissions (GHG) and the total non-renewable energy use (NREU) by the Life Cycle Assessment (LCA**) for all polyester binders was included on a cradle-to-factory gate approach. Specifically, the **FDCA production process starting from sugar beet was assessed in terms of GHG emissions and NREU**, which was based on **primary data**. Moreover, a more detailed analysis of the **impact of marine eutrophication and freshwater eutrophication was allowed for the sugar beet** cultivation since they are relevant in the production of a substance derived from a cultivated biomass feedstock.

The second part of the present thesis had as a main goal the valorisation of lignin as coating material. Currently, **lignin is attractive as a reinforcing filler for the preparation of polymer-based composites** due to its large number of functional groups and the **potentially favourable covalent and non-covalent interactions** that may arise between such highly-functional filler and the polymeric matrix. Particularly, an alternative strategy to achieve **enhanced dispersion level of the lignin filler within the polymer matrix is the preparation and use of lignin-based nanoparticles**. To this end, our first aim was to prepare the **nanolignin (NL) particles by ultrasonic treatment** of softwood kraft lignin to obtain lignin-water dispersions with an excellent colloidal stability. The second goal was initially to **incorporate the obtained lignin nanoparticles into a waterborne thermoplastic polyurethane** and successively **into epoxidized natural rubber to form nanocomposite materials** with increasing bio-filler concentration. For this scope, the effect of the filler type (NL vs. untreated lignin) and the concentration on a detailed characterization of the resulting nanocomposites was investigated.

3.
Green polyesters for polyurethane coatings

3.1 INTRODUCTION

Polyurethanes (PUs) are one of the most used coating materials in many manufacturing sectors (automotive, furniture, heavy duty) due to their excellent durability and mechanical properties[1]. PUs are actually the sixth most used polymers on a global scale with an annual production of over 12 million tons[2]. One of the emerging topics in modern PU technology is the exploitation of monomers and macromers from renewable resources to improve the environmental sustainability while preserving the excellent technical performances[3,4]. PU coatings are obtained by the stoichiometrically balanced mixture and crosslinking of polyols (polyether and frequently polyester oligomers) with polyisocyanates (see Figure 1). By a careful selection of different polyols and isocyanates, a variety of PUs with specific properties can be developed for a broad range of industrial applications like foams, paints, thermoplastics, fibers and adhesives[5-7].

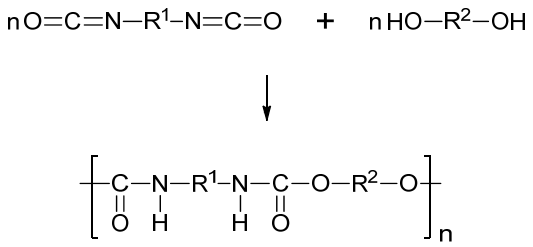

Figure 1. Reaction of a diisocyanate with a diol to form a polyurethane.

Polyester polyols are the largest fraction in the composition of PU coating material. There has been a certain ease of availability to obtain bio-based polyester precursors from biorefineries[8] where soybean oil-based is taking on a leading role[9,10], compared to, for example, isocyanates and diamines. Polyester polyols are made from aliphatic as well as aromatic diacids and

hydroxy functional monomers[11]. Within aromatic acids, 2,5-furandicarboxylic acid (FDCA) is a relatively "new" bio-based building block with a unique aromatic structure that is attracting great interest. Moreover, the production of furan derivatives from sugars, synthesized chemically from 5-hydroxymethylfurfural (HMF), has recently become a promising route in green chemistry and in catalysis studies[12]. In recent years, polyester polymers and copolymers based on FDCA have received special attention in many aspects regarding monomer synthesis, polymerization reactions, application[13,14] and characterization[15-17]. FDCA was mainly proposed as a green alternative to petrochemical-derived terephthalic acid to produce thermoplastic polyesters[18,19]. A recent paper[20] presented an overview of the developments and future prospects on bio-based polyesters from FDCA and other renewable resources. They can be used as biomaterials[21] with competitive properties[22] and potential applications as thermoplastics as well as elastomers[23].

Renewable raw materials may reduce the environmental impacts compared with petroleum based counterparts. These effects can be quantified by the Life Cycle Assessment (LCA) method whose aim is to determine the environmental impacts of products and processes by the evaluation of the entire life cycle. There has been a growing use of this method since it is necessary to take measures against global climate change, and to become less dependent on petroleum sources. An example case is the study of LCA applied to the bio-based polyester polylactic acid (PLA)[24]. In addition, an extensive number of studies have been reported in which the assessment on a life-cycle basis of the different impacts of bio-based products has been compared to conventional fossil-derived products[25,26] or to other bio-based products[27]. Concerning FDCA production, although there is a high industrial

interest in it, only a few papers are available in the open literature[28,29] in terms of greenhouse gas emissions (GHG) and non-renewable energy use (NREU). However, bio-based resources could be involved in other environmental burdens, which can be assessed by the LCA, as it is the case of eutrophication, acidification, ozone depletion, land-use change, biodiversity, soil degradation, air pollution and social impacts among others.

In spite of the large number of papers describing polyurethane coatings, there is a lack of information in the literature about polyester copolymers based on FDCA as precursors of PU coatings. Moreover, no specific study is reported in the literature concerning a cradle-to-gate LCA of polyester binders to represent the larger component of the coating material. Nowadays, although the possibility of using bio-based monomers to synthesise polyester was already demonstrated, no specific evaluation of their ecoprofiles is available, being LCA studies predominantly focused on bio-based polyester as packaging materials.

In the light of the above considerations, the aim of this work is to present a new class of polyester binders based on a suitable FDCA as precursors of PU coating materials. The new 100% bio-based structure was re-designed and obtained through the selection and copolymerization of four different monomers, all available from modern biorefinery downstreams. This new structure was developed together with 75% bio-based and two fossil-based polyester binders. The corresponding four PU coatings were obtained by crosslinking of a conventional polyisocyanate and the polyesters synthesized. Their technological performances were benchmarked between them. Moreover, the evaluation of the total impact of greenhouse gas emissions (GHG) and the total non-renewable energy use (NREU) by the Life Cycle Assessment (LCA) are included on the basis of a cradle-to-gate approach

separating the contributions due to the monomer mixture composition and those related to the copolymerization process, and considering an FDCA production process starting from sugar beet (primary data). Specifically, a finer analysis of the impact of marine eutrophication and freshwater eutrophication is allowed, providing relevant information about the environmental implications of the production of a chemical derived by biomass (sugar beet), as it is the case of the present study. The LCA on FDCA production for sugar beet cultivation was developed during my stay at Lund University in Sweden.

3.2 EXPERIMENTAL SECTION

3.2.1 Materials

All materials used in this study are commercially available. The conventional polyisocyanate used for crosslinking, called commercially Vestanat 1890/100, was supplied by Evonik Industries. It was a cycloaliphatic polyisocyanate based on isophorone diisocyanate (IPDI). The basic structure is the isocyanurate ring, its NCO-functionality is between two and three. 1,4-butanediol (1,4-BD), 1,2-propanediol (1,2-PD), 1,3-propanediol (1,3-PD), succinic acid (SA), adipic acid (AA), phthalic anhydride (Pht), glycerine (Gly) used for the synthesis of the polyesters and the solvents needed to reduce the viscosity such as butyl acetate (BA) and propylene carbonate (PCC) were all purchased from Sigma-Aldrich. FDCA monomer was provided by the Sinochem Jiangsu Co., Ltd. (Middle, Nanjing, China).

3.2.2 Monomer selection process

Suitable monomers were selected according to their functional role in the binder design and primary data availability in the Ecoinvent database version 3.2, and in the open literature. All the relevant information is summarized in Table 1. The data concerning succinic acid (SA) production came from the direct crystallization (SA-DC) process described by Cok et al. (2014).

Table1. Characteristics and functions of monomers for polyester binders.

Name of the monomer (acronym)	Family	The function in the material	Bio or fossil based	Reference for background data
Glycerine (Gly)	Polyols	Give residual –OH functions to the final polyester binder, allowing the crosslinking reaction with isocyanates	Fossil-based	Secondary data[30]
Glycerine (Gly)			Bio-based (Palm Oil)	
Phthalic anhydride (Pht)	Aromatic diacids	Increase the coating glass transition temperature Tg	Fossil-based	Secondary data[31]
2,5-Furandi-carboxylic acid (FDCA)			Bio-based (Sugar beet)	Primary data
Adipic acid (AA)	Aliphatic diacids	Increase coating flexibility and outdoor durability	Fossil-based	Secondary data[31]
Succinic acid (SA)			Bio-based (Corn starch)	Secondary data[27]
1,4-butanediol (1,4-BD)	Aliphatic diols	Increase polymer molecular weight	Fossil-based	Secondary data[32]
1,2-propanediol (1,2-PD)			Fossil-based	Secondary data[31]
1,3-propanediol (1,3-PD)			Bio-based (Corn sugar)	Secondary data[33]

3.2.3 Preparation - copolymerization of polyester (PEs) binders

Table 2 shows the composition of the four 4-monomers copolyester binders synthesized and considered in the present study for the evaluation of their ecoprofiles, and tested experimentally in PU coating formulations. Polyesters 3 and 4 (PE3_Fossil and PE4_Fossil) were designed and developed considering that all monomers are derived from fossil-based resources. The only difference between them is the change from 1,4-butanediol monomer to 1,2-propanediol monomer respectively. The latter presents a methyl side group and a secondary hydroxyl. This normally leads to a lower reactivity but at the same time it leads to the formation of sterically hindered ester groups in the polyester, which may be more stable towards hydrolysis. As for the polyester 2 (PE2_75%), the composition was mainly based on monomers from renewable resources with the exception of the phthalic anhydride monomer (partially bio-based, 75% renewable carbon). With regard to the aliphatic acids, the adipic acid has not a direct sustainable alternative so far. Therefore, the succinic acid was introduced as a renewable monomer[27]. As the molecular structures of the two diacids are different, it is supposed that some differences between polymer Tg and hydrolytic stability may occur. Moreover, moving from one binder to another, SA and 1,3-PD in PE2_75%, the polymers with a higher concentration of main chain ester groups and without methyl side groups will be produced. This may lead to an enhanced water sensitivity and possibly to lower Tg, which are effects to be evaluated. Regarding polyester 1 (PE1_100%), it was based on 100% bio-based monomers where the only difference between the two bio-based materials (PE2_75% and PE1_100%) is the nature of the aromatic acid, which replaces the fossil-based phthalic acid with the bio-based FDCA, respectively.

Table 2a. Polyester compositions of the two synthesized 75% and 100% bio-based polyester binders.

PE1_100% (monomers)	COMPOSITION (% w/w)	PE2_75% (monomers)	COMPOSITION (% w/w)
Gly	6.9	**Gly**	7.0
1,3-PD	34.0	**1,3-PD**	34.7
FDCA	38.4	**Pht**	37.9
SA	20.6	**SA**	20.4

Table 2b. Polyester compositions of the two synthesized fossil-based polyester binders.

PE3_Fossil (monomers)	COMPOSITION (% w/w)	PE4_Fossil (monomers)	COMPOSITION (% w/w)
Gly	6.7	**Gly**	6.4
1,2-PD	33.2	**1,4-BD**	37.4
Pht	39.1	**Pht**	36.5
AA	21.0	**AA**	19.7

The polymerization process was the same for all the four polyesters, and consisted in a bulk polycondensation at high temperature (from 150°C to 210°C) under dry nitrogen flow to remove water as by-product. The progress of each reaction was monitored by end group titration which monitored the residual acidity of polyesters, and stopped the polymerization when the acid number (AV) was < 15 mgKOH/g, using the following Equation:

$$\text{AV [mg KOH/g]} = \frac{V3 * 56.1 * N}{W2}$$

where: V3 = volume of KOH 0.1N consumed for sample titration; W2 = sample weight on the solid; 56.1 = molecular weight of KOH and N = normality of KOH (0.5N).

When polymerization was completed, the determination of the hydroxyl number for all polyester binders was calculated, using the following Equation:

$$N°OH\ [mg\ KOH/g] = \frac{(V2-V1) * 56.1 * N}{W1} + N°acid\ \ of\ sample$$

where: V1 = volume KOH 0.5 M used in sample titration; V2 = volume KOH 0.5 M used in titration of blank test ; W1 = sample weight as solid; 56.1 = molecular weight of KOH and N = normality of KOH (0.5N). Values of acid and hydroxyl numbers for all PE binders are shown in Table 3 together with the reation time of the synthesis.

Table 3. Acid number (AV), hydroxyl numbers (OHV) and reaction time of the copolymerizatio for all PEs.

	AV [mg KOH/g]	Time reaction (h)	OHV [mg KOH/g]
PE1_100%	14.5	9	51.0
PE2_75%	12.8	6	87.4
PE3_Fossil	6.8	4	80.4
PE4_Fossil	14.3	8	56.8

3.2.4 Preparation - crosslinking of polyurethane (PUs) coatings

The PU coatings were obtained by crosslinking with a polyisocyanate IPDI and the polyester binders synthesized on lab-scale. The corresponding PU coatings were named PU1 (from PE1_100%), PU2 (from PE2_75%), PU3 (from PE3_Fossil) and PU4 (from PE4_Fossil). The crosslinking was performed at 80°C for around 6 h and 1,4-Diazabicyclo [2.2.2]octane (DABCO) was used as a catalyst to crosslink the PU1 and the dibutyltin dilaurate (DBTDL) catalyst was used for the other PU coatings (see Figure 2). The reason was the incompatibility of the DBTDL with the propylene carbonate (PPC) solvent.

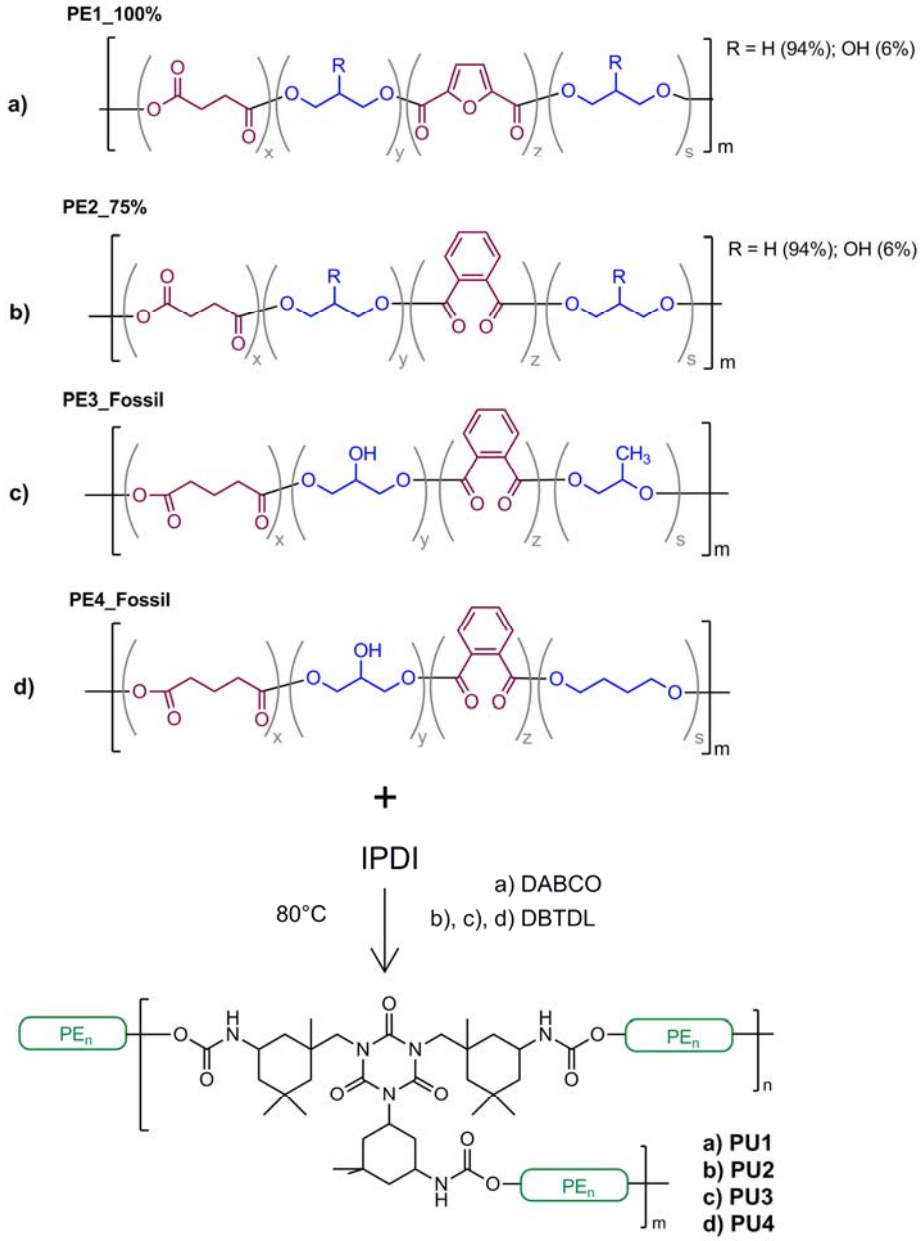

(x ≈ 0.20; y ≈ 0.065; z ≈ 0.38; s ≈ 0.35)

Figure 2. The corresponding PU coatings obtained by crosslinking with a polyisocyanate IPDI and the polyester binders.

Coatings with a thickness of 40-50 μm were bar-applied onto glass or metal substrates after dilution with butyl acetate solvent for PU2, PU3 and PU4 and PPC solvent for PU1 to reduce viscosity (solid content 30-50% w/w). All coatings passed the chemical resistance test after curing (MEK test > 100 double rubs according to ASTM D4752[34]) confirming that crosslinking has occurred.

3.2.5 PE binders and PU coatings characterization

3.2.5.1 Fourier Transform Infrared spectroscopy (FTIR) analysis

The extent of reaction upon PUs crosslinking was checked by monitoring the progressive disappearance of the NCO stretching located at 2260 cm^{-1} through FTIR analysis. The spectra were acquired using a Thermo Nicolet 760 FTIR Spectrophotometer with 64 accumulated scans performed from 4000 cm^{-1} to 700 cm^{-1} at 2 cm^{-1} resolution. The comparison of spectra acquired at different times allowed the estimation of the degree of the reaction. After 4 - 6 h the NCO peak completely disappeared indicating that the reaction ended.

3.2.5.2 Differential Scanning Calorimetry (DSC) analysis

Thermal analysis was performed on PE and PU samples using a DSC (MettlerToledo DSC/823e instrument) at a scan rate of 10°C min^{-1} under nitrogen flux. The measurements consisted of three runs (heating/cooling/heating) from 25 °C to 150 °C. The samples measured had a weight of around 10-15 mg.

3.2.5.3 Optical Contact Angle (OCA) – surface wettability

The wettability of the PU surfaces was studied performing contact angle measurements using an optical contact angle system (OCA-15-Plus, Dataphysics, Germany) equipped with a CCD photocamera and with a 500 μL Hamilton syringe to dispense liquid droplets. Measurements were made at room temperature by means of the sessile drop technique with dedicated software (SCA 2.0) determining the contact angle based on the Young Laplace fitting method. Pure water (H_2O) was used as probe liquid and the delivered volume was 2 μl with 0.5 μl/s as dispense speed. A minimum of 25 measurements were taken in different regions on the surface of each PU film and results were averaged.

3.2.5.4 Gel Permeation Chromatography (GPC)

The molecular weight of PE samples was estimated by means of gel permeation chromatography (GPC) using a Waters 510 high-performance liquid chromatography (HPLC) system equipped with a Waters 486 tunable absorbance detector set at λ = 300 nm, using THF as eluent. The sample (200 μL of PE in THF, 2 mg/mL) was injected into a system of columns connected in series (Ultrastyragel HR, Waters) and the analysis was performed at 30 °C and at a flow rate of 0.5 mL/min. The GPC system was calibrated against polystyrene standards in the 102-104 g/mol molecular weight range.

3.2.5.5 Bohlin Rheometer – viscosity measurement

A BOHLIN CVO 120 High Resolution rotational rheometer (Melvern instruments Ldt.) was used to determinate the viscosity of all polyester binders. A gradually increasing stress, from 0 to 500 Pa, was applied within 3

minutes and thirty evaluation points were linearly chosen for viscosity measurements. The analysis was performed by a plane-plate geometry of 20 mm diameter, at a fixed gap width of 800.

3.2.5.6 Buchholz Indentation test – hardness analysis

The indentation resistance (hardness) of the corresponding PU coatings were evaluated by Indentation Hardness Tester acc. to Buchholz, Model 263 (ISO 2815[35]) A metal block with testing force between a range of 4.90 N and 4.95 N (equivalent to 500 to 505 g) was applied on each coating surface for 30 seconds and the length (l) of the resulting indentation was measured using a microscope. The length of the indentation is inversely proportional to the hardness and the indentation resistance ($\acute{\alpha}_B$) values were obtained from the indentation length (Table 4) using the following Equation:

$$\text{Resistance (H)} = \frac{\text{Force}}{\text{Area}} = \frac{\text{cte}}{\text{Length (l)} * \text{width (w)}} = \frac{\text{cte}}{\text{Length (l)} * \text{cte}} = \frac{1}{\text{Length (l)}}$$

$$\acute{\alpha}_B = \frac{100}{\text{Length (l)}} \quad \text{where } l \text{ is in millimetres (mm)}$$

Table 4. Relationship between indentation length (l) and indentation resistance ($\acute{\alpha}_B$). The calculated error of the indentation resistance is as a function of the indentation length (taking $\Delta l = 0.1$ mm).

Coatings	Indentation length (l) (Average in mm)	Indentation resistance ($\acute{\alpha}_B$)
PU1	1.20	83
PU2	1.85	54
PU3	1.10	91
PU4	1.54	64

3.2.5.7 Pull-Off Adhesion testing

The adhesive properties of the resulting PU materials on different substrates (glass and aluminium chromed) were evaluated with a PosiTest AT-M Manual adhesion pull-off tester (DeFelsko, ASTM D4541-09[36]) by measuring the pulling force needed to detach a 20 mm-diameter aluminium dolly adhered to the films by means of epoxy adhesive (Araldite 2011, curing cycle: 50°C, 24 h). Three determinations of each sample were assessed.

3.2.5.8 Surface characterization

Surface tension on the corresponding coatings was evaluated by performing contact angle measurements with the same technique previously described. The procedure was followed using water (H_2O) and diiodomethane (CH_2Cl_2) (Sigma-Aldrich) because at least two liquids are necessary to compute surface tension. The surface energies and its polar and dispersive components were estimated by Wu's harmonic-mean method[37], enabling to discriminate between its components, using the following Equation of the interfacial tension γsl:

$$\gamma_{sl} = \gamma_{sv} + \gamma_{lv} - \frac{4\,\gamma_{sv}^{d}\,\gamma_{lv}^{d}}{\gamma_{sv}^{d} + \gamma_{lv}^{d}} - \frac{4\,\gamma_{sv}^{p}\,\gamma_{lv}^{p}}{\gamma_{sv}^{p} + \gamma_{lv}^{p}}$$

where the subscript *sv* and *lv* refer respectively to the solid and to the testing liquid and the subscripts *d* and *p* indicate the dispersive and polar components of surface tension so this formula is applied $\gamma_{sv} = \gamma_{sv}^{s} + \gamma_{sv}^{p}$.

3.3 LIFE CYCLE ASSESSMENT (LCA) ON POLYESTER BINDERS

3.3.1 Methodology

The LCA analysis was developed following the LCA methodology, which is standardised in the ISO 14040-14044 series by the International Organization of Standardization[38,39] (ISO 14040-14044). This study was focused on the 'Cumulative Energy Demand' (v1.09) method[40] which covers the impact category of non-renewable energy use (NREU) including fossil and nuclear energy and the 'Greenhouse Gas Protocol (GGP)' (v1.01) method which covers the impact category of GHG emissions. The GGP method was chosen to perform a Carbon Footprint of the different alternatives analysed. This method leads to measure the amount of greenhouse gases (in kg CO_{2eq}) emitted to the atmosphere and contributing to global climate change and includes emissions from fossil and biogenic carbon sources, emissions caused by land use change and carbon uptake by plants over a 100-year time horizon. To calculate carbon dioxide equivalents (CO_{2eq}) of all non-CO_2gases (CH_4, N_2O, SF_6, HFCs and CFCs) the 100-year IPCC global warming potentials (GWP) are used in (IPCC[41], 2007). The 100-year GWP is a metric used to describe the time-integrated radiative characteristics of well mixed greenhouse gases over a 100-year time horizon. In particular, for sugar production, the 'Recipe Midpoint (H)' (v1.12), method[42] based on the GWP100 (100-year timeframe), was also used to analyse the impact categories of marine eutrophication and freshwater eutrophication, as they are relevant in the production of a substance derived from a cultivated biomass feedstock, as it is the case of this study (sugar beet). The latter impact categories could not be used in all the study, as this information was not found in the literature for

the other steps. The choice of these categories of impact was related to the need of providing an evaluation of the impact of the studied production but also because the lack of other impact categories in literature. Specifically, GHG emissions was selected because it is one of the main environmental problems of the present century and the future. NREU category was used to provide a view of the impacts in relation not only to emissions but also to consumption, which is considered one of the most critical issues in the primary sector. The characterization factors of each emission used in GHG emissions for all polyester binders are shown in Table 5. The characterization factors for sugar production are shown in Table 6a. The characterization factors of each emission used in marine and freshwater eutrophication for sugar production are shown in Table 6b. A sensitivity analysis was also done for all polyesters with the aim of estimating the effects of choices made regarding methods and data on the outcome of the study (ISO 14044). In addition, a finer sensitivity analysis was developed on sugar production from sugar beet cultivation as primary data were added for PE1_100% production compared to the other polyesters (PE2_75% and PE3/PE4_Fossil). This analysis was tested through different LCA calculation allocations such as economic and energy. The functional unit is one kg of polyester binder, the basis to compare among all of them.

Table 5. Characterization factors of each emission in the environmental impact category GHG emissions together with the resulting emission equivalents for PE1_100%, PE2_75%, PE3 and P4_Fossil production.

Environmental impact category	Emissions	Characterization factors	Resulting emission equivalents
GHG emissions	Carbon dioxide (fossil)	1 kg CO_{2eq}	1.75 kg CO_{2eq} / kg PE1_100%
	Nitrous oxide	298 kg CO_{2eq}	2.75 kg CO_{2eq} /kg PE2_75%
			8.40 kg CO_{2eq} / kg PE3_Fossil
	Methane (fossil and biogenic)	25 kg CO_{2eq}	8.10 kg CO_{2eq} / kg PE4_Fossil

Table 6a. Characterization factors of each emission in the environmental impact category GHG emissions together with the resulting emission equivalents for sugar production from sugar beet cultivation.

Environmental impact category	Emissions	Characterization factors	Resulting emission equivalents
GHG emissions	Carbon dioxide (fossil)	1 kg CO_{2eq}	708 kg CO_{2eq}/ton sugar
	Nitrous oxide	298 kg CO_{2eq}	
	Methane (fossil and biogenic)	25 kg CO_{2eq}	

Table 6b. Characterization factors of each emission in the environmental impact category marine and freshwater eutrophication together with the resulting emission equivalents for sugar production from sugar beet cultivation.

Environmental impact category	Emissions	Characterization factors	Resulting emission equivalents
Freshwater Eutrophication	Phosphate (water)	1 kg $PO_4^{3-}{}_{eq}$	0.19 kg $PO_4^{3-}{}_{eq}$/ton sugar
	Phosphorous (water)	298 kg $PO_4^{3-}{}_{eq}$	
	Phosphorous (soil)	25 kg $PO_4^{3-}{}_{eq}$	
Marine Eutrophication	Ammonia (air)	0.40 kg $NO_3^{-}{}_{eq}$	3.2 kg $NO_3^{-}{}_{eq}$/ton sugar
	Ammonium, ion (water)	3.40 kg $NO_3^{-}{}_{eq}$	
	Cyanide (water)	2.35 kg $NO_3^{-}{}_{eq}$	
	Nitrate (air)	0.12 kg $NO_3^{-}{}_{eq}$	
	Nitrate (water)	1 kg $NO_3^{-}{}_{eq}$	
	Nitrite (water)	1.3 kg $NO_3^{-}{}_{eq}$	
	Nitrogen (water)	4.35 kg $NO_3^{-}{}_{eq}$	
	Nitrogen oxides (air)	0.17 kg $NO_3^{-}{}_{eq}$	
	Nitrogen, organic bound (water)	4.35 kg $NO_3^{-}{}_{eq}$	

3.3.2 System boundary

The LCA study on the production of all polyester binders was developed. Figure 3 shows the system boundary of the four polyester binders analysed (PE1_100%, PE2_75%, PE3_Fossil and PE4_Fossil) according to a cradle-to-

factory gate view. Within the system boundary, the contributions of different monomers and the contribution of the polymerization process were analysed separately up to the step of binder production.

As for the FDCA monomer, the simplified flow diagram for its production is shown in Figure 4, which also follows a cradle-to-factory gate approach. The FDCA production system is divided into five major phases: beet cultivation; transport of beet to the plant and the sugar production; conversion of fructose; conversion of 5-HMF and finally oxidation of 5-HMF to the FDCA. Within these main phases, the first two (Figure 4) were developed from primary data. Their multiple operational steps are present in the next point. The other phases were developed from the literature[28]. In addition, transport of the raw materials and the production of the farm equipment, such as beet harvesters and tractors used in the sugar production step, and the intermediate transport steps from sugar production to FDCA production, were outside the system boundaries and were not considered.

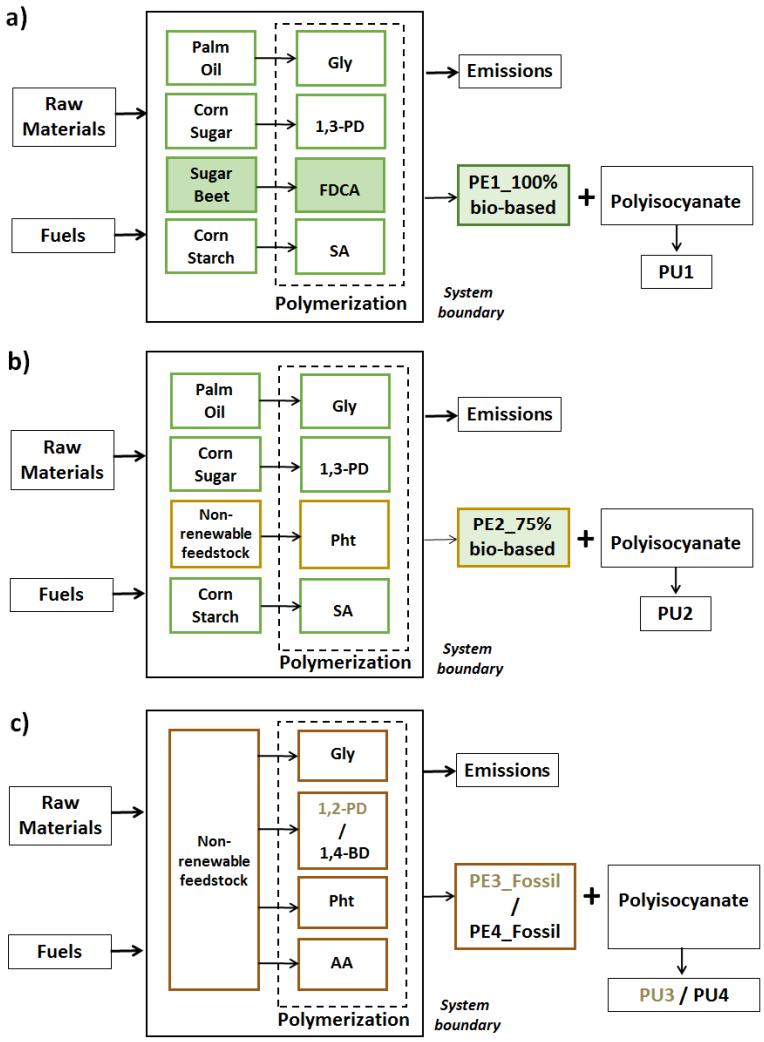

Figure 3. The system boundary of the different polyester binders. Green boxes represent the monomers from renewable resources for the bio-based polyester binders.

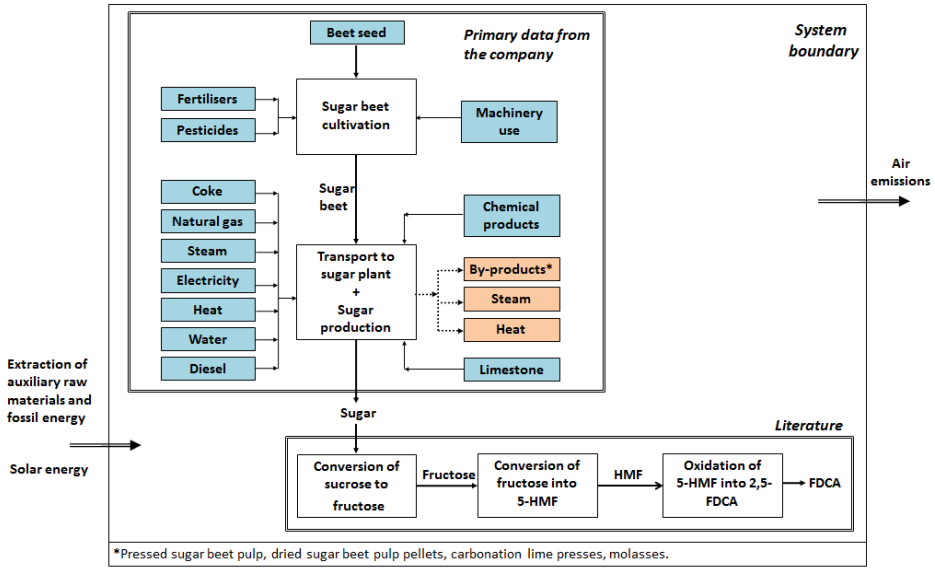

Figure 4. The system boundary of the FDCA production from sugar beet cultivation. Blue and orange boxes represent all the relevant inputs and outputs included in sugar beet cultivation and sugar production respectively.

3.3.2.1 Sugar production steps

The life cycle of sugar starts with beet cultivation. The warm and humid climate in addition to fertile soils, are perfect conditions for beet to grow due to the higher units of sugar obtained in this area of southern Sweden. The sugar found in beet is produced from the rays of the sun, water and carbon dioxide by photosynthesis. A sugar beet contains around 17.5 percent of sugar. The beet seeds are sown in March and in April and grow up until the harvest time, which starts in mid-September. The delivery of sugar beets is on-going until February and this period is known as the beet campaign. The production of biomass requires multiple operational steps, e.g. ploughing, sowing, fertilization and harvesting, which are shown in Figure 5. All the relevant inputs were included in for the beet cultivation and used in the farm

such as beet seeds, fertilisers, pesticides and machinery use (Figure 4). The latter includes manufacture of machinery, emissions of the phase of use, maintenance and use of fuel consumption. Its production was also included in the system. On the output side, emissions were also considered including nitrous oxide, nitrates, phosphates and carbon dioxide. Due to the large amount of rainfall in the region, irrigation water during the beet cultivation was not needed.

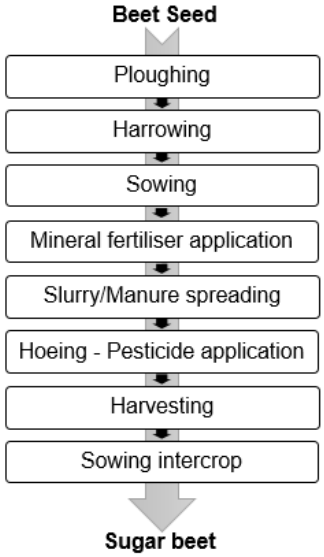

Figure 5. Scheme of the field work activities in the beet cultivation

After harvesting, the sugar beet is transported to the sugar mill where it is weighed and samples are taken to measure the sugar content and the amount of soil and stones present in the load. The beet is transported to the washing area where the first sub-process of the sugar production starts. This process is subdivided into eight sub-processes present in Figure 6. All the relevant inputs such as natural gas, diesel and coke production, heat, electricity, and steam, as well as water consumption and production of chemical products

were included for the sugar production and used in the mill (Figure 3). As for the water consumption input, due to the fact that the mill produces water, an insignificant contribution was present in the study. Consequently, the results obtained during the analysis were negligible. Waste solids were not considered in the system because they are not generated at the sugar mill. Emissions from fuels like carbon dioxide, methane, nitrous oxide, nitrogen oxides and sulphur dioxides were considered and included. In the washing area, large quantities of water are used and reused repeatedly to wash and handle the beet. Only a little water is added in the process since around a third part of this water evaporates in the evaporation process. A conveyor belt carries the clean beet to the slicing machine where it is cut into thin strips. The strips are taken to a diffusion device where the sugar is extracted in hot water. The resulting liquid obtained in this process is called raw juice. The remaining beet strips called beet pulp are pressed (pressed sugar beet pulp) and some parts are dried (dried sugar beet pulp pellets), which are molassed with approximatively 30% molasses. Then, they are used in the production of animal feed.

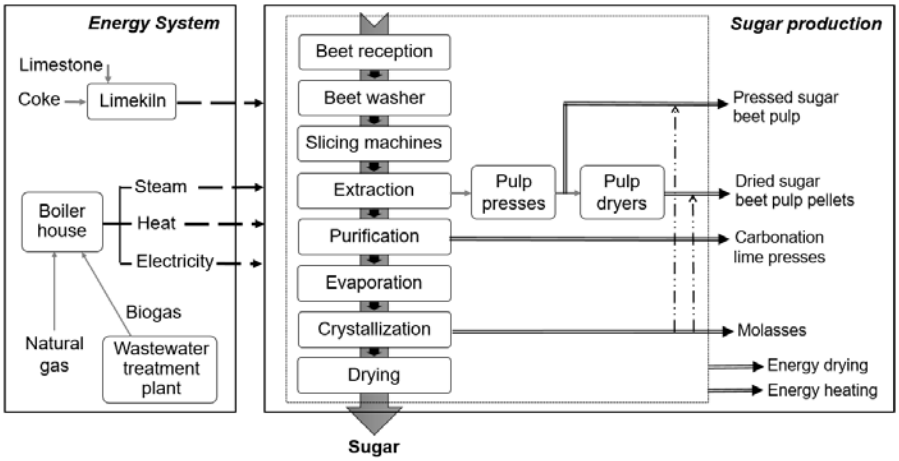

Figure 6. Scheme of sugar production and energy system at the sugar factory.

Purification of the raw juice takes place by adding slaked lime ($Ca(OH)_2$) and carbon dioxide (CO_2) to bind non-sugar substances together. Once the substances are filtered off, thin juice (pale yellow juice) remains with a sugar content of around 14 percent. The rest is mainly water. The filtered off lime is pressed and sold as soil conditioner (carbonation lime presses). Most of the remaining water (sugar beet contains around 75% water) is removed by evaporation in large vessels and then it is reused in the entire mill (thus Nordic Sugar is also water producing company). Thick juice with a high percentage of sugar is obtained (approximately 70 percent of sugar) but due to its high amount of water, still present in the juice, it is almost entirely removed by boiling it at a low pressure and under high temperature. A small amount of icing sugar is added to start the crystallization process since thick juice is now sufficiently concentrated to form crystals. This produces a mixture of sugar crystals and syrup called massecuite, which has a high sugar content. Sugar is extracted from the massecuite by a boiling process and it is centrifuged several times. The brown syrupy called molasses separated from the white sugar crystals is also used as animal feed. The white sugar is carefully washed out, scraped from the centrifuge, dried and saved. This is the final white sugar product. Finally, the sugar is stored in large silos ready to be packed for further transportation. At the sugar mill, an energy system supplies the sugar production. Electricity, steam and heat are produced in the boiler house by natural gas and biogas. Biogas is produced in the wastewater treatment plant. Normally, the electricity produced is not enough and it has to be bought from the grid to supply all the plant. The remaining steam (energy drying) is sold as drying animal feed and the remaining heat (energy heating) is sold to heat the houses that are close to the factory (district heating system nearby). In the lime kiln, the limestone is burned using coke as a solid fuel to produce $Ca(OH)_2$)

and CO_2, which are used in the purification part.

3.3.3 Data used in the study

As it is mentioned before in Table 1, all monomers (except FDCA) were selected according to their availability data in the Ecoinvent database version 3.2, and in the open literature for the study of life cycle on polyesters. As for FDCA production, in the two first steps (beet cultivation and sugar production), the analysis was performed with the most recent, primary and detailed data provided by a European country during the campaign of 2015. Emissions to air derived from crop management were calculated by the IPCC method[43] (2006) (IPCC 2006) to obtain the atmospheric emissions that are the precursors of climate change (carbon dioxide, nitrous oxide, methane). In the development of this calculation of emissions, some secondary data obtained from the literature[44] were used, as it is the case of the amount of nitrogen in animal manure, which was applied on the soil for sugar beet cultivation. Poultry manure with a 12.5 kg tot N/ton content, cattle manure with a 3.7 kg tot N/ton content and slurry pig with a 6.4 kg tot N/ton content. Emissions to water derived from crop management were based on literature data including regional specific climate and soil conditions and some assumptions were applied. The gross nitrogen leaching was estimated to be expressed as 30 kg N per hectare per year[45] and the gross phosphorous leaching was estimated to be expressed as 0.5 kg P per hectare per year[45]. The data used in the FDCA last 3 step's production (see Figure 3) were secondary obtained by Eerhart's work[28]. Some assumptions were needed in the conversion of fructose step for the impact category of GHG emissions. The energy that was considered was natural gas (same energy that was used in the sugar production step). Finally, all data were incorporated into the SimaPro LCA software, and into the

Ecoinvent database version 3.2 with an attributional system model that was used as a background source in some processes for FDCA production and the polyester binders. Whenever it was possible, models based on European technology (RER) were used within the system. However, some processes had models based only on the rest of the world's technology (ROW). In this case, they were used as a substitute to Europe's based models. The relevant data for the FDCA production is shown in Table 7. Inventory analysis for all polyester binders according to the composition is shown in Table 8. Finally, the inventory analysis for the sugar production is presented in Table 9.

Table 7. Relevant data on process data for 1 kg of FDCA production from beet cultivation.

GHG EMISSIONS:		
Sugar from beet (calculated)	0.70	kg CO_2eq / kg sugar
Fructose from sugar (assumption)	0.20	kg CO_2eq / kg fructose
FDCA from fructose (literature[28])	0.25	kg CO_2eq / kg FDCA
TOTAL GHG emissions FDCA from beet	**1.15**	**kg CO_2eq / kg FDCA**
NREU:		
Sugar from beet (calculated)	7.10	MJ / kg sugar
Fructose from sugar (literature[28])	3.90	MJ / kg fructose
FDCA from fructose (literature[28])	5.00	MJ / kg FDCA
TOTAL NREU FDCA from beet	**16.0**	**MJ / kg FDCA**

Table 8. Inventory analysis on process data for 1 kg of polyester productions. The data not shown in the table are from Ecoinvent. Energy refers the non-renewable energy use in each monomer.

Polyester binder	Input			Output		
	Materials			**Materials**		
PE1_100%	Gly	0.07	kg	PE1_100%	1.00	kg
	1,3-PD	0.35	kg			
	FDCA	0.40	kg			
	SA	0.20	kg			
	Energy			**Emissions to air**		
	Gly	x	x	Gly	x	x
	1,3-PD	21.80	MJ	1,3-PD	0.75	kg CO_2eq
	FDCA	6.15	MJ	FDCA	0.45	kg CO_2eq
	SA	6.80	MJ	SA	0.18	kg CO_2eq
PE2_75%	**Materials**			**Materials**		
	Gly	0.07	kg	PE2_75%	1.00	kg
	1,3-PD	0.35	kg			
	Pht	0.38	kg			
	SA	0.20	kg			
	Energy			**Emissions to air**		
	Gly	x	x	Gly	x	x
	1,3-PD	22.15	MJ	1,3-PD	0.75	kg CO_2eq
	Pht	x	x	Pht	x	x
	SA	6.65	MJ	SA	0.18	kg CO_2eq
PE3_Fossil	**Materials**			**Materials**		
	Gly	0.07	kg	PE3_Fossil	1.00	kg
	1,2-PD	0.33	kg			
	Pht	0.36	kg			
	AA	0.18	kg			
	Energy	x	x	**Emissions to air**	x	x
PE4_Fossil	**Materials**			**Materials**		
	Gly	0.06	kg	PE4_Fossil	1.00	kg
	1,4-BD	0.37	kg			
	Pht	0.36	kg			
	AA	0.18	kg			
	Energy	x	x	**Emissions to air**	x	x

Table 9. Inventory analysis on process data for 1 ton of sugar production from sugar beet cultivation.

Steps	Input			Output		
	Materials			**Materials**		
Sugar beet cultivation	Seeds	0.30	kg	Sugar beet	6.2	tons
	Fertilisers	0.26	ton	Emissions to air		
	Pesticides	0.33	kg	Nitrous oxide	0.62	kg
	Energy			Carbon dioxide	56.25	kg
	Machinery use[1]	1.2	ha	**Emissions to water**		
				Nitrate	2.90	kg
				Phosphate	0.05	kg
Transport to sugar plant + Sugar production	**Materials**			**Materials**		
	Sugar beet	6.2	ton	Sugar	1.00	ton
	Water	1.1	m^3	Pressed sugar beet pulp	0.16	ton
	Chemical products	1.9	kg	Pellets	0.04	ton
	Energy			Molasses	0.12	ton
	Diesel[2]	43.30	MJ	Carbonation lime P.	0.14	ton
	Transport[3]	434.70	tkm	Energy drying	0.14	GJ
	Natural gas	3.90	GJ	Energy heating	0.12	GJ
	Coke	0.26	GJ	**Emissions to air[4]**		
	Electricity	0.16	GJ	Carbon dioxide	0.25	ton
				Methane	0.01	kg
				Nitrous oxide	0.001	kg
				Nitrogen oxides	0.17	kg
				Sulfur dioxides	0.15	kg
				Emissions to water		
				Wastewater	7.03	m^3
				BOD	0.02	kg
				Total nitrogen	0.32	kg

[1]Manufacture of machinery, emissions of the phase of use, maintenance and use of fuel consumption are considered in agricultural stage.

[2] Internal transport trucks, bulk loaders bulk loading, forklifts transportation are included.

[3]Transport from farm to the factory.

[4]Those emissions are disaggregated from Ecoinvent database.

3.3.4 Comparison of the processing data with other sources from literature

Data concerning monomers selected for the 100% bio-based polyester binder were compared with other literature sources (Figure 7). Bio-based glycerine production (from palm oil) was compared with other glycerine production processes based on different biological feedstocks such as rape oil and soybean oil, taken from Ecoinvent[30,46]. All of them are based on global geographical coverage. The 1,3-PD production was compared with another 1,3-PD bio-based production taken from Urban and Bakshi's work[26] (2009). Both processes came from corn-derived glucose. The geographical coverage from Urban's work is based on U.S.A and Europe for DuPont's study[33] (2009). The process which was chosen to be compared in Urban and Bakshi's study was the bio-based 1,3-PD production with mass allocation in the process LCA study. For SA production, a comparative of three different processes was also analysed according to the data from Cok's study[27]. The three processes are direct crystallization (present study, SA-DC), electrodialysis (SA-ED) and ammonium sulphate (SA-AS) process. More recently[47] SA from algae feedstocks with a complete LCA analysis was described. However, SA is only a co-product in this process and the extrapolation of GHG and NREU data is not straightforward, so it was not possible to include it in the comparison. Finally, the FDCA production developed in this study was compared to two different processes obtained in Eerhart's study[28]. The difference between the processes (FDCA_1 and FDCA_2) to compare is the operating condition during the furanics conversion (temperatures between 200 ° C and 220 °C) and they are based on corn instead of beet.

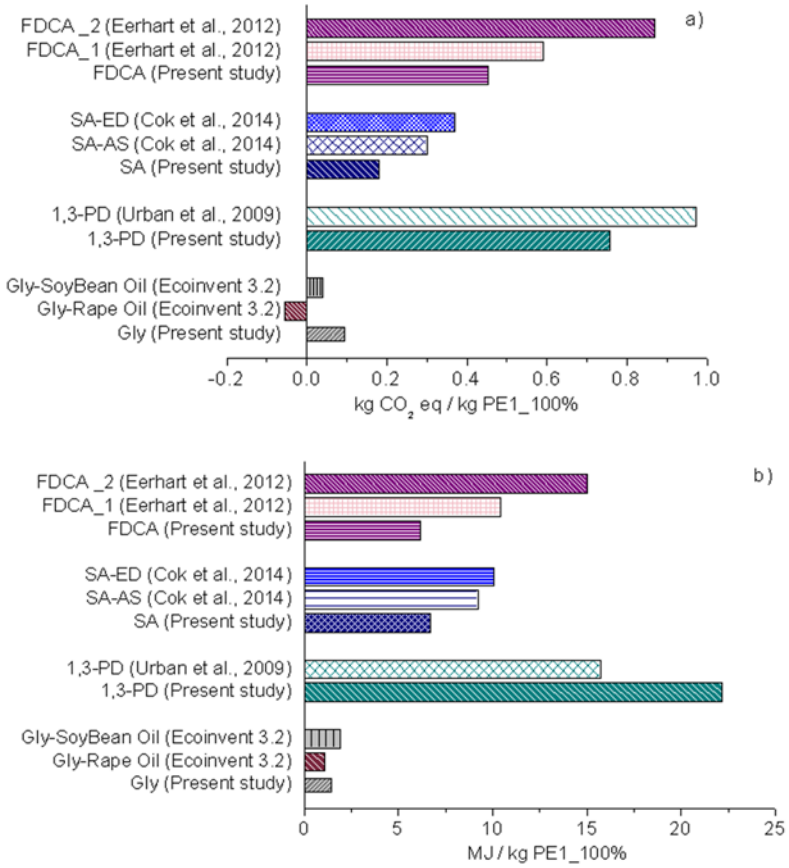

Figure 7. Comparison of the processing data with other sources from literature in bio-based Gly, SA, 1,3-PD and FDCA monomers: a) $kgCO_{2eq}$ / kg PE1_100% in terms of GHG emissions and b) MJ / kg PE1_100% in terms of non-renewable energy use.

In the case of Gly production the effect of different biological feedstock was noticed. A significant decrease of GHG emissions and NREU was observed by passing from palm oil feedstock to rape oil feedstock. The reduction of NREU was around 25%, and the decrease of the total GHG emissions was around 157%. The large difference derives from the CO2 from land transformation where the rape oil value is really low compared to the others (9.89-5 kg CO2 eq/kg PE1_100% for the Gly production with rape oil with respect to 0.220 and

0.223 kg CO2 eq/ kg PE1_100% for the Gly production with palm oil and soybean oil respectively). The reason is due to the change in land use in this process, which is not considered. Then, the impact on GHG performance for Gly production with rape oil is insignificant. A clear example of the importance to consider the land transformation in LCA studies since it refers to changing one kind of land cover to another. In the case of the Gly production from soybean oil feedstock a higher NREU value by around 24% for palm oil and 43% for rape oil was observed. Regarding GHG emissions, a reduction by around 58% was observed compared to Gly production from palm oil feedstock. This fact can be explained considering that biogenic CO_2 is lower for the Gly production from soybean oil feedstock which is around 0.003 kg $CO_{2\ eq}$/kg PE1_100% than for Gly production from palm oil feedstock which is around 0.13 kg $CO_{2\ eq}$/kg PE1_100%. When comparing the two alternative routes for 1,3-PD production, a reduction of GHG emissions by around 22% and an increase of non-renewable energy total use by around 30% was observed for 1,3-PD used in the present study in comparison to Urban's study. However, the reason for this discrepancy is not clear because any of the studies reveal the specific data used. As for SA (present study, SA-DC) production, a significant reduction was observed with respect to the other alternatives in terms of GHG emissions and NREU.

This comparison shows the different-case scenarios of each bio monomer in terms of GHG emissions and NREU. For SA production, the direct crystallization process (SA-DC) was chosen as base case in our study because it has more benefits than the other methods. In the Gly case, notwithstanding rape oil feedstock presented better results, it was decided to work with palm oil since it is one of the oil grades with higher production volume together with the soybean oil. As for 1,3-PD production, DuPont's study (2009) was

chosen due to the fact that it presents a geographical coverage based on the European Union (EU). Finally, in respect of FDCA production, a significant reduction in terms of GHG emissions (between 23-48%) and NREU (between 40-60 %) was obtained in our study (primary data) compare to the literature.

3.3.5 Allocation

Allocation was required in the sugar production phase for the obtainment of FDCA; the procedure defined by ISO 14044[39] is followed. Seven output flows are obtained in the sugar production, which are white sugar, molasses, dried sugar beet pulp (pellets), pressed sugar beet pulp, carbonation lime presses and energy as steam (energy drying) and heat (energy heating) (see Figure 6). Allocation of impacts are a very important methodological issue of LCA practitioners and its definition is 'Partitioning the input or output flows of a process or a product system between the product system under study and one or more other product systems' (ISO 14040-14044). Two different types of allocations, economic and energy, were studied and their allocation applications for the seven outputs are shown in Table 10. Both allocations were selected by some fundamental reasons: in the energy case, it was assessed due to the fact that sugar mills globally exist, which are bioethanol producers and therefore, an energetic purpose makes it a suitable alternative for this study even though in our specific case it is not produced. In the economic case, it was evaluated by its simplicity and ability to illustrate the properties of complex systems notwithstanding the prices may change over the years and an extended estimated price to a longer period and periodic controls may be needed to enhance its credibility. The data used for energy allocation (EnA) was completely primary. In the case of economic allocation (EA), secondary data were needed for energy outputs obtained from the

literature[48-50]. The rest of outputs were primary. EA was assessed in accordance with an estimated average price from the last ten years for sugar and the last five years for by-products that are produced at the factory. EnA was developed according to the amount of energy as low heating value in sugar and the other by-products. Carbonation lime presses output was excluded from the allocation analysis due to its insignificant value for economic allocation and lack of energy content for energy allocation. The price and energy value for each product were multiplied by the amount in tons of dry matter of each product to obtain the allocation percentage.

Table 10. The different percentages of the two applied allocations in sugar production from beet cultivation.

Product/ by-products	Economic allocation (EA) (%)	Energy allocation (EnA) (%)
Sugar	90.0	82.0
Dried sugar beet pulp (pellets)	5.0	11.0
Pressed sugar beet pulp	0.8	0.4
Molasses	3.5	6.0
Energy drying	0.5	0.7
Energy heating	0.2	0.6

The two allocations were compared during the study and no remarkable differences were observed as it is shown in Table 9 (percentage of sugar around 82-90%). For that reason, regarding FDCA production, the results from economic allocation in sugar production phase were selected and used as base case due to its more effective way to attribute mass and energy outputs to the same unit.

3.4 RESULTS AND DISCUSSIONS

3.4.1 Solubility tests on 100% bio-based polyester binder

In coating technology, a dilution solvent is normally needed in order to reduce the viscosity and to allow a correct film forming mechanism. Dilution with butyl acetate (BA) solvent was adequate for PE2_75%, PE3_Fossil and PE4_Fossil formulations. However, more polar solvents were needed for PE1_100% containing the FDCA monomer. Among the various solvents tested such as propylene carbonate (PPC), acetonitrile (AN), acetone (AC), tetrahydrofuran (THF) and ethyl acetate (EA), PPC was chosen as an optimal solution (see Figure 8). Moreover, PPC is considered an environmentally friendly solvent for the development of the sustainable coating[51]. The solubility parameter (δ) of the PCC solvent is 27.2 δ/MPa$^{1/2}$ whereas the BA solvent has a 17.4 δ/MPa$^{1/2}$ of solubility parameter[52]. Those different parameters suggest that PE1_100% binder is significantly more polar than the other three resins.

Figure 8. Solubility test on PE1_100%

3.4.2 Characterization on polyester binders

The glass-transition temperatures (Tg) of the copolyesters is represented in Figure 9. The PE1_100%, PE2_75% and PE4_Fossil binders showed a more flexible resin compared to PE3_Fossil as they contain linear chain extenders

like 1,4 BD and 1,3 PD without methyl side groups. According to the substitution of Pht with FDCA for bio-based polyesters (PE1_100% and PE2_75%), a small difference was observed, being less flexible PE_100% (- 8 °C).

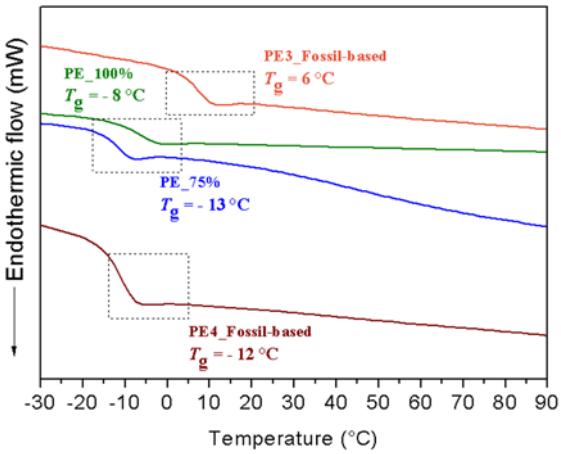

Figure 9. Differential scanning calorimetry curves of all polyester binders.

The molecular weight of PE samples was evaluated by gel permeation chromatography (GPC) analysis and it is reported in Table 11. The number average molecular weight (Mn) of the polyesters ranged from 1285 to 1775 g/mol and the weight average molecular weight (Mw) from 2578 to 4328 g/mol with a polydispersity index (PDI) between 1.8 and 2.5. All these values are suitable given the nature of polycondensation polymers. The viscosity values were measured for all PEs (70% dry) as a control test to develop the formulations for the coating's preparation (Table 11). A pseudoplastic behaviour for all of them was observed and a more viscous material on PE3_Fossil and PE1_100%, which were compensated with more solvent in the coating preparation.

Table 11. Molecular weights (Mn and Mw), polydispersity index (PDI) and viscosity (η) for all PE binders.

	Mn [g/mol]	Mw [g/mol]	PDI	η (Pa s)
PE1_100%	1775	3138	1.8	17
PE2_75%	1285	2578	2	nd
PE3_Fossil	1726	4328	2.5	26
PE4_Fossil	nd	nd	nd	5

3.4.3 Polyurethane (PU) coatings characterization

3.4.3.1 Differential Scanning Calorimetry (DSC) analysis

The thermal transitions of the crosslinked PU coatings are shown in Figure 10. Substituting the Pht monomer with FDCA monomer, a stiffer PU1 polymer backbone was formed, with a Tg value of + 14°C compared to + 3°C for PU2 (from PE2_75%). It is due to the fact that the FDCA structure is more symmetric and regular, which makes the interaction between the polymer's chains became stronger and therefore a raising of Tg was shown. In addition, it can be shown that the highest Tg is around + 34°C, corresponding to the fossil-based PU3 coating, containing 1,2-PD as a chain extender. PU1, PU2 and PU4 coatings only contain linear chain extenders like 1,4 BD and 1,3 PD (without methyl side groups) and therefore more flexible polymer structures were formed, showing a Tg value of 2 °C for PU4 and 3°C for PU2.

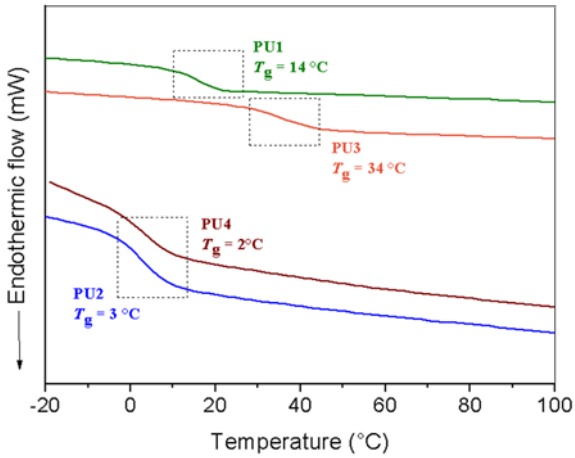

Figure 10. Differential scanning calorimetry curves of all PU coatings.

3.4.3.2 Buchholz Indentation tester – Hardness test

As the indentation behaviour is concerned in Table 12, the PU1 coating with FDCA-based polyester binder showed the highest hardness between the bio-based coatings (PU1 and PU2) thanks to the substitution of Pht with FDCA, which is in agreement with its higher Tg (14 and 3 °C respectively). However, the 100% fossil-based PU3 coating presented the highest hardness of all with a value of 91, which is in agreement with the highest Tg (+ 34°C).

Table 12: Hardness measurements onto glass using Buchholz Indentation tester.

	Average values [ά b]
PU1	83.3 ± 0.1
PU2	54.1 ± 0.2
PU3	91.0 ± 0.4
PU4	64.6 ± 0.2

3.4.3.3 Optical Contact Angle (OCA)- surface wettability

In respect of surface wettability, the contact angle data reported in Table 13 showed a good hydrophobic character in PU2 and PU4 coatings, without an

apparent effect of polyester composition. As far as PU1 coatings with FDCA-based polyester binder is concerned, a more hydrophilic character (80 °C) was observed. The reason may be caused by the more polar character of FDCA with respect to phthalic structures. In Figure 11, the images of contact angle measurements for all PU coatings are shown.

Table 13: Contact angle measurements onto glass using water.

	Average values [°]
PU1	80.0 ± 2.1
PU2	88.0 ± 3.4
PU3	83.0 ± 1.8
PU4	89.0 ± 2.6

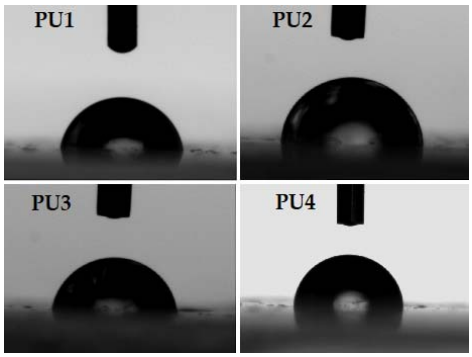

Figure 11. Imagines of contact angle measurements using water on PU coatings.

3.4.3.4 Pull-Off Adhesion testing

The adhesion was evaluated for coatings supported onto glass and chromated aluminium. As shown in Table 14, all PU coatings applied onto glass substrates showed an excellent adhesion with the highest bonding strength observed on PU1 coating (> 8 MPa), which is in agreement with its hydrophilic character. The measurements of PUs on aluminium substrate

showed a moderately good adhesion with the highest adhesion strength (around 1.8 MPa) found in PU4.

Table 14: Adhesion measurements onto glass and chromated aluminium using pull-off tester.

	Average values [MPa]	
	Glass	**Chromated Al**
PU1	> 8	1.3 ± 0.3
PU2	6.4 ± 1.2	1.0 ± 0.2
PU3	7.3 ± 2.3	1.1 ± 0.4
PU4	5.9 ± 2.1	1.8 ± 0.2

3.4.3.5 Surface characterization- OCA analysis

Surface energies and its polar and dispersive components are reported in Table 15. Values were estimated by Wu's harmonic-mean method. It is worthwhile to notice that for all PU coatings the dispersive component is predominant with respect to the polar one, which is related to the urethane groups. In addition, PU1 showed the highest surface tension value by around 43 mN/m constituting greater cohesive forces and therefore greater forces of adhesion, which is in agreement with the adhesion test results onto glass.

Table 15: Surface tension and its components determined for the four PU coating substrates using Wu method calculation.

Samples	SFT Polar [mN/m]	SFT Dispersive [mN/m]	SFT Total [mN/m]
PU1	9.7	33.6	43.3
PU2	6.7	32.2	38.9
PU3	8.9	32.8	41.7
PU4	5.2	33.5	38.6

3.4.3.6 Hydrolytic stability test

Finally, the hydrolytic stability of the PU coatings was investigated. Hydrolytic stability in polyester-based polyurethanes is known to be better in binders containing glycols with low concentration of ester groups, that is to say, glycols with longer hydrocarbon chains[53]. The hydrolytic stability in PU films was monitored over 30 days of continuous exposure to water at + 60°C. A detailed visual inspection excluded the formation of blisters, which is an indication of high adhesion onto the substrate, and overall, stability of the polymer network in the tested conditions. A more quantitative evaluation was made through contact angle and hardness measurements every 5 days, and results are shown in Figures 12 and 13. Results are expressed as percentage retention of the property over the time. As it is shown in Figure 12, a constant decrease of hydrophobicity is observed in all PU films throughout the 10th day of testing. After the 10th day, the superficial changes are more marked, as the large standard deviations showed. In particular, the PU1 coating with FDCA-based polyester binder showed a high decrease of hydrophobicity after the 25th day. At the end of the test, on the 30th day, the PU1 coating showed 15% less hydrophobicity than PU2, PU3 and PU4. In Figure 13, it is interesting to observe that there was an increase of hardness especially in PU3 coatings, whereas PU4 seems more stable. After one month of exposure, all those three PU coatings retained more than 90% of their initial hardness; it is worth underlining that the partial bio-based PU2 coating (from PE2_75%) was remarkably stable and it even tends to increase slightly its hardness upon ageing. The reason of this latter effect is unclear, possibly it is due to some morphological changes of the polyurethane induced by ageing (like a microphase segregation with formation of harder urethane domains). In any case, hydrolytic degradation can be excluded, because it would have involved

a dramatic decrease of molecular weight and consequently, a strong hardness decrease. This is particularly positive in view of potential application of bio-based PUs as protective coatings. Finally, PU1 coating showed a fast decreased of hardness with a value of 40% less after the 5th day of monitoring by indentation hardness test and it is maintained during the following 30 days. This tests may confirm the hydrophilic character of the PU1 based on FDCA. A hydrophilic material can absorb water faster by swelling the material and therefore, decreasing its hardness.

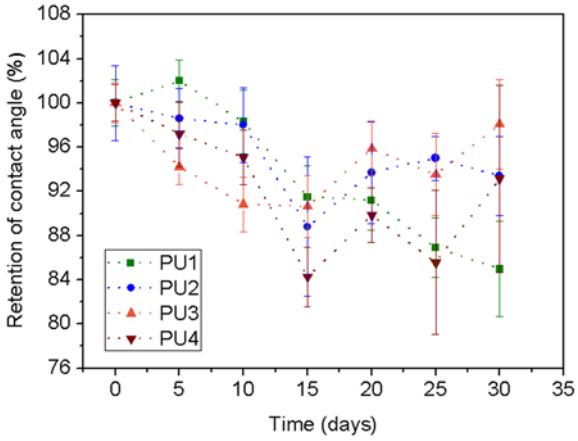

Figure 12. Hydrolytic stability monitoring by contact angle test.

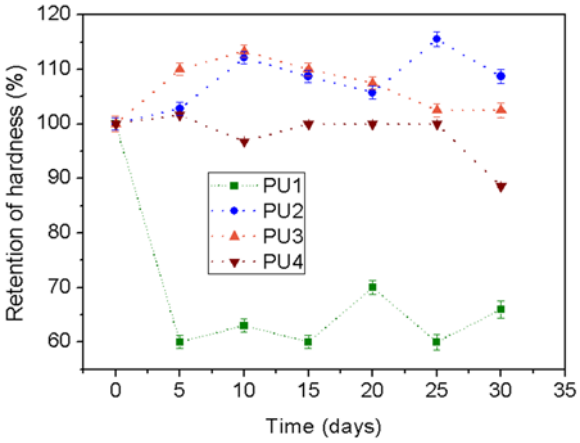

Figure 13. Hydrolytic stability monitoring by hardness test.

3.4.4 LCA analysis

The total NREU and GHG emissions of the four cases studied were evaluated for 1 kg of polyester, including the contribution of the choice of the monomer and the contribution of the polymerization process to produce the binder, which was the same for all polyesters considered.

Figure 14 shows the total impact of the GHG emissions with a value of 2.75 kg CO_2 eq/kg for PE_75% whereas PE_100% has a lower impact with a value of 1.75 kg CO_2 eq/kg. Both show a meaningful reduction compared to fossil-based polyesters (PE3_Fossil and PE4_Fossil) by around 67% and 79% respectively (8.4 kg CO_2 eq/kg and 8.1 kg CO_2 eq/kg). The substitution of the phthalic monomer with FDCA into the PE_100%, led to a significant reduction in the latter by around 36%.

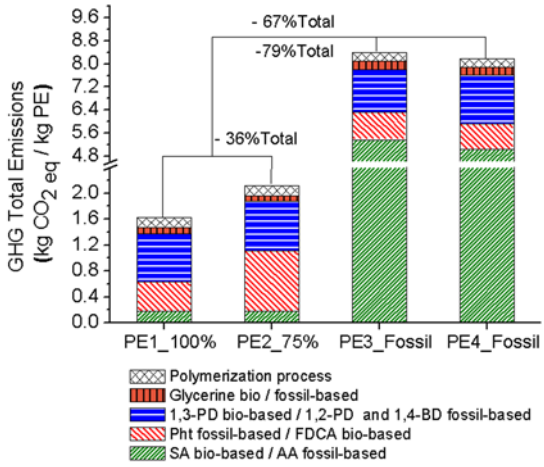

Figure 14. Total impact of the GHG emissions for PE_100% bio-based compared to PE_75% bio-based and PE3 / PE4_Fossil-based.

Figure 15 shows the total NREU of all polyesters where PE_100% presents the lowest reduction with a value of 39 MJ/kg, a 38% less of the total NREU than PE_75% with the substitution of the FDCA monomer and PE3 / PE4_Fossil (-

60%). Finally, the polymerization process showed a low contribution to the total cradle-to-factory gate emissions. Consequently, the next point of the study was focused on the analysis of the monomer mixture contributions showing which monomers had a bigger impact in terms of GHG and NREU.

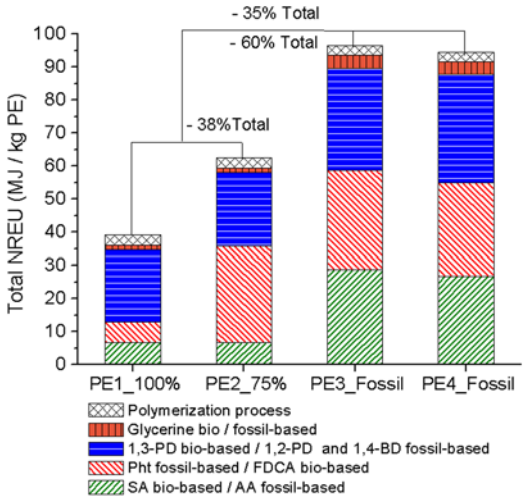

Figure 15. Total NREU for PE_100% bio-based compared to PE_75% bio-based and PE3 / PE4_Fossil-based.

3.4.4.1 Environmental impact assessment between the monomers

The monomer mixture contributions were analysed for each monomer family. Concerning the polyols family, bio-based glycerine (from palm oil) showed a significant reduction on the total GHG emissions by around 64% and non-renewable energy use by around 63% with respect to glycerine from epichlorohydrin (Figure 16). In Figure 17, it can be observed that the conversion from fossil-based 1,4-BD to fossil-based 1,2-PD produced only a slightly effect in terms of GHG emissions (-12%), but almost the same total NREU consumed (-6%). By contrast, it can be noticed that the change from fossil-based aliphatic diols to chemically similar bio-based aliphatic diols such

as 1,3-PD caused a remarkably lower impact for GHG emissions and NREU, namely 1,3-PD is featured with around -30% with respect to 1,4-BD/1,2-PD on non-renewable energy consumption, and around -53% compared to 1,4-BD/1,2-PD as far as GHG emissions are concerned.

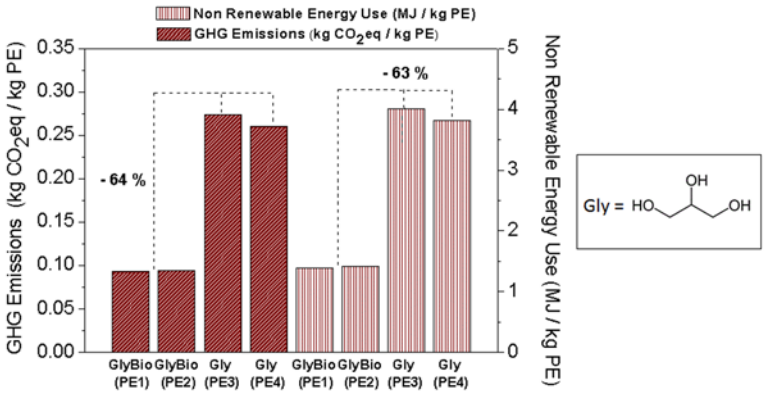

Figure 16. Comparison between bio-based glycerine (from palm oil) and fossil-based glycerine monomers in terms of GHG emissions and NREU.

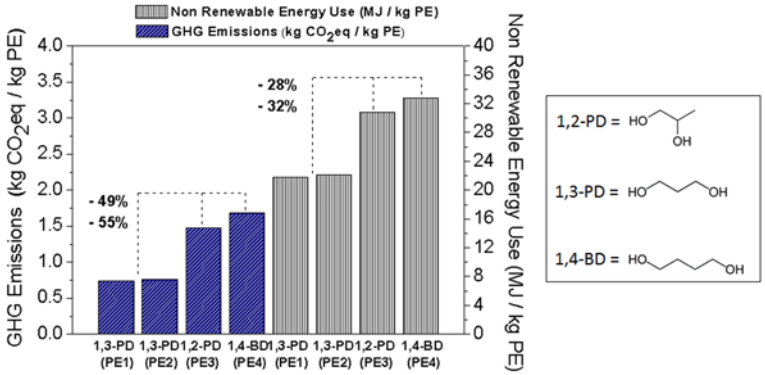

Figure 17. Comparison between diol monomers in terms of GHG emissions and NREU.

As for aromatic diacids (Figure 18), a marked decrease of GHG emissions and NREU was observed by changing the fossil-based aliphatic diacid with

succinic acid obtained from renewable sources. The reduction of the total GHG emissions were around 96%, and the decrease of NREU was around 75%. Finally, in aromatic diacids, the substitution of phthalic anhydride with FDCA showed a significantly low impact on the total GHG emissions by around 53%, and a remarkably low impact on the total non-renewable energy use by around 79% (Figure 19).

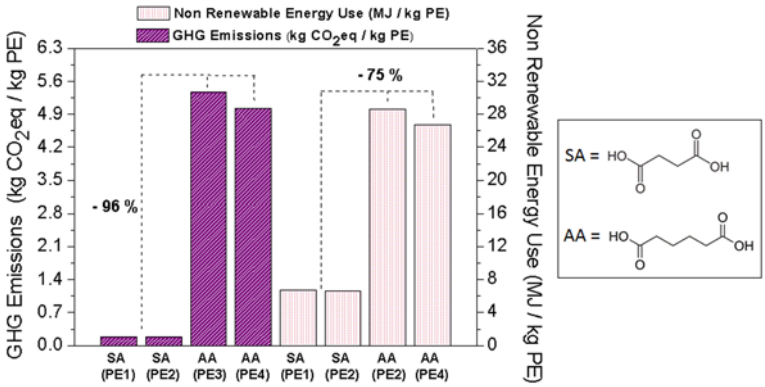

Figure 18. Comparison between adipic acid and succinic acid monomers in terms of GHG emissions and NREU.

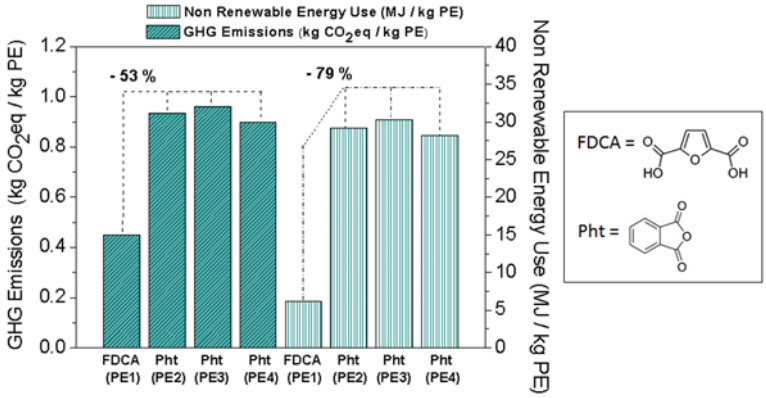

Figure 19. Comparison between phthalic anhydride and 2,5-furandicarboxylic acid monomers in terms of GHG emissions and NREU.

3.4.4.2 Environmental impacts on sugar production from beet cultivation

Contributions of sugar production from sugar beet cultivation in terms of non-renewable energy total use (NREU), total GHG emissions, total freshwater eutrophication and total marine eutrophication were evaluated for the reference of 1 ton sugar for the two allocations studied. The total emissions are divided into two major phases: sugar beet cultivation and the transport of sugar beet to the plant and the sugar production. In addition, the contribution percentage of the all multiple operational steps of the sugar production process was also assessed in the analysis. Emissions from sugar beet cultivation, machinery used in agricultural stage and raw materials production derive from the cultivation phase. Beet transport to the sugar factory, energy consumed and chemical products production derive from the sugar production phase. As it was mentioned before, the water consumption input had an insignificant contribution in the system due to the fact that the mill produces water. Therefore, this results obtained were not included during the analysis. Figure 20 shows the phosphorus in phosphate form in the freshwater with a total value of 0.19 kg PO_4^{3-}eq/ton sugar for the economic allocation and 0.18 kg PO_4^{3-}eq/ton sugar for energy allocation where the 53% of the total impact corresponds to sugar beet cultivation and the 47% of the total impact corresponds to sugar production. It should be noted that those emissions do not have a big impact on water due to clay soil, the dominating soil type in the southwest of Sweden, which reduces the phosphorus leakage. In Figure 21, nitrogen in nitrate form. The total NO_3^- emission equivalent to the economic allocation presented a value of 3.2 kg NO_3^-eq/ton sugar and almost the same value for energy allocation (3.0 kg NO^{3-}eq/ton sugar). The

biggest impact of this total came from the sugar beet cultivation phase. In fact, the figure 21b also shows that the 79% of these total emissions (90%) derived from the emissions to water as a consequence of leaching formation. The reason is the big amount of nitrogen used in fertilizers. The rest of the steps showed a lower percentage of 9% being less representative.

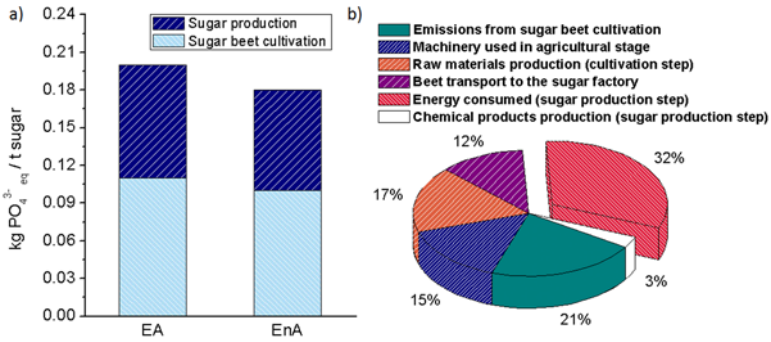

Figure 20. Total impact of phosphate emission (PO_4^{3-}) equivalents caused in freshwater eutrophication in sugar production from sugar beet cultivation for all allocations divided into the major phases and the total PO_4^{3-} contribution percentage of all the multiple operational steps of the sugar production.

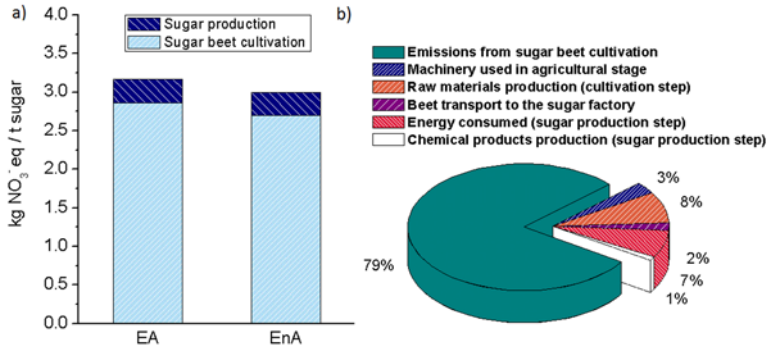

Figure 21. Total impact of nitrate emission (NO_3^-) equivalents caused in marine eutrophication in sugar production from sugar beet cultivation for all allocations divided into the major phases and the total NO_3^- contribution percentage of all the multiple operational steps of the sugar production.

Figure 22 shows the total impact of the GHG emissions in sugar production from sugar beet cultivation with a value of 670 and 708 kg CO_{2eq}/ton sugar for energy and economic allocation respectively. It is noteworthy that, those total impacts belong to 52% of the sugar beet cultivation phase and 48% to the production phase as can be observed in Figure 22. At a more detailed level (see Figure 22b), it can be noted that the biggest impact came from the fossil energy consumed in the sugar production phase with a 39% followed by the emissions to air during the process of the cultivation phase with 28%. In addition, the most important precursor emissions originated from climate change are carbon dioxide (CO_2), nitrous oxide (N_2O) and methane (CH_4) being the latter the less representative one, which represented 67%, 29% and 4% of the total emissions respectively. The CO_2 emissions were mainly derived from heat production representing 46% of the total CO_2 emissions whereas the N_2O emissions were principally originated from the emissions to air from sugar beet cultivation (21.5% of the total GHG emissions).

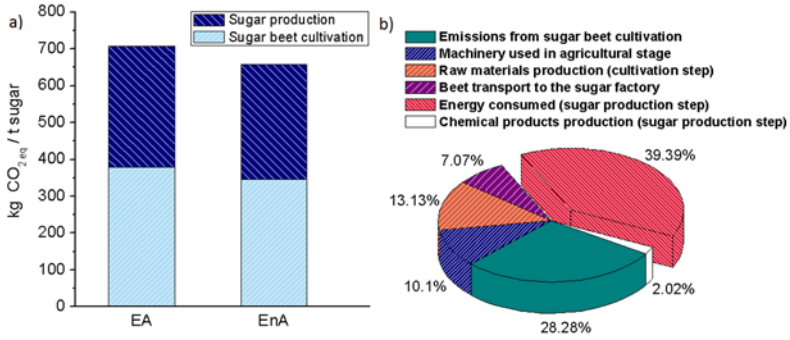

Figure 22. Total impact of GHG emissions in sugar production from sugar beet cultivation for all allocations divided into the major steps and the GHG contribution percentage of all the multiple operational steps of the sugar production.

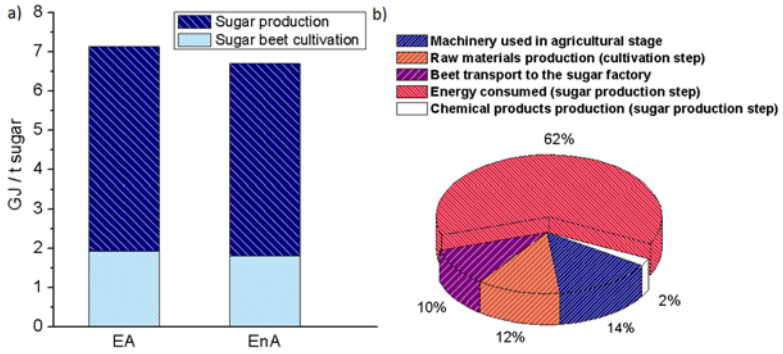

Figure 23. The total of NREU in sugar production from sugar beet cultivation for all allocations divided into the major phases and the NREU contribution percentage of all the multiple operational steps of the sugar production.

Finally, the total NREU in the sugar production from sugar beet cultivation into the major phases is observed in Figure 23 with a value of 6.70 and 7.10 GJ/ton for energy and economic allocations. As it is emphasised in the figure, the biggest consumption derived from the sugar production phase represented by 74% of the total consumption, and which is caused mainly by the natural gas production (62% of this 74% total). At a more detailed level of each step of the system, the use of machinery in the agricultural stage, production of raw materials used in the agricultural stage and the beet transport to the factory represent around 12% of the total consumption. The production of chemical products in the production step only show a 2% (Figure 23b).

3.4.4.3 Sensitivity analysis

A sensitivity analysis for all polyesters was performed with the aim of assessing the reliability of the results and conclusions of the present work. Modifications on the calculation of category indicator results were introduced with the purpose of observing how much were they affected. These

assumptions were based on the calculation methodology, whose aim was to compare the Greenhouse Gas Protocol (GHG protocol) method[54] to the IPCC 2013 Global Warming Potential with a timeframe of 100 years (100a) (v1.0) method[55] for the case of GHG emissions. In relation to NREU, the aim was to compare the Cumulative Energy Demand (CED) method[40] to the IMPACT 2002+ (v2.12) method[56] taking the impact of the non-renewable energy in the case of the last method. A deviation between the different methods was calculated by subtracting the total impacts values of each monomer.

In Table 16, the calculation methodology between the GHG protocol and IPCC 2013 GWP 100a methods in all four 4-monomers polyester showed small differences. All the deviations were less than 0.42. As far as aliphatic diols (1,4-BD/1,2-PD/1,3-PD) and aromatic diacid (Pht/FDCA) are concerned, the calculation of the total GHG emissions resulted less affected by the chosen methodology.

Table 16a. Sensitivity analysis (GHG protocol- IPCC 2013 GWP 100a) for PE1_100% and PE2_75%.

kg CO_2 eq / kg PE	**PE1_100%**			**PE2_75%**		
	GHG protocol	**IPCC 100a**	**Deviation**	**GHG protocol**	**IPCC 100a**	**Deviation**
SA	0.18	0.18	*0.00*	0.18	0.18	*0.00*
Pht FDCA	0.45	0.45	*0.00*	0.93	0.95	*- 0.02*
1,3PD	0.74	0.74	*0.00*	0.76	0.75	*0.01*
GlyBio	0.09	0.25	*- 0.16*	0.09	0.26	*- 0.17*

Table 16b. Sensitivity analysis (GHG protocol- IPCC 2013 GWP 100a) for PE3_Fossil and PE4_Fossil.

kg CO_2 eq / kg PE	PE4_Fossil			PE3_Fossil		
	GHG protocol	**IPCC 100a**	**Deviation**	**GHG protocol**	**IPCC 100a**	**Deviation**
AA	5.03	4.63	*0.40*	5.37	4.95	*0.42*
Pht	0.90	0.92	*- 0.02*	0.96	0.98	*- 0.02*
1,4BD 1,2PD	1.68	1.70	*- 0.02*	1.48	1.50	*- 0.02*
Gly	0.26	0.26	*0.00*	0.27	0.28	*- 0.01*

In the case of bio-based glycerine (see Table 16a), there was a significant increase in the total GHG emissions by around 65% with the IPCC 2013 GWP 100a method. This is due to the fact that the IPCC method does not take into account the CO_2 uptake in its calculation. The bio-based monomer glycerine has a greater impact on the cultivation process than the others (see Table 16b). In the case of AA with the IPCC 2013 GWP 100a method, a small decrease in the total GHG emissions was present (around 8%). This is because the IPCC 2013 GWP 100a method characterization factor for the nitrous oxide emission is lower than the GHG protocol method characterization factor. Then, the total GHG emission is slightly lower in IPCC 2013 GWP 100a method with respect to the GHG protocol method.

Table 17a. Sensitivity analysis (CED - IMPACT 2002+) for PE1_100% and PE2_75%.

MJ/kg PE	PE1_100%			PE2_75%		
	CED	IMPACT 2002+	Deviation	CED	IMPACT 2002+	Deviation
SA	6.80	6.80	*0.00*	6.67	6.67	*0.00*
Pht FDCA	6.14	6.14	*0.00*	29.19	29.10	*0.09*
1,3PD	21.80	21.80	*0.00*	22.18	22.18	*0.00*
GlyBio	1.40	0.53	*0.87*	1.42	0.54	*0.88*

In Table 17, the comparison between the CED and IMPACT 2002+ methods in all the four 4-monomers polyester showed some differences. Deviations showed a maximum value of 0.88 among all of them. Aliphatic diols (1,4-BD/1,2-PD/1,3-PD), aliphatic diacids (AA/SA) and the aromatic diacid (FDCA/Pht) showed similar values with regards to the calculation methodology in the NREU. By comparison, for the bio-based glycerine (according to the IMPACT 2002+ method) the total NREU decreased by over 62%. This is because in the IMPACT 2002+ method, the non-renewable biomass value is not taken into account.

Table 17b. Sensitivity analysis (CED - IMPACT 2002+) for PE3_Fossil and PE4_Fossil.

MJ/kg PE	PE4_Fossil			PE3_Fossil		
	CED	IMPACT 2002+	Deviation	CED	IMPACT 2002+	Deviation
AA	26.78	26.80	*- 0.02*	28.61	28.60	*0.01*
Pht	28.14	28.10	*0.04*	30.03	30.00	*0.03*
1,4BD 1,2PD	32.83	32.80	*0.03*	30.84	30.90	*- 0.06*
Gly	3.82	3.81	*0.01*	4.01	4.01	*0.00*

3.5 CONCLUSIONS AND FUTURE PERSPECTIVES

Different polyester binders suitable as intermediates to produce polyurethane coatings were designed, synthesized and technologically characterized. Monomers derived from both conventional (oil based) and renewable sources were used. The different physical properties of the coatings suggest potentially differentiated applications. The technological evaluation showed a stiffer PU1 coating (from PE1_100%) and a more hydrophilic character leading not only to better adhesion but also to a more moisture-sensitive surface. Potential applications in the field of metal coating may be interesting (coil coating, automotive), especially as intermediate layers/primers where the high adhesion of the material and recoatability are needed. The harder PU3 coating (from PE3_Fossil) is more scratch resistant and could be proposed as a mechanically protective coating in the automotive or furniture sectors. However, softer PU4 and PU2 materials are more suitable as candidates for metal coil coatings, where an excellent post-cure flexibility and formability of the painted metal strip are needed. A further improvement for the FDCA-based coating (PU1) may be counterbalanced with other more hydrophobic monomer which compensates its hydrophobicity.

The LCA methodology was applied for the evaluation of environmental impacts related to the production of all polyester binders. In particular, the monomer mixture contributions were analysed for each monomer family. The introduction of a fraction of monomers from renewable sources may significantly reduce the total GHG emissions and the total NREU. More specifically, in the replacement of adipic acids (a C_6 aliphatic diacid) with the relatively similar succinic acid (a C_4 aliphatic diacid), it was observed a total of GHG emissions by around -96% and a total of NREU ones by around -75%.

In the case of the substitution of the Pht monomer with the FDCA monomer, the total of GHG emissions and the total of NEHRU ones were reduced by around -96% and -75% respectively. As for diol monomers, the introduction of 1,3-PD monomer showed a significant reduction (≈52% in terms of GHG emissions and 30% in terms of NREU) compared to 1,2-PD and 1,4-BD. In the case of the introduction of bio-based glycerine, the reduction was remarkable in terms of GHG emissions (-64%) and NREU (-63%). According to the polymerization process, a very low contribution to the total cradle-to-factory gate emissions was shown. Overall, the evaluation of environmental impacts related to the complete production of the PE_100% binder compared to the other three PEs demonstrated this significant reduction in terms of GHG emissions (-79% compared to fossil-based polyesters and -36% compared to PE_75%) and in terms of NREU (-60% compared to fossil-based polyesters and -38% compared to PE_75%). In addition, the sensitivity analysis for all PEs based on the calculation methodology showed a few differences in the total results. Finally, the environmental impact study on the biomass (sugar beet) attested that economic and energy allocations did not show remarkable differences in the impacts. In terms of eutrophication, it was observed that the big impact of the total NO_3^- emissions equivalent came from the emissions to water as a consequence of leaching formation during the beet cultivation. As for the total PO_4^{3-} emission equivalents, the biggest impact derived from the energy consumed in the sugar production phase. However, those total emissions do not have a big impact on water since the soil is formed by clay (typically from southwest of Sweden) and it may reduce the phosphorus leakage.

However, those results are preliminary, as other environmental burdens are not covered in this study. A further improvement of environmental benefits

in this sector related to the primary data needed to refine LCA calculations including other impact categories like eutrophication, which are relevant for all products derived from biomasses and biorefinery processes.

3.6 REFERENCES

1. Zia KM, Bhatti HN, Ahmad Bhatti I (2007) Methods for polyurethane and polyurethane composites, recycling and recovery: A review. React Funct Polym 67: 675-692.

2. Benyahya S, Boutevin B, Caillol S, Lapinte V, Habas JP (2012) Optimization of the synthesis of polyhydroxyurethanes using dynamic rheometry. Polym Int 6:918-925.

3. Pfister DP, Xia Y, Larock RC (2011) Recent advances in vegetable oil-based polyurethanes. ChemSusChem 4:703-717.

4. Vilela C, Sousa AF, Fonseca AC, Serra AC, Coelho JFJ, Freire CSR, Silvestre AJD (2014) The quest for sustainable polyesters – Insights into the future. Polym Chem 5:3119-3141.

5. Helou M, Carpentier J-F, Guillaume S (2011) Poly(carbonate-urethane): an isocyanate-free procedure from a,x-di(cyclic carbonate) telechelic poly(trimethylene carbonate)s. Green Chem 13:266-271.

6. Annunziata L, Diallo AK, Fouquay S, Michaud G, Simon F, Brusson J-M, Carpentier J-F, Guillaume SM (2014) α,ω-Di(glycerol carbonate) telechelic polyesters and polyolefins as precursors to polyhydroxyurethanes: an isocyanate-free approach. Green Chem 16:1947-1956.

7. Van Velthoven JLJ, Gootjes L, Van Es DS, Noordover BAJ, Meuldijk J (2015) Poly(hydroxy urethane)s based on renewable diglycerol dicarbonate, Eur Polym J 70:125-13.

8. Islam MR, Beg MDH, Jamari SS (2014) Development of vegetable-oil-based polymers. J Appl Polym Sci 131:40787.

9. Miao S, Callow N,Wang P, Liu Y, Su Z, Zhang S (2013) soybean oil-based polyurethane networks: Shape-memory effects and surface morphologies. J Am Oil Chem. Soc 90:1415-1421.

10. Pan X, Webster DC (2012) New biobased high functionality polyols and their use in polyurethane coatings. ChemSusChem 5:419-429.

11. Zhang C, Ding R, Kessler MR (2014) Reduction of epoxidized vegetable oils: A novel method to prepare bio-based polyols for polyurethanes. Macromol Rapid Commun 35:1068-1074.

12. Tong X, Ma Y, Li Y (2010) Biomass into chemicals: Conversion of sugars to furan derivatives by catalytic processes. Appl Catal A Gen 385:1-13.

13. Sousa AF, Vilela C, Fonseca AC, Matos M, Freire CSR, Gruter GJM, Coelho JFJ, Silvestre AJD (2015) Biobased polyesters and other polymers from 2,5-furandicarboxylic acid: A tribute to furan excellency. Polym Chem 6:5961-5983.

14. Cao M, Zhang C, He B, Huang M, Jiang S (2017) Synthesis of 2,5-furandicarboxylic acid-based heat-resistant polyamides under existing industrialization process. Macromol Res 25:722-729.

15. Wilsens CHRM, Verhoeven JMGA, Noordover BAJ, Hansen MR, Auhl D, Rastogi S (2014) Thermotropic polyesters from 2,5-furandicarboxylic acid and vanillic acid: Synthesis, thermal properties, melt behavior, and mechanical performance. Macromolecules 47:3306-3316.

16. Wu B, Xu Y, Bu Z, Wu L, Li BG, Dubois P (2014) Biobased poly(butylene 2,5-furandicarboxylate) and poly(butylene adipate-co-butylene 2,5-furandicarboxylate)s: From synthesis using highly purified 2,5-furandicarboxylic acid to thermo-mechanical properties. Polym 55:3648-3655.

17. Kwiatkowska M, Kowalczyk I, Kwiatkowski K, Szymczyk A, Rosłaniec Z (2016) Fully biobased multiblock copolymers of furan-aromatic polyester and dimerized fatty acid: Synthesis and characterization. Polym 99:503-512.

18. Jacquel N, Saint-Loup R, Pascault JP, Rousseau A, Fenouillot F (2015) Bio-based alternatives in the synthesis of aliphatic-aromatic polyesters dedicated to biodegradable film applications. Polym 59:234-242.

19. Wang J, Liu X, Jia Z, Liu Y, Sun L, Zhu J (2017) Synthesis of bio-based poly(ethylene 2,5-furandicarboxylate) copolyesters: Higher glass transition temperature, better transparency, and good barrier properties. J Polym Sci Part A Polym Chem 55:3298-3307.

20. Zia KM, Noreen A, Zuber M, Tabasum S, Mujahid M (2016) Recent developments and future prospects on bio-based polyesters derived from renewable resources: A review. Int J Biol Macromol 82:1028-1040.

21. Yu Z, Zhou J, Cao F, Wen B, Zhu X, Wei P (2013) Chemosynthesis and characterization of fully biomass-based copolymers of ethylene glycol, 2,5-furandicarboxylic acid, and succinic acid. J Appl Polym Sci 130:1415-1420.

22. Papageorgiou GZ, Papageorgiou DG, Terzopoulou Z, Bikiaris DN (2016) Production of bio-based 2,5-furan dicarboxylate polyesters: Recent progress and critical aspects in their synthesis and thermal properties. Eur Polym J 83:202-229.

23. Zhou W, Zhang Y, Xu Y, Wang P, Gao L, Zhang W, Ji J (2014) Synthesis and characterization of bio-based poly(butylene furandicarboxylate)-b-poly(tetramethylene glycol) copolymers. Polym Degrad Stab 109:21-26.

24. Vink ETH, Davies S (2015) Life Cycle Inventory and impact assessment data for 2014 ingeo polylactide production. Ind biotechnol 11:167-180.

25. Adom F, Dunn JB, Han J, Sather N (2014) Life-Cycle fossil energy consumption and greenhouse gas emissions of bioderived chemicals and their conventional counterparts. Environ Sci Technol 48:14624-14631.

26. Urban RA, Bakshi BR (2009) 1,3-Propanediol from Fossils versus Biomass: A Life Cycle Evaluation of Emissions and Ecological Resources. Ind Eng Chem Res 48:8068-8082.

27. Cok B, Tsiropoulos I, Roes AL, Patel MK (2014) Succinic acid production derived from carbohydrates: An energy and greenhouse gas assessment of a platform chemical toward a bio-based economy. Biofuels, Bioprod Biorefining 8:16-29.

28. Eerhart AJJE, Faaij APC, Patel MK (2012) Replacing fossil based PET with biobased PEF; process analysis, energy and GHG balance. Energy Environ Sci 5:6407-6422.

29. Isola C, Sieverding HL, Raghunathan R, Sibi MP, Webster DC, Sivaguru J, Stone JJ (2017) Life cycle assessment of photodegradable polymeric material derived from renewable bioresources. J Clean Prod 142:2935–2944.

30. Jungbluth N, Dinkel F, Doka G, Chudacoff M, Dauriat A, Spielman M, Sutter J, Kljun N, Keller M, Schleiss K (2007) Life cycle inventories of bioenergy. Ecoinvent report No. 17, Swiss Centre for LCI, Dübendorf.

31. Althaus H-J, Chudacoff M, Hischier R, Jungbluth N, Osses M, Primas A (2007) Life Cycle Inventories of chemicals. Ecoinvent report No. 8, Swiss Centre for LCI, Dübendorf .

32. Sutter J (2007) Life Cycle Inventories of petrochemical solvents. Ecoinvent final report No. 22, v2.0. Swiss Centre for LCI, Dübendorf, CH.

33. Dupont Tale and Lyle Bio Products (DT&L) (2009) Life Cycle Analysis Overview-Susterra/Propanediol.http://www.duponttateandlyle.com/sites/default/files/Susterra%20LCA.pdf, accessed 12/06/2017.

34. ASTM D4752 – 10 (2015) standard practice for measuring MEK resistance of ethyl silicate (inorganic) zinc-rich primers by solvent rub.

35. ISO 2815:2003 (2003) Paints and varnishes - Buchholz indentation test.

36. ASTM D4541 – 09 (2009) Standard Test Method for Pull-Off Strength of Coatings Using Portable Adhesion Testers.

37. Wu S (1973) Polar and Nonpolar Interactions in Adhesion. J Adhes 5:39-55.

38. ISO 14040:2006 (2006) Environmental Management – Life Cycle Assessment – Principles and Framework. Geneva, Switzerland.

39. ISO 14044:2006 (2006) Environmental Management – Life Cycle Assessment – Requirements and Guidelines. Geneva, Switzerland.

40. Frischknecht R, Jungbluth N, Althaus H-J, Doka G, Heck T, Hellweg S, Hischier R, Nemecek T, Rebitzer G, Spielmann M, Wernet G (2007) Overview and Methodology. Ecoinvent report No. 1, Swiss Centre for LCI, Dübendorf.

41. IPPC Intergovernmental Panelon Climate (2007) IPCC Fourth Assessment Report, Climate Change. https://ipcc.ch/publications_and_data/ar4/syr/en/contents.html, accessed 01/11/2017.

42. Goedkoop M, Heijungs R, Huijbregts M, De Schryver A, Struijs J, Van Zelm R (2008) Environmental mechanism. Source: Recipe 2008. A life cycle impact assessment method which comprises harmonised category indicators at the midpoint and the endpoint level. First edition, v 1.12. Report I: Characterization, May 2013 revision.

43. IPCC Guidelines for National Greenhouse Gas Inventories, Volume 4, Chapter 11 (2006). http://www.ipcc-nggip.iges.or.jp/public/2006gl/vol4.html, accessed 01/11/2017.

44. http://www.greppa.nu/om-greppa/om-projektet/in-english.html, assessed 13/10/2017.

45. Börjesson P, Tufvesson LM (2011) Agricultural crop-based biofuels - Resource efficiency and environmental performance including direct land use changes. J Clean Prod 19:108-120.

46. Omni Tech International, The United Soybean Board, 2010. Life Cycle Impact of Soybean Production and Soy Industrial Products. http://biodiesel.org/reports/20100201_gen-422.pdf, accessed 07/06/2017.

47. Gnansounou E, Kenthorai Raman J (2016) Life cycle assessment of algae biodiesel and its co-products. Appl Energy 161:300-308.

48. http://www.scb.se/hitta-statistik/statistik-efter-amne/energi/prisutvecklingen-inom-energiomradet/energipriser-pa-naturgas-och-el/pong/tabell-och-diagram/genomsnittspriser-per-halvar-2007/priser-pa-naturgas-for-industrikunder-2007/, assessed 13/10/2017.

49. Lundgren J, Ekbom T, Hulteberg C, Larsson M, Grip CE, Nilsson L, Tunå P (2013) Methanol production from steel-work off-gases and biomass based synthesis gas. Appl Energy 112:431-439.

50. Börjesson P, Lantz M, Andersson J, Björnsson L, Möller BF, Fröberg M, Hanarp P, Hulteberg C, Iverfeldt E, Lundgren J (2017) Methane as vehicle fuel – a well to wheel analysis. The Swedish Knowledge Centre for Renewable Transportation Fuels, Sweden .

51. Demire Y (2015) Sustainability and economic analysis of propylene carbonate and polypropylene carbonate production processes using CO_2 and propylene oxide. J Chem Eng Process Technol 6:236.

52. Barton AFM (1985) Handbook of solubility parameters and other cohesion parameters. CRC Press Inc, Florida.

53. Furukawa, M, Shiiba T, Murata S (1999) Mechanical properties and hydrolytic stability of polyesterurethane elastomers with alkyl side groups. Polymer 40:1791-1798.

54. IPPC Intergovernmental Panelon Climate, 2007. IPCC Fourth Assessment Report, Climate Change. https://ipcc.ch/publications_and_data/ar4/syr/en/contents.html, accessed 12/06/2017.

55. IPPC Intergovernmental Panelon Climate, 2013. IPCC Fifth Assessment Report, Climate Change: The Physical Science Basis. http://www.ipcc.ch/report/ar5/wg1/, accessed 12/06/2017.

56. Jolliet O, Margni M, Charles R, Humbert S, Payet J, Rebitzer G, Rosenbaum RK (2003) IMPACT 2002+: A New Life Cycle Impact Assessment Methodology. Int J Life Cycle Assess 8:324-330.

4.
Lignin as functional filler

4.1 INTRODUCTION

Lignin is a natural aromatic polymer found in the wall of cellular plants, where it accounts for about 15%-25% of the wooden matter[1]. At present, several million tons per year of lignin are recovered in the waste streams of pulp and paper factories and in biorefineries fed with lignocellulosic biomass[2,3]. Such large abundance, second only to cellulose and hemicellulose, makes lignin particularly interesting as valuable renewable source of aromatics for the development of high performance and environmentally friendly polymer-based materials. However, despite such great potential, lignin is still enormously underutilized at industrial scale, as its fate is typically to be burnt as low-cost fuel for energy generation. Indeed, only a restricted fraction of the lignin produced annually is currently recovered for higher value-added applications, that typically include its incorporation in formulations for additives, fillers and dispersants for composites, plastics and rubbers[4,5]. This relatively limited range of commercial applications is largely related to the vast chemical heterogeneity, poor reactivity and difficult processability of the available lignins, the latter aspect being closely associated with the highly branched and hydrogen-bonded three-dimensional structure of such amorphous material[6-8].

In the attempt to tackle some of these limitations, several chemical and chemical-physical strategies have been proposed in the last few years to enhance the exploitability of lignin as macromonomer for the production of polymeric materials. To this end, different fractionation approaches (pH-induced precipitation, membrane-assisted ultrafiltration and solvent extraction) have been used to improve the miscibility of lignin in common solvents while better controlling its chemical, structural and physical

properties[9-19]. In addition, highly specific chemical functionalization reactions have been applied to lignin to improve its reactivity, add functionalities to its structure and allow easier incorporation as reactive material into bio-based thermoplastic, thermosetting polymers, including polyurethanes, polyesters, phenolics and epoxies, and rubbers[20-28].

The large number of functional groups present in lignin (e.g., aliphatic and aromatic hydroxyls, carbonyls, carboxyls) makes this material particularly attractive as reinforcing filler for the preparation of polymer-based composites, due to the potentially favourable covalent and non-covalent interactions that may arise between such highly-functional filler and the polymeric matrix. In this respect, different attempts have been made involving the incorporation of lignin particles (generally in the 10-100 μm range) into plastics and rubbers[29-31]. Typically, it was shown that straightforward addition of lignin into the target matrix yielded little or no effect on the mechanical properties of the corresponding composite. Therefore, appropriate chemical modification strategies were required to improve filler/matrix compatibility by introducing new functional groups on the lignin particle surface *via* nitration[32], esterification[33-35], silanization[36], butyration or urethane-bond formation[37].

An alternative strategy to achieve enhanced dispersion level of the lignin filler within the polymer matrix is the preparation and use of lignin-based nanoparticles. With respect to their micrometer-sized (or larger) counterpart, nanolignin (NL) particles are characterized by a larger surface-to-volume ratio that is expected to lead to a more efficient interaction with the polymer matrix. As a result, improved dispersion and matrix-to-filler interfacial load transfer may be anticipated, thus prospecting improved mechanical properties of the NL-based polymer composite[38]. To obtain lignin-based nanoparticles, different

approaches have been adopted so far, that include the formation of NL colloids by self-assembly[39] and the application of chemical[40,41], mechanical[42] or ultrasonic[43,44] treatments to the pristine material. Contingent upon the process employed, particle dimensions of few-tens to few-hundreds of nm can be achieved. In particular, ultrasonication appears to be especially interesting as it allows to obtain stable colloidal suspensions of NL particles as small as 10-50 nm by simple physical treatment (*viz.*, cavitation), thus avoiding the need of (hazardous) chemical pre- or post-treatments on the material (typically, no solvent fractionation is required) and potentially leading to a more environmentally favourable overall process (as water is the typically employed dispersing medium).

Despite the clear scientific and technological impact of NL as fully bio-based reinforcing filler with enhanced water-dispersion stability, only surprisingly few examples of its application in polymer-based nanocomposite materials have recently appeared in the literature[42,45-47]. In particular, it was shown that lignin nanoparticles obtained by high-shear mechanical treatment could be completely homogenized to diameters in the 100 nm range and readily dispersed within the polymer matrix poly(vinyl alcohol). This led to improved thermal stability of NL-based composite systems compared to materials incorporating untreated lignin[42]. On the other hand, natural rubber-based nanocomposites were obtained by addition of colloidal polyelectrolyte complexes (100 nm average size) obtained from lignin and poly(diallyldimethylammonium chloride). The resulting materials were shown to exhibit enhanced thermal stability and mechanical properties thanks to the strong filler-to-matrix adhesion[45]. Finally, lignin nanoparticles obtained by acidolysis were employed to improve the thermal, mechanical and wettability properties of bio-derived polymeric matrices such as poly(lactic

acid) and wheat gluten[46,47]. Based on these recent results, it is evident that no demonstrations of polymer-based nanocomposites reinforced with NL obtained by ultrasonic treatment have been reported to date, notwithstanding the great potential of this approach in view of the development of more environmentally sustainable lignin treatment processes. Indeed, the few reports on ultrasonication of lignin mainly focused on the characterization of the effects of this treatment on the chemical, physical and morphological properties of lignin[43,48-50], with no detailed investigation on the use of such ultrasonically treated lignin nanoparticles in nanocomposite systems.

Accordingly, in this work NL particles were prepared by ultrasonically treating a commercially available softwood kraft lignin to obtain stable colloidal water dispersions. A thorough chemical, physical and morphological characterization of the NL systems was carried out and compared with the parent untreated material. The obtained lignin nanoparticles were initially incorporated into a epoxidized natural rubber (ENR) in order to investigate the possibility to replace carbon black that is usually used as filler in rubber composites[51-54]. As reported in the literature, polymeric materials from renewable resources, added as additives to rubber blends and vulcanizated, influence on vulcanization process, tensile strength properties and dynamical-mechanical properties. Therefore, they were evaluated. Successively, the obtained lignin nanoparticles were also incorporated into a waterborne thermoplastic polyurethane to form nanocomposite materials with increasing bio-filler concentration. Such polymeric matrix was chosen because of the wide industrial applicability of polyurethanes that find use in a large variety of technological fields[55]. The effect of filler type (NL *vs.* untreated lignin) and concentration on the chemical-physical, thermal and morphological

characteristics of the resulting nanocomposites was investigated and the reinforcing effect was discussed based on mechanical tests.

4.1.1 Epoxidized natural rubber and vulcanization process

Epoxidized natural rubber (ENR) is a modified natural rubber with a random distribution of epoxy groups along with the polymer backbone[54]. These epoxy groups in ENR are readily reacted with nucleophilic reagents, which impart ENR the miscibility with other polymers active fillers by reactive compatibilization[54,56,57].

Vulcanization is the process by which rubber molecules are cross-linked with each other by heating the liquid rubber in the presence of sulfur[58,59]. Cross-linking increases the rubber's strength and elasticity by about ten times, but the amount of cross-linking must be controlled to avoid creating a brittle and inelastic substance. The process of vulcanization was accidentally discovered in 1839 by Charles Goodyear towards the end of the 19th century when he dropped some rubber containing sulfur onto a hot stove. Vulcanization with sulfur is still the chosen method to process unsaturated elastomers like natural rubber in the tyre manufacture technology. The reaction does not directly involve the opening of C=C double bond, but the substitution reaction of allylic hydrogen atoms by sulfur[60] (Figure 1).

The vulcanization reaction is very slow (24-48 h), therefore other chemicals are used to improve the efficiency of the process. In the base recipe, ZnO is used to promote sulfur decomposition, stearic acid to improve the solubility of ZnO into the polymer, and organic accelerants such as 2-mercaptobenzothiazole (2MPBTA) to speed-up the crosslinking reaction.

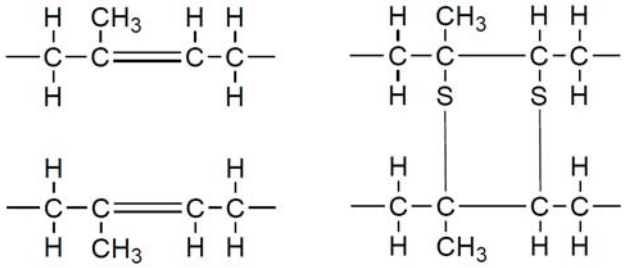

Figure 1. Vulcanization process with sulfur

4.2 NANOLIGNIN (NL) PARTICLES

4.2.1 Experimental section

4.2.1.1 Materials

Softwood kraft lignin (Indulin AT) was commercially available and supplied by MeadWestvaco.

4.2.1.2 Preparation of nanolignin (NL) particles

Nanolignin (NL) was prepared *via* an ultrasonication treatment using a Sonic & Materials VCX130 sonicator tip at a frequency of 20 kHz, 130 W power and 95% oscillation amplitude. The parent kraft lignin (from here on referred to as IND, 10 mg) was dispersed in deionized water (10 mL) and treated for 2, 4 and 6 h. The resulting dispersions (0.1 wt.% lignin in water) were named NL-2h, NL-4h and NL-6h, respectively. An ice bath was used to avoid excessive heating of the dispersion due to the exothermicity of the ultrasonication process.

4.2.1.3 Material characterization

4.2.1.3.1 Transmission electron microscopy (TEM)

TEM micrographs were acquired on NL fractions at increasing times of ultrasonic treatment using a Philips CM 200 electron microscope operating at 200 kV equipped with a Field Emission Gun filament. For sample preparation, few drops of lignin (IND or NL) suspension in water were deposited on a 200 mesh carbon-coated copper grid and air-dried for several hours before analysis. A Gatan US 1000 CCD camera was used and 2048x2048 pixels images with 256 grey levels were recorded.

4.2.1.3.2 UV-vis spectroscopy

UV-vis spectroscopy was carried out on solid IND and NL samples dissolved in dimethyl sulfoxide (DMSO) at room temperature using an Evolution 600 UV−vis spectrophotometer (Thermo Scientific) in the 250-600 nm wavelength range with a scan speed of 100 nm/min and a bandwidth of 5 nm. A liquid cell of 1 cm path length with quartz window was used. The use of DMSO enables complete solubilization of the IND and NL powders but limits the absorption spectral range to wavelengths longer than 260 nm.

4.2.1.3.3 Fourier-transform infrared (FTIR) spectroscopy

FTIR spectra were collected on a Nicolet 760-FTIR spectrophotometer on IND and NL solid samples (powder). Spectra were obtained from 64 accumulated scans performed from 4000 cm^{-1} to 700 cm^{-1} at 2 cm^{-1} resolution.

4.2.1.3.4 Differential scanning calorimetry (DSC)

DSC analyses were carried out on 10 ± 1 mg solid state lignin samples using a Mettler-Toledo DSC/823e instrument at a scan rate of 20 °C min^{-1} under nitrogen flux. The measurements consisted of three runs (heating/cooling/heating) from 25 °C to 200 °C. The glass transition temperature (Tg) of the materials was evaluated as inflection point in the second heating run.

4.2.1.3.5 Gel Permeation Chromatography (GPC)

The molecular weight of IND and NL samples was estimated by means of gel permeation chromatography (GPC) using a Waters 510 high-performance liquid chromatography (HPLC) system equipped with a Waters 486 tunable

absorbance detector set at λ = 300 nm, using THF as eluent. The sample (200 μL of IND and NL in THF, 2 mg/mL) was injected into a system of columns connected in series (Ultrastyragel HR, Waters) and the analysis was performed at 30 °C and at a flow rate of 0.5 mL/min. The GPC system was calibrated against polystyrene standards in the 102-104 g/mol molecular weight range.

4.2.2 Results and discussion

4.2.2.1. Morphology and water-suspension stability of lignin (nano)particles

Transmission electron microscopy (TEM) analysis was used to investigate the morphology and dimensions of lignin particles before and after ultrasound treatment for different processing times (2 h, 4 h and 6 h). As shown in Figure 2 where the corresponding TEM images are presented, the morphology of lignin nanoparticles was found to be irregular in shape throughout the entire sonication process. Concurrently, a notable decrease in particle size accompanied by a reduction of inter-particle aggregation was observed for increasing ultrasonication times. Pristine untreated lignin (IND) was characterized by the presence of large agglomerates with dimensions in the 1-3 μm range (Figure 2a), likely arising from the strong intermolecular forces (typically, hydrogen bonds) acting between macromolecular lignin chains combined with the high insolubility of kraft lignin in water. By increasing ultrasonic treatment time, such agglomerates are found to progressively disaggregate and the average particle dimension to decrease by several orders of magnitude. In particular, after 6h of ultrasound treatment, a water dispersion of submicrometric lignin particles could be obtained, with minimum size in the 10 nm – 50 nm range (Figure 2d). This clearly indicates

that successful formation of NL could be achieved. These results are in good agreement with recent literature reports where comparable particle dimensions were obtained on wheat straw and Sarkanda grass lignins.[43] In order to evaluate the effect of ultrasonication time on the further particle size reduction, lignin was also treated for 9h. However, no significant size modifications were observed for longer treatment times (Figure 3), likely due to a less efficient cavitation effect on nanoparticle dimension in the range of a few tens of nanometers. As a result, the characterizations that will be presented in the following will be based on NL-6h.

To assess the stability of the NL dispersion in water, settling experiments were performed on ultrasound-treated (NL-6h) and pristine (IND) systems. As shown in Figure 4a. the as-obtained water dispersion containing NL-6h exhibits a dark brown tint resulting from the presence of homogeneously distributed lignin nanoparticles successfully suspended within the entire liquid volume. The same dispersion was found to maintain such homogeneous tint for over 15 months without any noticeable formation of solid precipitate (Figure 4b), clearly indicating the excellent water-dispersion stability of the ultrasonically treated NL-based system. Conversely, the as-prepared untreated IND water suspension (obtained by magnetically stirring a 1 mg/ml dispersion of pristine lignin in water for 12 h) evidenced poor homogeneity immediately after interruption of the stirring process. In particular, all lignin material was found to settle down as solid precipitate already after 5 min at rest, as a result of the highly hydrophobic character of pristine kraft lignin that preferentially forms agglomerates and aggregates in water ultimately resulting in solid/liquid phase segregation.

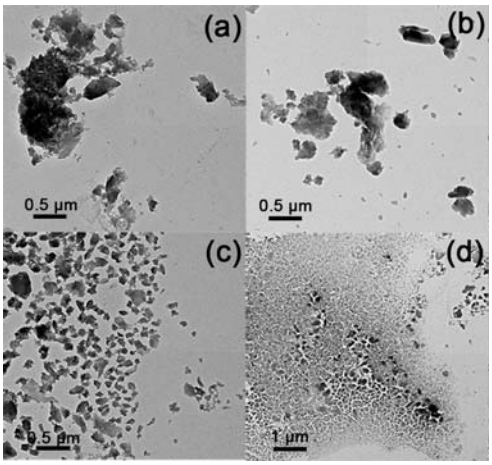

Figure 2. TEM images of kraft lignin particles at increasing ultrasound treatment times: (a) pristine material (0 h), (b) 2 h, (c) 4 h and (d) 6 h.

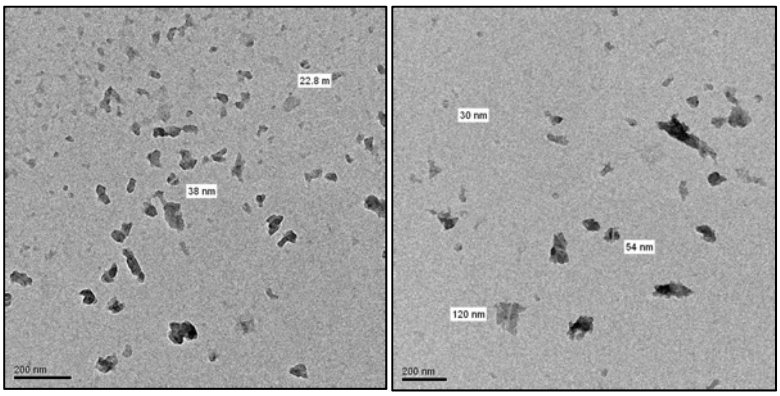

Figure 3. TEM images of NL-6h: (a) lignin nanoparticles after ultrasound treatment for 6 h), with indication of particle size as measured by TEM, (b) lignin nanoparticles after ultrasound treatment for 9 h.

Figure 4. Photographic images of water dispersions of ultrasonically treated NL-6h and pristine IND lignin (a) after dispersion process and (b) after 15 months at rest.

4.2.2.2 UV–vis spectroscopy on lignin (nano)particles

UV–vis spectroscopy was used to qualitatively investigate the compositional evolution of lignin as a result of the ultrasonic treatment. In this respect, possible changes in the type and amount of conjugated moieties in lignin occurring during the ultrasonication process may lead to modifications of its UV-vis absorption response. Figure 5 presents the UV-vis absorption spectra of IND and NL-6h samples. In both cases, a maximum is observed at 280 nm which is ascribable to the presence of non-condensed phenolic groups in guaiacyl units that are characteristic of softwood lignin[19,61]. In addition, a shoulder centered at 340 nm is present in the absorption spectra of both IND and NL-6h, although with different relative intensities. This absorption feature is attributable to the presence of conjugated moieties such as α-carbonyl groups and esters of hydrocinnamic acids that are also present in softwood lignin[62]. This signal is found to exhibit a slight decrease in intensity in NL-6h compared to pristine IND, likely suggesting that during the ultrasonication treatment partial loss of conjugation in lignin may occur due to the interaction of conjugated species with radical species forming as a result of the cavitation process[48,49].

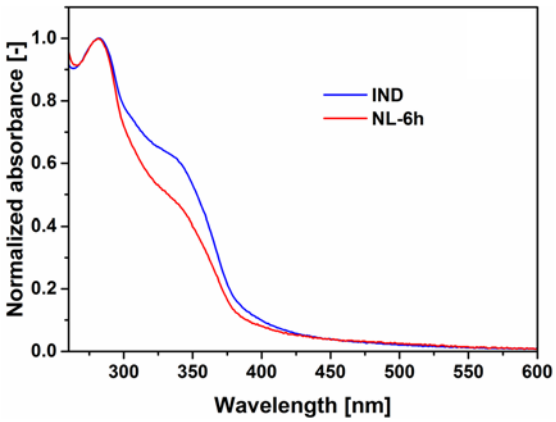

Figure 5. UV-vis spectra of untreated pristine lignin (IND) and lignin (nano)particles (NL-6h).

4.2.2.3 Fourier-transform infrared spectroscopy (FTIR) on lignin (nano)particles

To investigate the chemical modifications potentially occurring to lignin during the ultrasonication process, FTIR spectra were collected on both IND and NL-6h (Figure 6). The absorption intensities of the spectra were normalized with respect to the signal at 1515 cm^{-1}, corresponding to the C=C stretching vibrations of the aromatic ring.[48]. The parent material exhibits a wide absorption band in the 3700-3050 cm^{-1} range that is typically associated with stretching vibrations of -OH groups present in lignin. In particular, two main vibrational components can be distinguished in this region at 3420 cm^{-1} (peak) and 3230 cm^{-1} (weak shoulder), ascribable to stretching vibrations of intramolecular and intermolecular hydrogen bonded hydroxyl groups, respectively. As opposed to this, the treated NL-6h material only exhibits a single sharp absorption peak centered at 3420 cm^{-1}, whose intensity is found to increase at increasing ultrasonic treatment times (see Figure 7). These results indicate that the ultrasonication process may induce partial oxidation

to lignin that results in the formation of a higher concentration of –OH moieties in the macromolecule as compared to the parent material, ultimately leading to increased polarity in the treated system. As evidenced by the FTIR analysis, these additional hydroxyl functionalities are more likely to establish intramolecular rather than intermolecular hydrogen-bonding interactions, thus leading to lower inter-particle attractions when dispersed into polar media. Consistently, markedly improved stability in water is observed for NL-6h suspensions compared to pristine IND (see Figure 6b). No significant modifications are observed in the characteristic signals attributed to C-H stretching vibrations in methyl and methylene groups, clearly detectable in the 3050-2800 cm^{-1} spectral region for both untreated and treated materials. In the C=O stretching region, IND only shows a very weak shoulder centered at 1700 cm^{-1}, ascribable to the relatively low concentration of carbonyl moieties (e.g., conjugated aldehydes and carboxylic acids) in the parent material, as also observed in previous studies on similar systems[63]. Upon ultrasonic treatment, a broader shoulder at around 1710 cm^{-1} is formed (C=O stretching in carbonyl and carboxyl groups), accompanied by the appearance of an additional sharp signal centered at 1640 cm^{-1}, whose intensity is found to increase with ultrasonic treatment time (see Figure 7). This latter signal may be ascribed to C=O stretching vibrations resulting from the contribution of intramolecular hydrogen-bonded carboxylic acids that may form during the ultrasonication process. Interestingly, these observations are in good agreement with the modifications found in the 3700-3050 cm^{-1} range on –OH stretching vibrations, where the formation of oxidized species during the sonication process resulted in a sharp increase of the signal associated to the stretching vibrations of intramolecular hydrogen-bonded –OH groups in NL-6h. Further evidence of the oxidative effect of ultrasounds on the lignin

macromolecule may be inferred by considering the signal observed at 1268 cm^{-1} (C=O and C-O vibrations in guaiacyl units present in lignin) whose intensity is found to increase compared to the parent material as a result of the ultrasound treatment. The region characteristic of the aromatic skeletal C=C and C-C stretching vibrations in lignin does not appear to be affected by the ultrasonication process, as the strong signal found at 1600 cm^{-1} is observed with comparable intensities in both parent and treated materials. This observation indicates that in the conditions employed in the present study the sonication process does not affect the aromaticity of lignin. Similarly, no significant modifications due to the ultrasonic process are found in the 1480-1300 cm^{-1} (vibrations of phenolic O-H groups combined with aliphatic C-H in methyl groups) and 1250-800 cm^{-1} (C=O, C-H and C-O in-plane and out-of-plane deformations in guaiacyl, syringyl and p-hydroxyphenyl units) spectral ranges, where similar signals with comparable intensities are observed in both IND and NL-6h.

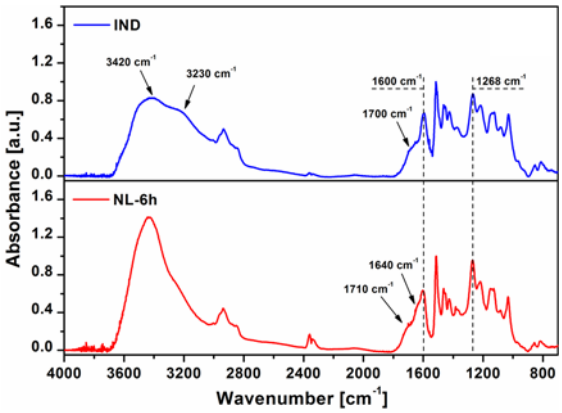

Figure 6. Fourier-transform infrared spectra of untreated pristine lignin (IND) and lignin (nano)particles (NL-6h).

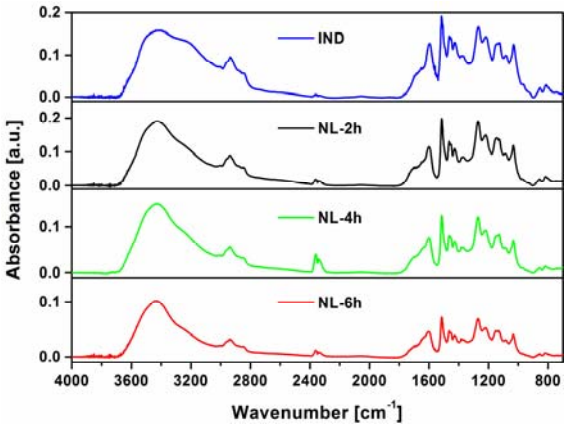

Figure 7. Fourier-transform infrared spectra of NL at increasing ultrasound treatment times (2 h, 4 h, 6 h). The FTIR spectrum of pristine untreated lignin (IND) is also shown.

4.2.2.4 Differential Scanning Calorimetry (DSC) on lignin (nano)particles

In order to assess the effect of ultrasonic treatment on the thermal behavior of lignin, DSC analysis was performed on both IND and NL-6h samples. As shown in Figure 8, no significant variations were observed after ultrasonication, as comparable Tg were found in pristine and treated material, with values lying in the typical temperature ranges observed on softwood lignins (153 °C and 151 °C for IND and NL-6h, respectively)[61]. Tg is directly related to the mobility of the macromolecular chains, which may be affected by a complex interplay between several factors including the molecular weight of the material, the presence of chemical or physical crosslinks and the presence of strong intermolecular interactions between the macromolecular chains such as intermolecular hydrogen bonds. As previously observed (Figure 6), the ultrasonication process was found to reduce the extent of intermolecular hydrogen-bonded hydroxyl-mediated interactions.

Considering these observation, a noticeable reduction of Tg may have been expected upon treatment. However, further analysis through gel permeation chromatography (GPC) revealed a slight increase of Mn and Mw after the ultrasonication process accompanied by a broadening of the molecular weight distribution (Figure 9 and Table 1).

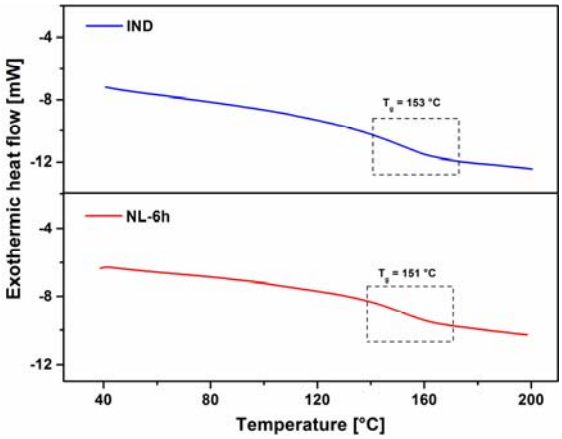

Figure 8. Differential scanning calorimetry curves of untreated pristine lignin (IND) and lignin nanoparticles (NL-6h).

These results may indicate that in the experimental conditions employed in this study cavitation may have occurred to some extent during the ultrasonic treatment[50]. Accordingly, partial oxidative coupling may have taken place leading to a higher degree of branching in lignin and ultimately yielding increased chain length, molecular weight and thus prospective increased Tg. Based on these considerations, the negligible modifications in Tg observed *via* DSC prior to and after ultrasonic treatment may be the result of these two counteracting effects (decrease in intermolecular hydrogen bonding *vs.* increase in molecular weight).

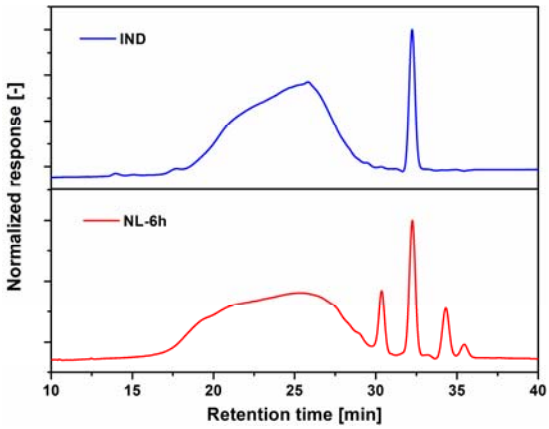

Figure 9. Gel permeation chromatography chromatograms of pristine IND and NL-6h.

Table 1. Molecular weights (Mn and Mw) and polydispersity index (PDI) of IND and NL-6h.

	Mn [g/mol]	**Mw [g/mol]**	**PDI**
IND	2480	7590	3.0
NL-6h	2550	11140	4.4

4.3 EPOXIDIZED NATURAL RUBBER COMPOUND

4.3.1 Experimental section

4.3.1.1 Materials

All materials used in this study are commercially available. The epoxidized natural rubber (ENR) used as matrix material for the nanocomposites was supplied by Manuli Industries SpA. It presents a degree of epoxidation of 50%, T_g = -24°C and a density of 1020 kg/m^3. The zinc oxide (ZnO), stearic acid (StA), 2-mercaptobenzothiazole (2MPBTA) and sulfur (S) used as components needed for the formulation of pre-vulcanized rubbers were supplied by Sigma Aldrich and used as they were received.

4.3.1.2 Sample preparation - Brabender mixer

The preparation of the samples were performed by mixing the lignin (IND), nanolignin (NL) particles, epoxidized natural rubber (ENR) and the components required (5 phr ZnO, 2 phr StA, 1 phr 2MPBTA and 2,25 phr S) for vulcanization onto a two rolls mixer, called Brabender, whose volume was 55 cc, at a temperature lower than 100 ºC with a rotor speed of 40 rpm for 9 min. This temperature was chosen in order to mix all the materials without starting the vulcanization process. The formulation of the rubber (nano)compounds with those materials as parts per 100 by weight of the rubber polymer (phr) are presented in Table 2. The mass amount of IND and NL in the ENR matrix was 10% and 40% and the samples were named ENR/IND-10, ENR/NL-10, ENR/IND-40 and ENR/NL-40 respectively. During mixing, torque and temperature values were recorded and controlled to prevent an early vulcanization process at this stage. The process continued until the plateau was reached for the two values, indicative of obtaining a

sufficiently homogeneous mixture. A curve example during the mixing is shown in Figure 10.

Table 2. Formulation of rubber (nano)composites.

	IND (%)	NL (%)	ZnO (phr)	StA (phr)	2MPBTA (phr)	S (phr)
ENR			5	2	1	2.5
ENR/IND-10	10		5	2	1	2.5
ENR/IND-40	40		5	2	1	2.5
ENR/NL-10		10	5	2	1	2.5
ENR/NL-40		40	5	2	1	2.5

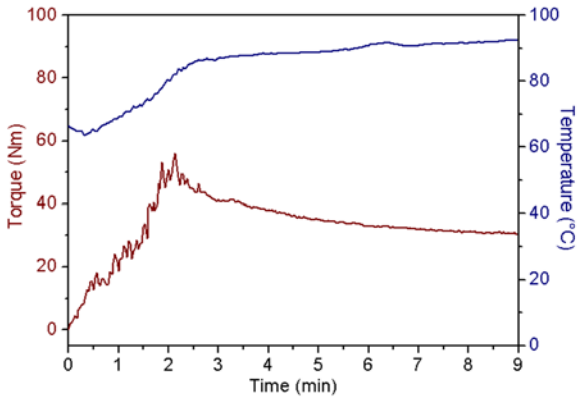

Figure 10. Example of the ENR/IND-10 system curve during the mixing time by brabender mixer. Brown line presents the applied torque and blue line shows the material temperature during the mixing time.

4.3.1.3 Vulcanization process

The vulcanization process is an important step in this part of the study and its components play an important role since they help to accelerate the process. The vulcanization is represented using vulcanization curves and the dynamic modulus-time trend obtained in the vulcanization process is monitored obtaining a graph as shown in Figure 11.

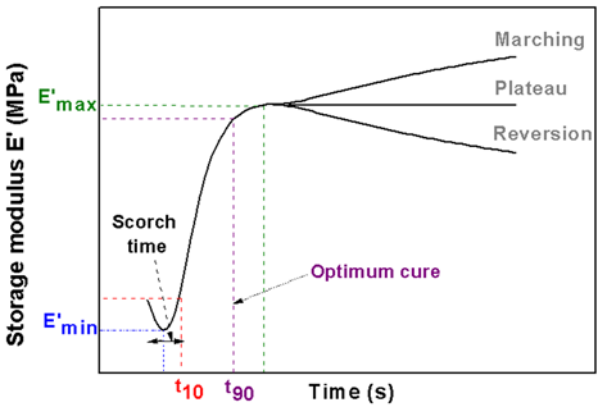

Figure 11. Vulcanization curves with the four process parameters measured.

The initial increase after the start of the test is due to the onset of vulcanization. The final plateau is related to the crosslinking density, whereas the eventual reversion with storage modulus decreases after reaching a maximum involves thermal instability of some formed bonds. Four process parameters are usually measured and reported: lowest achievable modulus (E'_{min}), highest achievable modulus (E'_{max}), scorch-time and optimum vulcanization time (t_{90}). The so-called scorch-time is the maximum time allowed for the processing and forming of the compound in the chosen experimental conditions, and it is roughly related to the gel-point of the rubber. The optimal vulcanization time is normally given as t_{90}, that represents the time at a given temperature after until 90% of the maximum storage modulus is achieved[67]. In addition, the time in which the module E' reaches 10% of its maximum value (t_{10}) is also often reported (see Figure 11) as a vulcanization parameter.

The vulcanization process in this study of the blends was performed by molding in a hydraulic press at a temperature of 151 °C and a pressure of 200 bars for a time equal to the characteristic time of each compound. The characteristic times used during vulcanization in press and previously

discussed (t_{10}, t_{90}, scorth time) where obtained for all materials by means of dynamic-mechanical analysis (DMA), a crucial step in the rubber technology to optimize material performances.

4.3.1.4 Material characterization

4.3.1.4.1 Dynamic mechanical analysis - Vulcanization parameters

Dynamic mechanical analysis (DMA) was carried out on the non-vulcanized samples in order to obtain the optimal vulcanization time (t_{90}) by SCA mode by means of a Mettler DMA/SDTA861 equipment. The specimen diameter used was 6 mm, whereas the thickness was 2 mm. The temperature was set to 150°C for 90 minutes. Frequency and applied load were 1.67 Hz and 20 N, respectively.

4.3.1.4.2 Dynamic mechanical analysis - Mechanical performance

DMA analyses were performed on all rubber (nano)composites vulcanized in order to assess the elastic (M') and dissipative (M'') moduli using a Mettler Toledo DMA/SDTA861 instrument in strain amplitude sweep at room temperature (25°C). The frequency was kept constant (0.1 Hz) and the deformation scanning was from zero to 200 microns.

4.3.1.4.3 Swelling tests

Swelling tests were performed on all rubber (nano)composites vulcanized with pure anhydrous butylacetate solvent at ambient temperature (25°C) in order to determine the degree of crosslinking. The analysis was based on

Flory-Rehner theory, which argues that swelling is related to the cross-link density in the material[68]. The following equation was used:

$$-\ln(1-v_2)-v_2-\chi v_2^2=\frac{\rho V_1}{M_c}v_2^{1/3}$$

where:

$v_2=\frac{V_0}{V}=\frac{V_0}{V_0+n_1V_1}$ is the volumetric fraction of solvent in the polymer-solvent gel; V_0 is the initial volume of rubber (nano)composites; n_1 is the number of moles of solvent present in the re-swelling system; V_1 is the solvent molar volume; χ is the parameter of polymer-solvent interaction based on Flory-Huggins theory; ρ is the rubber density and Mc is the number average molecular weight between crosslinks.

4.3.1.4.4 Tensile tests

Tensile measurements were conducted at room temperature using a Zwick/Roell Z010 (Zwick Roell Italia, Genova, Italy) equipped with a 10 kN load cell and a longstroke extensometer. All specimens were tested according to the standard test method ASTM D412[69]. A minimum of five samples were tested in each case to obtain average values.

4.3.2 Results and discussion

4.3.2.1 Vulcanization behavior

Lignin has plenty of acidic functional groups involving carboxyl and phenolic groups, which can interact with basic rubber ingredients. Therefore, a retardant effect on the rubber vulcanization based on lignin composites may be observed[70-72]. In this part of the study, the effect of the direct mixing of IND/NL and rubber on the vulcanization behavior of all systems was

investigated by DMA analysis and summarised in Figure 12. The vulcanization characteristics of the rubber (nano)composites were expressed in terms of the vulcanization time, t_{10} and optimum curing time (t_{90}), as well as the minimum and maximum modulus (E'_{min} and E'_{max}, respectively). From the vulcanization parameters in Table 3, t_{10} and t_{90} progressively increased at increasing filler loading (IND and NL) into the ENR matrix. This indicated that the retardant effect of the filler on the vulcanization of rubber (nano)composites took place. However, the retardant vulcanization effect with the introduction of IND was weaker than the one found with the incorporation of NL, that is, the t_{10} and t_{90} for ENR/IND systems were much lower than the ENR/NL ones. In rubber composites, E'_{min} and E'_{max} are dependent on the filler dispersion, filler-rubber network and rubber–rubber network. As it is reported in Figure 13a and b, with the incorporation of IND in the rubber matrix, the E'_{min} and E'_{max} were slightly increased at increasing lignin content. However, with the incorporation of NL in the rubber matrix, the E'_{min} and E'_{max} were slightly reduced at increasing lignin content. In the DMA curves shown in Figure 12, the reversion process after reaching the maximum value of the storage modulus (E') seemed to occur for all systems. A measure of the reversion grade, represented as delta modulus (ΔE'), for each system can be calculated as $E'_{max} - E$ (t=t'), where the chosen time was at 4000 s and their values are shown in Table 4. The highest ΔE' was observed for ENR/IND-40 followed by ENR/NL-10 system. The lowest reversion was found for ENR/NL-40 system. It may be attributable to the reversion of polysulfide bonds, i.e the polysulfide bonds regress to monosulfide bonds. In fact, this phenomenon is activated at temperatures close to vulcanization (around 155 °C)[73]. According to t_{90} value of each sample, the vulcanization process was performed by heat press at 150°C and 200 bar.

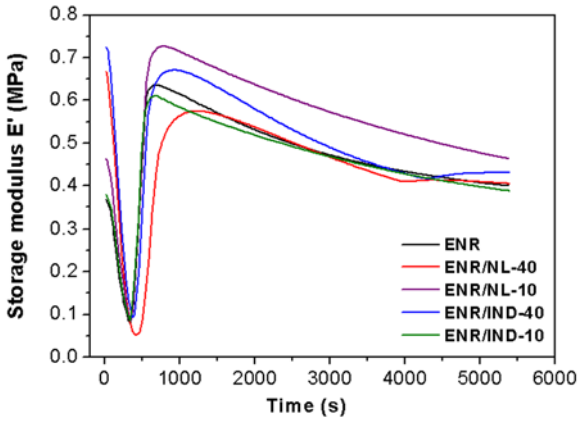

Figure 12. Dynamic mechanical analysis curves of all systems at different filler loadings including the unfilled ENR matrix as reference.

Table 3. Optimum vulcanization time (t_{90}) and vulcanization time at 10% (t_{10}) of rubber (nano)composites measured by dynamic mechanical analysis curves.

	t_{10} (min)	t_{90} (min)
ENR	5.35	8.90
ENR/IND-10	5.74	8.80
ENR/IND-40	6.25	10.20
ENR/NL-10	5.90	9.30
ENR/NL-40	7.40	13.15

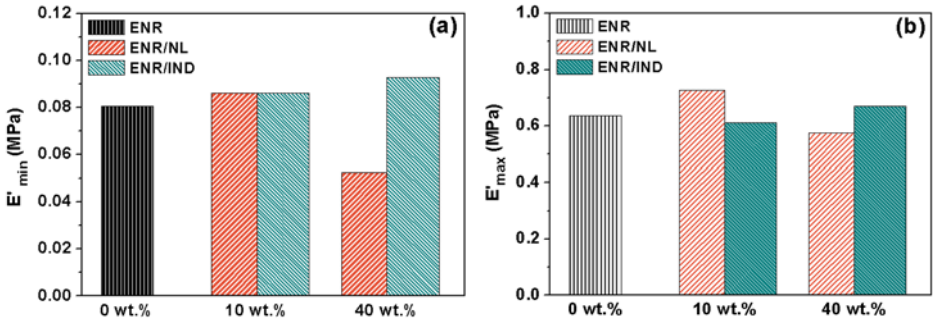

Figure 13. a) E′ $_{min}$ and b) E′ $_{max}$ of all systems at different filler loadings including unfilled ENR matrix as reference.

Table 4. Delta modulus (ΔE′) of rubber (nano)composites for the reversion process.

	ΔE′ (MPa)
ENR	0.20
ENR/IND-10	0.18
ENR/IND-40	0.24
ENR/NL-10	0.21
ENR/NL-40	0.16

4.3.2.2 Crosslinking density of rubber (nano)composite materials

The crosslinking density measurements of the rubber (nano)composites at varying filler loading were carried out on swelling tests based on Flory-Rehner's theory. The unfilled ENR matrix system was included as reference. In Table 5, the average molecular weight between crosslink (Mc) and crosslinking density (Vc) of the rubber compounds were presented. The crosslinking density (Vc) consistently increased with increasing filler content, indicating the non-destructive effect of lignin on the network structure of ENR/IND and ENR/NL composites. In particular, ENR/IND-40 composites showed the highest Vc showing a more compact crosslinking network.

Table 5. Average values and standard deviation of average molecular weight between crosslink (Mc) and crosslinking density (Vc) by swelling tests for all systems at different filler loadings.

	Swelling tests	
	Mc (g/mol)	**Vc (mol/cm^3) *10^{-4}**
ENR	6034.7 ± 161.4	1.70 ± 0.08
ENR/IND-10	4890.1 ± 249.8	2.06 ± 0.06
ENR/IND-40	4285.1 ± 330.8	2.71 ± 0.15
ENR/NL-10	5143.5 ± 184.9	2.03 ± 0.09
ENR/NL-40	5096.3 ± 218.6	2.20 ± 0.12

4.3.2.3 Dynamic mechanical properties of rubber (nano)composite materials

The storage modulus (E') of the obtained rubber (nano)composite materials at different filler loadings was investigated by means of DMA analysis at ambient temperature (25°C) as it is illustrated in Table 6. The unfilled ENR matrix system was included as a reference.

The E' of the rubber (nano)composites increased with increasing filler content (IND and NL). The increase in E' indicated a higher stiffness of materials compare to the unfilled rubber matrix. In particular, a slight increase in the storage modulus was observed in highly filled composites (40 wt.% IND) with respect to the filled nanocomposites (40 wt.% NL) increasing from 0.66 MPa to 0.71 MPa (3.5% of error). The introduction of lignin nanoparticles (NL), should have demonstrated an improvement in the filler-matrix interactions compared to the introduction of microlignin particles, which is characteristic of the nano-size dimension with the matrix. This analysis was developed as a preliminary test to observe the initial trend of elastic behaviour of the samples.

Table 6. Storage modulus E' values for all the systems at different filler loadings including the unfilled ENR matrix system as reference. The analysis was carried out with a margin of error between 2 and 3.5% for each sample.

	E' (MPa)
ENR	0.40 ± 2.0%
ENR/IND-10	0.47 ± 2.3%
ENR/IND-40	0.71 ± 3.5%
ENR/NL-10	0.49 ± 2.4%
ENR/NL-40	0.66 ± 3.3%

4.3.2.4 Tensile properties of rubber (nano)composite materials

The mechanical properties of the (nano)composite materials at increasing filler loadings were investigated by means of tensile tests on dog-bone specimens (Figure 14). Stress-strain curves of all systems are presented in Figure 15, where distinctive responses can be observed. Figure 16 and 17 summarise the trends observed on tensile modulus at 2% ($E_{2\%}$), 100% ($E_{100\%}$) and 300% ($E_{300\%}$) strain, tensile strength σ_u and elongation at break ε_{br} for all systems including the unfilled ENR matrix as reference.

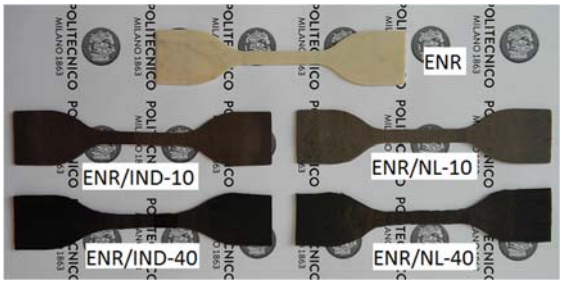

Figure 14. Dog-bone specimens of all systems including the unfilled matrix as reference.

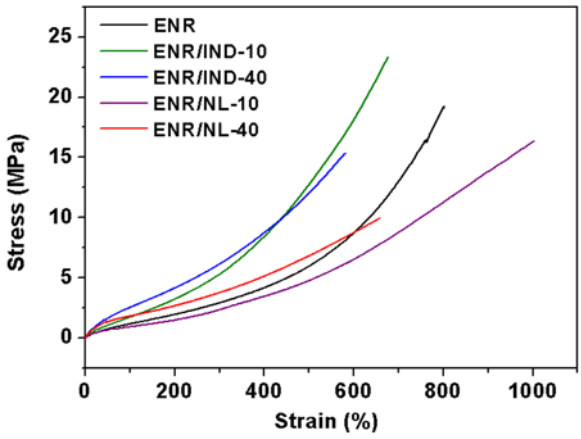

Figure 15. Strain-stress curves of ERN, ERN/IND-10, ERN/IND-40, ERN/NL-10 and ERN/NL-40 systems.

Tensile modulus at 2%, 100% and 300% strain was calculated by stress-strain curve for each sample. As it is reported in Figure 16, the addition of fillers (IND and NL) improved the stiffness of the rubber matrix in terms of tensile modulus values at 2% of elongation, specially for the systems with high filler content (40wt.%) (ENR/IND-40 $E_{2\%}$ = 5.5 MPa, ENR/NL-40 $E_{2\%}$ = 4.9 MPa, ENR $E_{2\%}$ = 2.2 MPa) where IND showed 10% more of stiffness. The results followed the same trend as the results obtained in the DMA analysis (see Table 6). The reinforcing efficiency of filler on rubber materials can be measured by means of the reinforcing index (RI), which can be defined as the ratio of the modulus at 100% strain to the modulus at 300% strain[54,74,75]. A higher value of RI corresponds to a higher reinforcing effect and a stronger rubber-filler interaction. Table 7 shows the reinforcing index (RI) of all systems and it is observed that the 100% and 300% modulus of all filled materials slightly increased compared to the unfilled material (ENR). Especially for the systems with IND as filler. The variation of RI followed a similar trend as the modulus. The RI for ENR/IND-10 system indicated the strongest lignin– rubber interactions. The composites containing NL as filler did not improve the reinforcing effect with respect to IND as filler. These preliminary negative trends are in line with recent literature reports on the reinforcing effect of a lignin on rubber and may be correlated to the poor interfacial interaction due to direct mixing of lignin and rubber since, unfortunately, lignin shows little or no reinforcing effect if it is directly mixed with rubber[76]. It is believed to be the following two factors which cause this phenomenon: the large size of lignin particles and the lack of strong interfacial interactions between lignin and rubber matrix[54]. This trend could have changed with the incorporation of nano-scale dimensions establishing a high surface/volume ratio characteristic of the nanolignin with the matrix, but the directly mixed seemed not to

improve. A reduction of the size of lignin particles down to the nanoscale was expected to lead to improved filler-matrix interactions, thereby leading to improve mechanical response. However, the experimental evidence demonstrated that directly mixing NL into ENR did not yield the expected results, likely due to unefficient level of dispersion and limited chemical affinity between lignin and rubber. Possible surface functionalization of lignin nanoparticles made by silanization is discussed in the future perspectives.

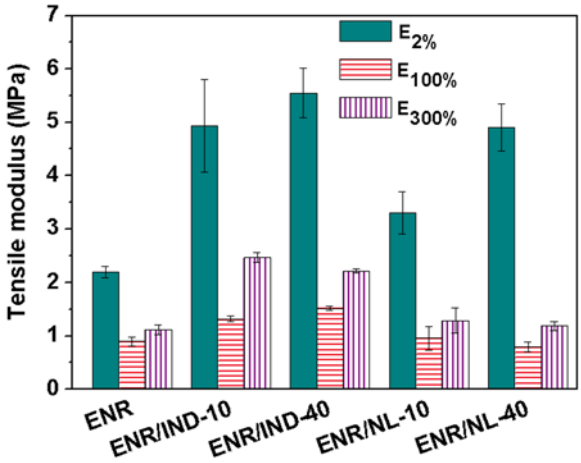

Figure 16. Values of tensile modulus at 2% ($E_{2\%}$), 100% ($E_{100\%}$) and 300% ($E_{300\%}$) for all (nano)composite systems at varying filler loading. The unfilled ERN matrix is also included as reference. Error bars indicate the standard deviation out of at least five measurements on different specimens.

Table 7. Modulus values at 100% ($E_{100\%}$) and 300% ($E_{300\%}$) and reinforcing index (RI) of vulcanized ENR, ENR/IND-10, ENR/IND-40, ENR/NL-10 and ENR/NL-40 systems.

	$E_{100\%}$	$E_{300\%}$	RI
ENR	0.90	1.12	1.24
ENR/IND-10	1.32	2.48	1.88
ENR/IND-40	1.52	2.22	1.46
ENR/NL-10	0.96	1.29	1.34
ENR/NL-40	0.80	1.19	1.49

According to the ultimate tensile strength response of the composite materials as a function of filler loading (Figure 17a), a decrease of σ_u was found with increasing filler content (IND and NL), especially for ENR/NL. The values decreased from 21 MPa (reference ENR) to 17.2 MPa (ENR /NL-10), 15.3 MPa (ENR /IND-40) and 9.7 MPa (ENR /NL-40). Only a very slight increase of σu was observed in the ENR/IND-10 system with a value of 23 MPa. In particular, in the case of ENR/IND-10 systems, σ_u values (23 MPa) comparable to those found for the unfilled PU matrix (21 MPa) are observed. Therefore, this results suggested that the inclusion of the fillers did not show a reinforcing effect on ENR matrix. Regarding elongation at break (Figure 17b), a significant decrease of ε_{br} was observed in ENR/IND systems in comparison to the reference (ENR = 835%, ENR/IND-10 = 661% and ENR/IND-40 = 582%). However, in the case of ENR/NL systems, especially for ENR/NL-10, comparable results were found (≈ 840 %). Therefore, the incorporation of a 10 % of filler did not affect the elongation at break. However, with the increasing percentage of filler (40 wt.% NL-6h) into the matrix, the elongation value at break decreases 660%.

These mechanical characteristics indicate that the addition of nanosized lignin particles allows to improve the stiffness of the rubber matrix material without significantly affecting its elongation at break with 10% of NL-filler, although a decrease of toughness was noted in both ENR/IND and ENR/NL composites at increasing filler loading. However, the improvement in the rubber matrix with the nanolignin particles compared to microlignin particles was not observed.

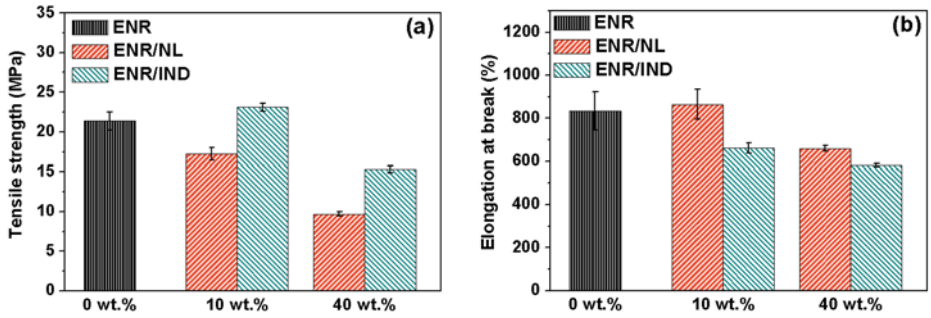

Figure 17. Values of (a) tensile strength σ_u and (b) elongation at break ε_{br} for all (nano)composite systems at varying filler loading. The unfilled ERN matrix is also included for reference. Error bars indicate the standard deviation out of at least five measurements on different specimens.

4.4 POLYURETHANE DISPERSION

4.4.1 Experimental section

4.4.1.1 Materials

All materials used in this study are commercially available. The polyurethane used as matrix material for the nanocomposites was supplied by ICAP-SIRA Chemicals and Polymers S.p.A. in the form of aqueous dispersion (Idrocap 954). It was based on hexamethylene diisocyanate (HMDI) and on a macrodiol obtained from adipate of mixed glycols and polypropylene glycol, the latter derived from renewable sources.

4.4.1.2 Preparation of waterborne polyurethane- based (nano)-composites

The aqueous PU solution (35% w/w) and the appropriate IND or NL suspensions were thoroughly mixed by stirring. The mass amount of IND and NL in the PU matrix was 5%, 10% and 20% and the samples were named PU/IND-5, PU/NL-5, PU/IND-10, PU/NL-10, PU/IND-20 and PU/NL-20 respectively. Water in each mixture was allowed to evaporate for 2 days at room temperature under a fume-hood and for 1 day in a vacuum oven at 50°C, until constant weight was reached. Solid samples used for characterization were obtained by hot-press molding. An example of molded polyurethane-based (nano)composite samples is shown in Figure 18.

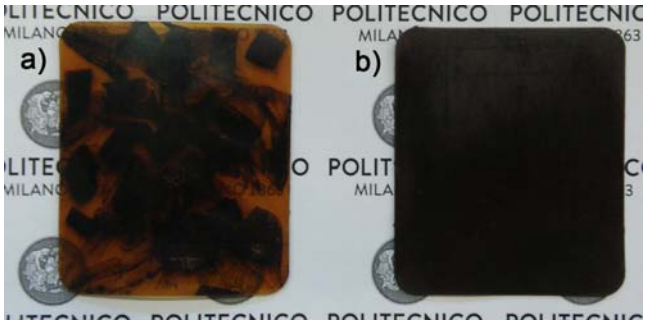

Figure 18. Photographic image of molds of (a) PU/IND and (b) PU/NL composite systems at 10 wt.% filler loading.

4.4.1.3 Materials characterization

4.4.1.3.1 Scanning electron microscopy (SEM)

SEM analyses were performed on cryo-fractured IND and NL-PU composites using a Carl Zeiss EVO 50 Extended Pressure scanning electron microscope (acceleration voltage of 15.00–17.50 kV) to evaluate the filler particle distribution in the polymer matrix.

4.4.1.3.2 Thermo-gravimetric analysis (TGA)

TGA measurements were obtained on solid state samples (approximate weight 15 mg) by means of a Q500 TGA system (TA Instruments). The samples were heated from ambient temperature to 800 °C at a scan rate of 20 °C min^{-1} both in air and nitrogen atmosphere.

4.4.1.3.3 Tensile tests

Tensile properties were determined at room temperature by means of a Zwick/Roell Z010 (Zwick Roell Italy) equipped with a 10 kN load cell and a longstroke extensometer. All specimens were tested according to the standard test method ASTM D638 (Type I specimen, dimensions down-scaled to 30%,

namely 15 mm gage length, 4 mm width of narrow section, 2 mm thickness). At least five samples were tested for each experimental condition to obtain average values.

4.4.2 Results and discussion

4.4.2.1 Scanning Electron Microscopy (SEM) of (nano) composite materials

To obtain lignin-based nanocomposite materials, NL-6h particles were incorporated at varying concentrations into a thermoplastic PU matrix and the resulting composite materials were characterized in terms of thermal and mechanical properties. To qualitatively evaluate the level of dispersion of the fillers in the polymeric matrix, SEM analysis was employed on PU/NL-10 nanocomposites (10 wt.% NL-6h in PU) and compared with the corresponding PU/IND-10 composite material (10 wt.% IND in PU). As shown in Figure 19a, the introduction of micrometer-sized lignin particles into the PU matrix results in the formation of large agglomerates clearly visible as protruding features on the top surface of the sample. Similarly, the cryo-fractured section of PU/IND-10 systems highlights the poor level of dispersion of pristine lignin within the polymeric system, with the presence of large aggregates and defects randomly dispersed throughout the bulk of the material. As opposed to this, PU/NL-10 systems show an excellent level of dispersion and distribution of NL particles into the PU polymer matrix, as confirmed by the relatively smooth surface of these systems and the absence of any noticeable aggregate within the volume of the samples (Figure 19b). SEM images of all investigated filler concentrations are presented in Figure 20, which followed the same trend. Given the importance of a high quality dispersion of the reinforcing filler in the polymeric matrix for high-

performance composite materials, these evidences may anticipate improved mechanical properties of PU/NL compared with PU/IND systems, as will be discussed in the following sections.

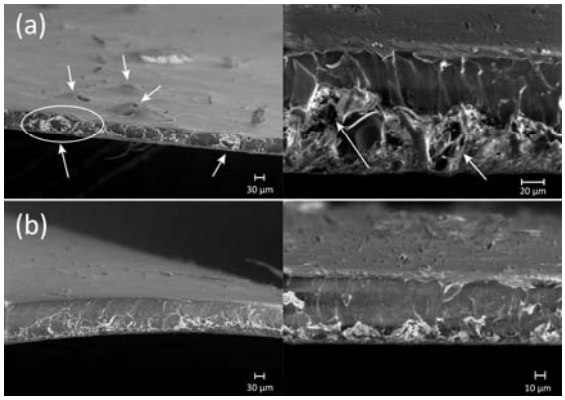

Figure 19. SEM images of (a) PU/IND composites and (b) PU/NL nanocomposites. In both samples 10 wt.% filler loading was employed. White arrows indicate lignin agglomerates.

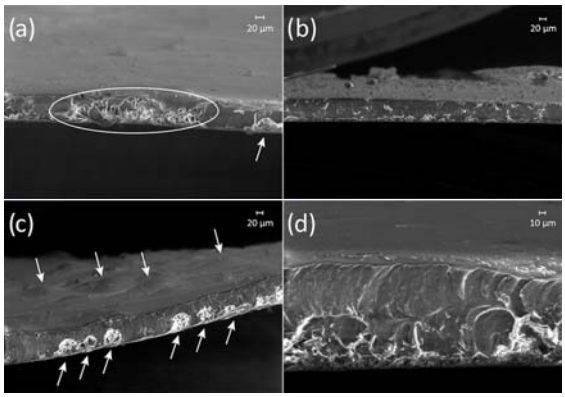

Figure 20. SEM images of PU/IND and PU/NL (nano)composites: (a) PU/IND-5, (b) PU/NL-5, (c) PU/IND-20 and (d) PU/NL-20.

4.4.2.2 Thermo-gravimetric analysis (TGA) of (nano) composite materials

The thermal stability of the obtained (nano)composite materials was investigated by means of thermo-gravimetric analysis (TGA) in nitrogen atmosphere. The results are presented in Figure 21, where TGA curves of PU/NL nanocomposites at increasing NL-6h loading are compared with the corresponding systems based on pristine micrometer-sized lignin particles (PU/IND). All materials exhibit a three-step thermal degradation profile which reflects the thermolytic response of the unfilled PU matrix. In particular, a first weight loss (~ 8-10%) is found in the 200-300 °C temperature range that can be associated with cleavage of the urethane bonds in the polymeric matrix[64]. Between 300 °C and 400 °C another ~20% thermal degradation step is observed that may be ascribed to the decomposition of ether and ester linkages. Finally, a third major weight-loss region is observed above 400 °C as a result of the complete depolymerization and thermal degradation of the polymer. The addition of NL-6h leads to a slight improvement of the thermolytic stability compared to the unfilled PU matrix at high temperatures (> 400 °C), as indicated by the increase in the maximum mass loss derivative temperature (T_{DTGmax}) observed in PU/NL nanocomposites for increasing NL-6h loading (Table 8). Similarly, the char mass residue at 750 °C ($R_{750\ °C}$) is found to progressively increase in PU/NL systems with the addition of increasing amounts of NL-6h ($R_{750\ °C}$ = 3%, 5%, 9% for PU/NL-5, PU/NL-10 and PU/NL-20, respectively) ultimately leading to improved stability compared with the unfilled PU matrix ($R_{750\ °C}$ = 1%). On the contrary, no clear trends are observed for PU/IND composites in this high temperature region at increasing filler loading, likely due to a relatively poorer stabilizing effect of IND at high temperatures. In the lower temperature region (< 300 °C), no significant

modifications with respect to the thermal response of unfilled PU are observed irrespective of the type of lignin-based filler employed (IND vs. NL-6h), although a relatively more stable behavior is observed on PU/NL nanocomposites. Indeed, these systems exhibit higher thermal degradation temperatures at 10% ($T_{10\%}$) and 50% ($T_{50\%}$) mass loss as compared with the IND-based counterpart. In particular, slightly improved thermal stability is observed on PU/NL nanocomposites with respect to unfilled PU in terms of $T_{50\%}$ values (Table 8).

Table 8. Thermal degradation temperatures at 10% (T_{10}) and 50% (T_{50}) mass loss, final char residue at 750 °C ($R_{750\ °C}$) and maximum mass loss derivative temperature (T_{DTGmax}) for PU/IND and PU/NL composites at different filler loadings, as obtained from TGA in nitrogen atmosphere.

	$T_{10\%}$ [°C]	$T_{50\%}$ [°C]	$R_{750°C}$ [%]	T_{DTGmax} [°C]
PU	308	433	1	442
PU/IND-5	290	428	2	442
PU/IND-10	294	431	8	443
PU/IND-20	294	431	7	442
PU/NL-5	307	434	3	445
PU/NL-10	300	433	5	443
PU/NL-20	305	436	9	445

These trends may be associated with the higher thermal stability of NL-6h compared with unfilled PU and with untreated IND at high temperatures (see Figure 22), as also observed in recent reports on analogous systems[42,48]. The thermo-oxidative properties of the lignin-based composite materials were investigated by means of TGA under air flux, and similar trends as those observed under N_2 atmosphere were observed on all systems, further

confirming the positive stabilizing effect of the addition of NL-6h especially at high filler loadings.

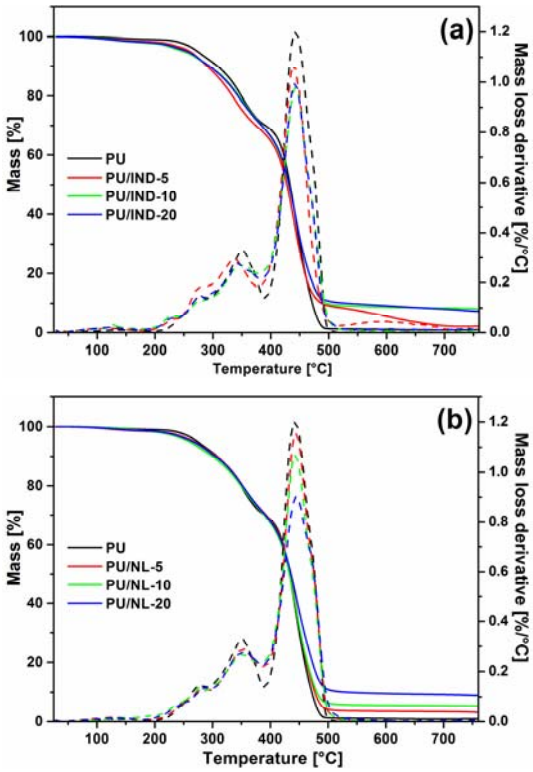

Figure 21. Thermo-gravimetric analysis curves (under nitrogen atmosphere) for (a) PU/IND composite and (b) PU/NL nanocomposite materials at different filler loadings.

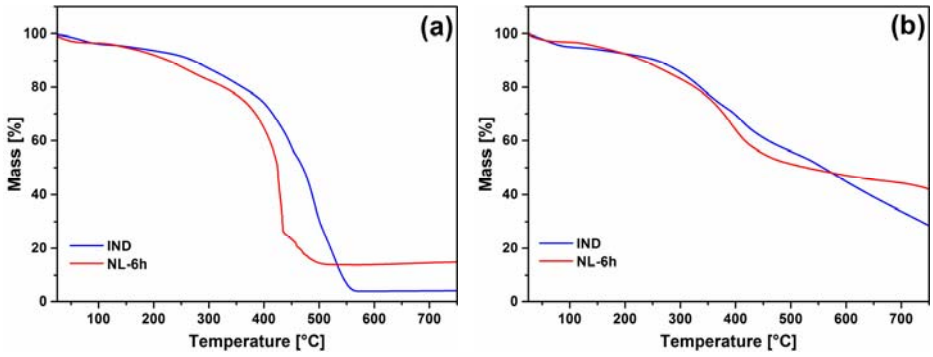

Figure 22. Thermo-gravimetric analysis curves for IND and NL in (a) air and (b) N_2 atmosphere.

4.4.2.3 Tensile properties of (nano) composite materials

The mechanical properties of the composite materials at increasing filler loadings were investigated by means of tensile tests on dog-bone specimens (Figure 23). Figure 24 summarizes the trends observed on elastic modulus E, ultimate tensile strength σ_u and elongation at break ε_{br} for all systems (the unfilled PU matrix was also included for reference). Representative stress-strain curves of PU/IND, PU/NL and unfilled PU matrix are presented in Figure 24a, where distinctive responses can be clearly observed depending on the nature of reinforcing filler employed. Compared to the unfilled PU matrix, PU/NL nanocomposite materials exhibit a progressive increase in elastic modulus for increasing NL-6h loadings, leading to E values of 45.4 MPa, 52.5 MPa and 65.6 MPa for PU/NL-5, PU/NL-10 and PU/NL-20 systems, respectively (Figure 24b). As a result, a twofold increase in elastic modulus is observed in highly filled nanocomposites (20 wt.% NL-6h) with respect to the unfilled matrix material (33.0 MPa). This trend is in line with previous studies on the reinforcing effect of lignin nanoparticles in polymer-based nanocomposites[46,47] and may be correlated with the ability of nanolignin to

establish effective (non-covalent) interactions with the polymer matrix due to the high surface/volume ratio characteristic of the nano-scale dimensions resulting from the ultrasonication process. As opposed to the case of PU/NL, unclear trends are observed on the elastic modulus of composite materials based on untreated lignin. Indeed, E values in the 50 MPa range are found for all PU/IND systems irrespective of the amount of lignin present in the composite. This behavior may be explained by considering the poor level of dispersion of micrometer-sized untreated lignin particles in the PU matrix (SEM analysis, Figure 19 and Figure 20) that may prevent efficient filler/matrix interactions, thus ultimately leading to limited mechanical reinforcing effect. Additionally, the large lignin aggregates observed both on the surface and in the bulk of PU/IND composite samples may act as defect sites that may induce the formation of cracks during the mechanical test, ultimately leading to limited reinforcing effect and relatively poor reproducibility of the results (as evidenced by the non-negligible magnitude of the error bars observed in Figure 24b for PU/IND composite systems). Indeed, visual inspection of the dog-bone specimens employed for tensile tests clearly highlighted uneven distribution of the filler in PU/IND systems which was not observed in PU/NL systems (Figure 23). When examining the ultimate tensile strength response of the composite materials as a function of filler loading (Figure 24c), a marked decrease of σ_u is found in the case of PU/IND systems, with values dropping from 6.1 MPa (PU/IND-5) to 3.8 MPa (PU/IND-20). On the contrary, a slight increase of σ_u is observed in NL-based nanocomposites especially for high filler content systems. In particular, in the case of PU/NL-20 systems, σ_u values (6.5 MPa) comparable to those found for the unfilled PU matrix (6.9 MPa) are observed. This behavior indicates that the addition of nanosized lignin particles allows to improve the stiffness of

the polymeric matrix material without significantly affecting its fracture toughness, although a decrease of elongation at break is observed on both PU/IND and PU/NL composites at increasing filler loading (Figure 24d). These mechanical characteristics (higher elastic modulus accompanied by preserved strength) may widen the use of such materials to low deformation applications where greater structural integrity is required, such as for instance in the automotive interior field or in the footwear field[65,66].

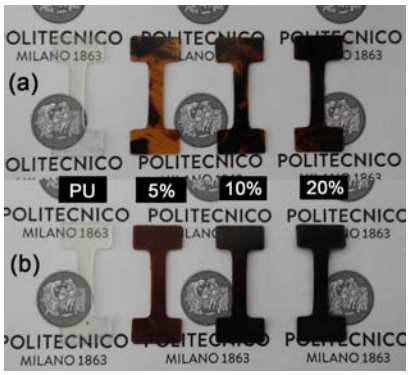

Figure 23. Photographic image of representative dog-bone samples of (a) PU/IND and (b) PU/NL composite systems at varying filler loading. For comparison, the unfilled PU matrix system is also presented (transparent samples).

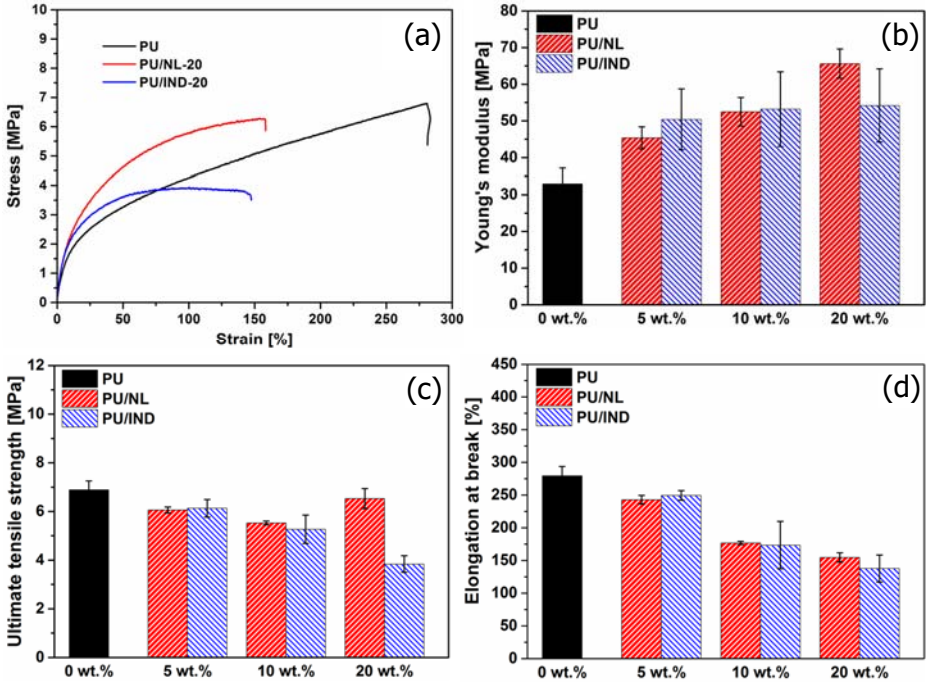

Figure 24. (a) Representative strain-stress curves of PU, PU/IND-20 and PU/NL-20 systems. Average values of (b) elastic modulus E, (c) ultimate tensile strength σ_u and (d) elongation at break ε_{br} for all (nano)composite systems at varying filler loading. The unfilled PU matrix is also included for reference. Error bars indicate the standard deviation out of at least five measurements on different specimens.

4.5 CONCLUSIONS AND FUTURE PERSPECTIVES

Firstly, a straightforward approach was presented in this work to obtain lignin nanoparticles suitable to be used as bio-based fillers in polymer nanocomposites. Such approach consists in the ultrasonic treatment of a commercially available softwood kraft lignin to yield lignin/water dispersions characterized by an excellent colloidal stability. By suitably tuning the ultrasonic treatment time, a remarkable decrease in lignin particle size could be attained, leading to the formation of lignin nanoparticles of around 10-50 nm. UV-vis spectroscopy evidenced that a partial loss of conjugated moieties (α-carbonyl groups and esters of hydrocinnamic acids) may occur upon the treatment as a result of the interaction between lignin and the radical species forming during the ultrasonication process. In addition, the FTIR spectroscopy showed that the ultrasonication treatment may impart some chemical modifications to lignin, resulting in an increased oxidation of NL compared to the parent material. This gives rise to an increased polarity in NL that well correlates with the markedly improved stability in water compared to pristine lignin.

The obtained NL particles were initially incorporated at varying concentrations into a ENR matrix and vulcanization parameters, density crosslinking and mechanical properties of the resulting (nano)composite materials were assessed. The vulcanization process indicated that the retardant vulcanization effect with the introduction of IND was weaker than the effect found with the incorporation of NL. The crosslinking density of the systems increased with increasing filler content. This indicated the non-destructive effect of lignin in the network structure (ENR/IND and ENR/NL composites). In particular, ENR/IND-40 composites showed the highest Vc demonstrating a more compact crosslinking network. Finally, these

mechanical characteristics indicated that the use of nanosized lignin particles allowed to improve the stiffness of the rubber matrix material without affecting its elongation at break, especially for ENR/NL-10. Nevertheless, a decrease of fracture toughness was observed at increasing filler loading. However, the addition of nanosized lignin particles did not show an improvement in the matrix-filler interactions of the mechanical properties compared to microsized lignin particles. This trend was also observed with the storage modulus E' values by DMA analysis. A further improvement in the interfacial interactions between lignin/nanolignin and rubber matrix is needed. The reduction of the particles in the lignin was not enough to reduce polarity and improve the chemical affinity between the filler and the matrix. Then, a future step in this research may be the use of a coupling agent (such as silanes) to improve or increase the adhesion between the interfaces. These molecules have a structure as $R_{(4-n)}$-Si-$(R'0X)_n$ (n=1,2) where R is an alkoxy group, R 'is an alkyl bond and X is an organic functional group.

Successively, the obtained NL particles were incorporated at varying concentrations into a thermoplastic PU matrix and the morphological, thermal and mechanical properties of the resulting (nano)composite materials were assessed. SEM analysis on NL-based nanocomposites evidenced an excellent level of dispersion and distribution of NL particles into the PU matrix as opposed to untreated lignin. In addition, a slight improvement of thermal stability was observed on NL-based nanocomposites compared with systems incorporating untreated lignin, especially at high temperatures (> 400 °C), which was associated with the higher thermal stability of the nano-sized bio-based filler. Finally, tensile tests on the (nano)composites at increasing filler loading evidenced significantly improved mechanical properties of the systems incorporating NL particles compared to pristine lignin in terms of

elastic modulus, ultimate tensile strength and elongation at break. These trends were correlated with the ability of NL to establish effective non-covalent interactions with the polymer matrix due to the high surface/volume ratio characteristic of the nano-scale dimensions resulting from the ultrasonication process. The results of this study give a clear demonstration of a viable environmentally friendly strategy to obtain waterborne polyurethane-based nanocomposites reinforced with NL in a straightforward manner and provide further evidence of the potential of lignin nanoparticles as fully bio-derived fillers for advanced nanocomposite applications.

4.6 REFERENCES

1. Gellerstedt G, Henriksson G (2008) Lignins: Major sources, structure and properties. In monomers, polymers and composites from renewable resources; Belgacem MN, Gandini A, Eds, Elsevier: Amsterdam. Chapter 9, 201-224.

2. Ragauskas AJ, Beckham GT, Biddy MJ, Chandra R, Chen F, Davis MF, Davison BH, Dixon RA, Gilna P, Keller M, Langan P, Naskar AK, Saddle JN, Tschaplinski TJ, Tuskan GA, Wyman CE (2014) Lignin valorization: improving lignin processing in the biorefinery. Science 344:1246843-1 - 1246843-10.

3. Tuck CO, Pérez E, Horváth IT, Sheldon RA, Poliakoff M (2012) Valorization of biomass: deriving more value from waste. Science 337:695-699.

4. Andrzej VAK (2011) Challenges in industrial applications of technical lignins. BioResources 6:3547-3568.

5. Lora J (2008) Industrial commercial lignins: sources, properties and applications, In Monomers, polymers and composites from renewable resources; Belgacem MN, Gandini A, Eds, Elsevier: Amsterdam. Chapter 10, 225-241.

6. Calvo-Flores FG, Dobado JA, Isac-Garcia J, Martin-Martinez FJ (2015) lignin and lignans as renewable raw materials. John Wiley and Sons, Ltd.: Chichester.

7. Doherty WOS, Mousavioun P, Fellows CM (2011) Value-adding to cellulosic ethanol: Lignin polymers. Ind Crops Prod 33:259.

8. Hatakeyama H, Hatakeyama T (2010) Lignin structure, properties, and applications, in Biopolymers; Abe A, Dusek K, Kobayashi S, Eds, Springer: Berlin, Vol. 232, 1-63.

9. Alekhina M, Ershova O, Ebert A, Heikkinen S, Sixta H (2015) Softwood kraft lignin for value-added applications: Fractionation and structural characterization. Ind Crops Prod 66:220-228.

10. Arshanitsa A, Ponomarenko J, Dizhbite T, Andersone A, Gosselink RJA, Van der Putten J, Lauberts M, Telysheva G (2013) Fractionation of technical lignins as a tool for improvement of their antioxidant properties. J Anal Appl Pyrolysis 103:78-85.

11. Boeriu CG, Fiţigău FI, Gosselink RJA, Frissen AE, Stoutjesdijk J, Peter F (2014) Fractionation of five technical lignins by selective extraction in green solvents and characterisation of isolated fractions. Ind Crops Prod 62:481-490.

12. Colyar KR, Pellegrino J, Kadam K (2008) Fractionation of pre-hydrolysis products from lignocellulosic biomass by an ultrafiltration ceramic tubular membrane. Sep Sci Technol 43:447-476.

13. Cui C, Sun R, Argyropoulos DS (2014) Fractional precipitation of softwood kraft lignin: isolation of narrow fractions common to a variety of lignins. ACS Sustainable Chem Eng 2:959-968.

14. Dodd AP, Kadla JF, Straus SK (2015) Characterization of fractions obtained from two industrial softwood kraft lignins. ACS Sustainable Chem Eng 3:103-110.

15. Helander M, Theliander H, Lawoko M, Henriksson G, Zhang L, Lindström ME (2013) Fractionation of technical lignin: molecular mass and ph effects. BioResources 8:2270-2282.

16. Li H, McDonald AG (2014) Fractionation and characterization of industrial lignins. Ind Crops Prod 62:67-76.

17. Saito T, Perkins JH, Vautard F, Meyer HM, Messman JM, Tolnai B, Naskar AK (2014) Methanol fractionation of softwood kraft lignin: impact on the lignin properties. ChemSusChem 7:221-228.

18. Toledano A, Serrano L, Garcia A, Mondragon I, Labidi J (2010) Comparative study of lignin fractionation by ultrafiltration and selective precipitation. Chem Eng J 157:93-99.

19. Passoni V, Scarica C, Levi M, Turri S, Griffini G (2016) Fractionation of industrial softwood kraft lignin: solvent selection as a tool for tailored material properties. ACS Sustainable Chem Eng 4:2232-2242.

20. Bonini C, D'Auria M, Emanuele L, Ferri R, Pucciariello R, Sabia AR (2005) Polyurethanes and polyesters from lignin. J Appl Polym Sci 98:1451-1456.

21. Cateto CA, Barreiro MF, Rodrigues AE, Brochier-Salon MC, Thielemans W, Belgacem MN (2008) Lignins as macromonomers for polyurethane synthesis: A comparative study on hydroxyl group determination. J Appl Polym Sci 109:3008-3017.

22. Duval A, Lawoko M (2014) A review on lignin-based polymeric, micro- and nano-structured materials. React Funct Polym 85:78-96.

23. Gandini A, Belgacem MN (2008) Lignins as components of macromolecular materials, in Monomers, polymers and composites from renewable resources; Belgacem MN, Gandini A, Eds, Elsevier: Amsterdam. Chapter 11, 243-271.

24. Isikgor FH, Becer (2015) Lignocellulosic biomass: a sustainable platform for the production of bio-based chemicals and polymers. CR Polym Chem 6:4497-4559.

25. Laurichesse S, Avérous L (2014) Chemical modification of lignins: Towards biobased polymers. Prog Polym Sci 39:1266-1290.

26. Saito T, Perkins JH, Jackson DC, Trammel NE, Hunt MA, Naskar AK (2013) Development of lignin-based polyurethane thermoplastics. RSC Adv 3:21832-21840.

27. Thanh Binh NT, Luong ND, Kim DO, Lee SH, Kim BJ, Lee YS, Nam JD (2009) Synthesis of Lignin-Based Thermoplastic Copolyester Using Kraft Lignin as a Macromonomer. Compos Interfaces 16:923-935.

28. Griffini G, Passoni V, Suriano R, Levi M, Turri S (2015) Polyurethane coatings based on chemically unmodified fractionated lignin. ACS Sustainable Chem Eng 3:1145-1154.

29. Kaewtatip K, Thongmee J (2013) Effect of kraft lignin and esterified lignin on the properties of thermoplastic starch. Mater Des 49:701-704.

30. Thakur VK, Thakur MK, Raghavan P, Kessler MR (2014) Progress in green polymer composites from lignin for multifunctional applications: A Review. ACS Sustainable Chem Eng 2:1072-1092.

31. Luo X, Mohanty A, Misra M (2013) Lignin as a reactive reinforcing filler for water-blown rigid biofoam composites from soy oil-based polyurethane. Ind Crops Prod 47:13-19.

32. Zhang L, Huang J (2001) Effects of nitrolignin on mechanical properties of polyurethane–nitrolignin films. J Appl Polym Sci 80:1213-1219.

33. Sailaja RRN, Deepthi MV (2010) Mechanical and thermal properties of compatibilized composites of polyethylene and esterified lignin. Mater Des 31:4369-4379.

34. Maldhure AV, Chaudhari AR, Ekhe JD (2011) Thermal and structural studies of polypropylene blended with esterified industrial waste lignin. J Therm Anal Calorim 103:625-632.

35. Dehne L, Vila Babarro C, Saake B, Schwarz KU (2016) Influence of lignin source and esterification on properties of lignin-polyethylene blends. Ind Crops Prod 86:320-328.

36. Yeo J-S, Seong D-W, Hwang S-H (2015) Chemical surface modification of lignin particle and its application as filler in the polypropylene composites. J Ind Eng Chem 31:80-85.

37. Zhang C, Wu H, Kessler MR (2015) High bio-content polyurethane composites with urethane modified lignin as filler. Polym 69:52-57.

38. Schaefer DW, Justice RS (2007) How nano are nanocomposites?. Macromolecules 40:8501-8517.

39. Qian Y, Deng Y, Qiu X, Li H, Yang D (2014) Formation of uniform colloidal spheres from lignin, a renewable resource recovered from pulping spent liquor. Green Chem 16:2156-2163.

40. Lievonen M, Valle-Delgado JJ, Mattinen M-L, Hult E-L, Lintinen K, Kostiainen MA, Paananen A, Szilvay GR, Setala H, Osterberg M (2016) A simple process for lignin nanoparticle preparation. Green Chem 18:1416-1422.

41. Frangville C, Rutkevičius, M, Richter AP, Velev OD, Stoyanov SD, Paunov VN (2012) Fabrication of environmentally biodegradable lignin nanoparticles. ChemPhysChem:13:4235-4243.

42. Nair SS, Sharma S, Pu Y, Sun Q, Pan S, Zhu JY, Deng Y, Ragauskas AJ (2014) High shear homogenization of lignin to nanolignin and thermal stability of nanolignin-polyvinyl alcohol blends. ChemSusChem 7:3513-3520.

43. Gilca IA, Popa VI, Crestini C (2015) Obtaining lignin nanoparticles by sonication. Ultrason Sonochem 23:369-375.

44. Zimniewska M, Kozłowski R, Batog J (2010) Nanolignin modified linen fabric as a multifunctional product. Mol Cryst Liq Cryst 484:43-50.

45. Jiang C (2013) Nano-lignin filled natural rubber composites: Preparation and characterization. Express Polym Lett 7:480-493.

46. Yang W, Kenny JM, Puglia D (2015) Structure and properties of biodegradable wheat gluten bionanocomposites containing lignin nanoparticles. Ind Crops Prod *74*:348-356.

47. Yang W, Fortunati E, Dominici F, Kenny JM, Puglia D (2015) Effect of processing conditions and lignin content on thermal, mechanical and degradative behavior of lignin nanoparticles/polylactic (acid) bionanocomposites prepared by melt extrusion and solvent casting. Eur Polym J 71: 126-139.

48. García A, Erdocia X, González Alriols M, Labidi J (2012) Effect of ultrasound treatment on the physicochemical properties of alkaline lignin. Chem Eng Process 62:150-158.

49. Seino T, Yoshioka A, Fujiwara M, Chen K-L, Erata T, Tabata M, Takai M (2001) ESR studies of radicals generated by ultrasonic irradiation of lignin solution. An application of the spin trapping method. Wood Sci Technol 35:97-106.

50. Wells JrT, Kosa M, Ragauskas AJ (2013) Polymerization of Kraft lignin via ultrasonication for high-molecular-weight applications. Ultrason Sonochem *20*:1463-1469.

51. Kosikova B, Alexy P, Gregorova A (2003) Use of lignin products derived from wood pulping as environmentally desirable component of composite rubber materials. Wood Research 48:62-67.

52. Kosikova B, Gregorova A, Osvald A, Krajcovicova J (2007) Role of lignin filler in stabilization of natural rubber-based composites. J Appl Polym Sci 103:1226-1231.

53. Jiang C, He H, Yao X, Yu P, Zhou L, Jia D (2015) In situ dispersion and compatibilization of lignin/epoxidized natural rubber composites: reactivity, morphology and property. J Appl Polym Sci 132.

54. Bahl K, Miyoshi T, Jana SC (2014) Hybrid fillers of lignin and carbon black for lowering of viscoelastic loss in rubber compounds. Polymer 55: 3825-3835.

55. Engels HW, Pirkl HG, Albers R, Albach RW, Krause J, Hoffmann A, Casselmann H, Dormish J (2013) Polyurethanes: versatile materials and sustainable problem solvers for today's challenges. Angew Chem Int Ed 52: 9422-9441.

56. Schon F, Gronski W (2003) Filler networking of silica and organoclay in rubber composites: Reinforcement and dynamic-mechanical properties. Kautschuk Gummi Kunststoffe 56:166-171.

57. Hashim AS, Kohjiya S (1994) Curing of epoxidized natural-rubber with p-phenylenediamine. J Polym Sci A- Polym Chem 32:1149-1157.

58. Akiba M, Hashim AS (1997) Vulcanization and crosslinking in elastomers. Prog Polym Sci 22:475-521.

59. Ghosh P, Katare S, Patkar P, Caruthers JM, Venkatasubramanian V, Walker KA (2003) Sulfur vulcanization of natural rubber for benzothiazole accelerated formulations: From reaction mechanisms to a rational kinetic model. Rubber Chemistry and Technology 76:592-693.

60. Dogadkin BA (1958) The mechanism of vulcanization and the action of accelerators. J Polym Sci A- Polym Chem 30:351-361.

61. Gellerstedt G (2015) Softwood kraft lignin: Raw material for the future. Ind Crops Prod 77:845-854.

62. Gärtner A, Gellerstedt G, Tamminen T (1999) Determination of phenolic hydroxyl groups in residual lignin using a modified UV-method. Nord Pulp Pap Res J 14:163-170.

63. Faix O (1992) Fourier Transform Infrared Spectroscopy, in Methods in lignin chemistry; Lin SY, Dence CW, Eds, Springer-Verlag: Heidelberg. Chapter 5, 233–241.

64. Chattopadhyay DK, Webster DC (2009) Thermal stability and flame retardancy of polyurethanes. Prog Polym Sci 34:1068-1133.

65. Abdeen ZI (2017) In rubber nano blends – preparation, characterization and applications; Markovic G, Visak PM, Eds., Springer International Publishing: Cham. Chapter 4, 89-103.

66. Smart SK, Edwards GA, Martin DJ (2010) In rubber nanocomposites – preparation, properties and applications; Thomas S, Stephen R, Eds, John Wiley & Sons (Asia) Pte Ltd: Singapore**.** Chapter 10, 239-254.

67. Blow CHCM (1993) Manuale di tecnologia della gomma, ed. G. editore.

68. Xia Z (2013) Determination of crosslinking density of hydrogels prepared from microcrystalline cellulose. J Appl Polym Sci 127:4537-4541.

69. ASTM D412-06a (2013) Standard test method for vulcanized rubber and thermoplastic elastomers- tension.

70. Kosıková B, Gregorová A (2005) Sulfur-free lignin as reinforcing component of styrene–butadiene rubber. J Appl Polym Sci 97:924-929.

71. Kumaran M G, De SK (1978) Utilization of lignins in rubber compounding. J Appl Polym Sci 22:1885-1893.

72. Jiang C, He H, Jiang H, Ma L, Jia DM (2013) Nano-lignin filled natural rubber composites: Preparation and characterization. eXPRESS Polymer Lett 7:480-493.

73. Mark JE, Erman B, Roland CM (2013) The Science and Technology of Rubber, Academic Press, 4ed, 337-340.

74. Luginsland H, Frohlich J, Wehmeier A (2002) Influence of different silanes on the reinforcement of silica-filled rubber compounds. Rubber Chem Technol 75:563-579.

75. Barrios VAE, Garcia-Ramirez M (2003) Effect of functionalization on sbr's interaction with carbon black and silica. Int J Polymeric Mater 52:985-998.

76. Doughty JB (1967) US Pat. 3,325,427.

5.
Conclusions

The research work presented in this thesis can be divided into two main parts one dealing with the development and environmental study of a new class of polyester binder based on FDCA suitable as precursor of PU coating materials compared to fossil-based alternatives and the other focusing on the preparation of the nanolignin (NL) particles by ultrasonic treatment of softwood kraft lignin to obtain lignin-water dispersions with an excellent colloidal stability. Successively, the incorporation of the obtained lignin nanoparticles into a waterborne thermoplastic polyurethane and into epoxidized natural rubber to form nanocomposite materials with increasing bio-filler concentration.

In the field of renewable raw materials to obtain biopolymers for the industry, the main goal is the replacement of fossil-based materials to decrease their impact on the environment and human beings, which is a concept based on the principles of green engineering and chemistry, and sustainability. Following this strategy, the development and LCA study of biopolymers such as polyester, polyurethane and lignin were investigated for several applications of the industry. In particular, in the first main objective of the present work, the re-design of the new class of polyester binder based on FDCA as precursors of PU coating materials was realized as schematized in the following:

- **Selection and copolymerization of four different monomers**, all available from modern **biorefinery downstreams**. The selection was according to their functional role in the binder design and primary data availability in the Ecoinvent database and in the open literature.
- This **new class of polyester (100%bio-based)**, which was formed by **glycerine, acid succinic, furandicarboxylic and 1,3-propanediol**, was

compared to three other polyester binders. One of them was formed by **75% bio-based** (Phthalic anhydride). The other two were **100% fossil-based**.

- The PU coatings were obtained by **crosslinking with a polyisocyanate IPDI and the polyester binders** synthesized on lab-scale.

After that, technological validation was performed on all PU coatings, especially for the new precursor of PU1 (based on FDCA), in order to evaluate the performances and possible applications for the industry. The results attested that:

- **PU1 coating** showed a **stiffer material** and a more hydrophilic character leading not only to a **better adhesion** but also to a more **moisture-sensitive surface**.
- Potential applications in the **field of metal coating,** mainly in coil coating and automotive as an **intermediate layers or primers** where a high adhesion of the materials and recoatability are needed.

Finally, environmental impact assessment on the PE binder's production was evaluated in terms of GHG emissions and NREU for a cradle-to-factory gate approach. The results testified that:

- **PE_100% showed a meaningful reduction** of the total impact of the **GHG emissions compared to fossil-based polyesters** (PE3_Fossil and PE4_Fossil) by around **79%** respectively.
- **PE_100% compared to PE_75%** (substitution of the phthalic monomer with FDCA) **led to a significant reduction** of the total impact of the **GHG emissions** by around **36%.**

- **PE_100% presented the highest reduction** with a 38% less **of the total NREU** than PE_75% with the substitution of the FDCA monomer and a 60% less than PE3 / PE4_Fossil.
- The **polymerization process showed a low contribution** to the total cradle-to-factory gate emissions.

The second main objective of the present research was the preparation of nano-particles of kraft lignin by ultrasonication treatment to obtain stable colloidal water dispersions for 2, 4 and 6h.

Interesting results in the NL characterization can be summarised as follows:

- **Successful formation of NL** was achieved **after 6h of treatment** with a minimum size in the **10 nm – 50 nm range**.
- **Excellent water-dispersion stability** of the ultrasonically treated NL-based system **for over 15 months** without any noticeable formation of solid precipitate.
- An increased oxidation of NL compared to the parent material was found as a result of ultrasonication treatment use, giving an **increased polarity in NL** that was well **correlated with the markedly improved stability in water** compared to pristine lignin.

The obtained NL particles were initially incorporated at varying concentrations into a ENR matrix (10% and 40%). The results of the characterization can be outlined as follows:

- The vulcanization process indicated that **the retardant vulcanization effect with the introduction of IND was weaker than** the effect found with **the incorporation of NL.**
- **The use of nanosized lignin particles allowed to improve the stiffness of the rubber matrix material** without affecting its elongation at break, especially for **ENR/NL-10.** Nevertheless, a

decrease of fracture toughness was observed **at increasing filler loading**.

- The **addition of nanosized lignin particles did not show an improvement in the matrix-filler interactions** of the mechanical properties compared to microsized lignin particles.

Finally, the obtained NL particles were incorporated at varying concentrations into a thermoplastic PU matrix (5%, 10% and 20%). The resulting nanocomposite materials were characterized and can be summarized as follows:

- An **excellent level of dispersion and distribution of NL particles into the PU matrix** as opposed to untreated lignin was evidenced by SEM analysis.
- An **improvement of thermal stability was observed on NL-based nanocomposites** compared with systems incorporating untreated lignin, **especially at high temperatures (> 400 °C),** which was associated with the higher thermal stability of the nano-sized bio-based filler.
- **Ability** of NL to **establish effective non-covalent interactions with the polymer matrix** due to the **high surface/volume ratio characteristic of the nano-scale dimensions** resulting from the ultrasonication process.
- **Higher elastic modulus** accompanied by preserved strength with highly filled nanocomposites (**20 wt.% NL-6h**).
- **Low deformation applications** with a greater structural integrity is required, for instance in the **automotive interior field or in the footwear field.**

>>
Appendix 1

GLOSSARY

PE	Polyester
PU	Polyurethane
PLA	Polylactic acid
Gly	Glycerine
1,3-PD	1,3-Propanediol
SA	Succinic Acid
1,2-PD	1,2-Propanediol
1,4-BD	1,4-butanediol
AA	Adipic acid
Pht	Phthalic anhydride
BA	Butyl acetate
IPDI	Isophorone diisocyanate
HMDI	Hexamethylene diisocyanate
PCC	Propylene carbonate
FDCA	2,5-Furandicarboxylic acid
HMF	5-hydroximethilfurfural
PTA	Terephthalic acid
PEF	Polyethylene furanoate
PET	Polyethylene terephthalate
MEG	Monoethylene glycol
ENR	Epoxidized natural rubber
IND	Softwood kraft lignin INDULIN AT
DMSO	Dimethyl sulfoxide
ZnO	Zinc oxide
StA	Stearic acid
2MPBTA	2-mercaptobenzothiazole

S	Sulfur
EPA	Environmental Protection Agency
LCA	Life Cycle Assessment
LCI	Life Cycle Inventory Analysis
LCIA	Life Cycle Impact Assessment
FU	Functional Unit
ALCA	Attributional Life Cycle Assessment
CLCA	Consequential Life Cycle Assessment
GWP	Global Warming Potential
GHG	Greenhouse gas emissions
GGP	Greenhouse gas Protocol
CED	Cumulative Energy Demand
NREU	Non-renewable energy use
ROW	Rest of the word's technology
RER	European technology
LLDPE	Linear low-density polyethylene
MWL	Milled Wood Lignin
MWEL	Milled Wood Enzymatic Lignin
CEL	Cellulose Enzymatic Lignin
VOCs	Volatile organic compounds
Tg	Glass transition temperature
TGA	Thermo-gravimetric analysis
AV	Acid number
OHV	Hydroxyl numbers
FTIR	Fourier Transform Infrared spectroscopy
DMA	Dynamic-Mechanical analysis
DSC	Differential Scanning Calorimetry

OCA	Optical Contact Angle
GPC	Gel Permeation Chromatography
TEM	Transmission electron microscopy
SEM	Scanning electron microscopy

>>
Appendix 2

PUBLICATIONS

- Articles in international journals with referee

1. Maria Nelly **Garcia Gonzalez**, Marinella Levi, Stefano Turri (2017) *Development of polyester binders for the production of sustainable polyurethane coatings: Technological characterization and life cycle assessment.* Journal of Cleaner Production 164, 171-178.

2. Maria Nelly **Garcia Gonzalez**, Marinella Levi, Stefano Turri, Gianmarco Griffini (2017) *Lignin nanoparticles by ultrasonication and their incorporation in waterborne polymer nanocomposites*. Journal of Applied Polymer Science. 45318.

3. Maria Nelly **Garcia Gonzalez**, Pål Börjesson, Marinella Levi, Stefano Turri. *Development and life cycle assessment of polyurethane coatings from polyester binders containing 2,5-furandicarboxylic acid.* Journal of Polymers and the Environment. Submitted 17-11-2017.

- Proceedings of national and international congresses

4. **Oral presentation**: Maria Nelly **Garcia Gonzalez.** *Life Cycle Assessment of different polyester binders for the production of sustainable polyurethane coatings*. 24 June 2016. Convegno dell'associazione rete italiana LCA 2016, Ravenna (Italy).

5. **Poster presentation.** Maria Nelly **Garcia Gonzalez.** *Life cycle assessment on bio-based polymer 2,5-Furandicarboxylic Acid from sugar beet cultivation*. 7-11 May 2017. SETAC Conference Europe 27th annual meeting, Brussels (Belgium).

6. **Poster presentation.** Maria Nelly **Garcia Gonzalez** *Nanoparticles from softwood kraft lignin as bio-derived fillers in polymer-based nanocomposites*. 16-19 May 2017. International Symposium on Grids & Clouds, La Rochelle (France).

7. **Oral presentation.** Maria Nelly **Garcia Gonzalez.** *Polymer nanocomposites based on lignin nanoparticles: development, characterization and potential applications*. 14 June 2017. 25th edition, European Biomass Conference and Exhibition, Stockholm (Sweden).

Journal of Cleaner Production 164 (2017) 171–178

Contents lists available at ScienceDirect

Journal of Cleaner Production

journal homepage: www.elsevier.com/locate/jclepro

Review

Development of polyester binders for the production of sustainable polyurethane coatings: Technological characterization and life cycle assessment

Maria Nelly Garcia Gonzalez*, Marinella Levi, Stefano Turri

Department of Chemistry, Materials and Chemical Engineering "Giulio Natta", Politecnico di Milano, Piazza Leonardo da Vinci 32, 20133 Milano, Italy

ARTICLE INFO

Article history:
Received 29 July 2016
Received in revised form
21 June 2017
Accepted 21 June 2017
Available online 23 June 2017

Keywords:
Life cycle assessment
Greenhouse gas emissions
Non-renewable energy use
Bio-based monomers
Polyester
Polyurethane coating

ABSTRACT

Polyurethane (PU) coatings are used in many industrial applications, like in the furniture and automotive sectors. The main objective of the present work is the re-design of polyester binder for PU coatings using a selection of monomers derived from biorefinery. A preliminary comparative evaluation of technological performances of the corresponding PU coatings is presented, showing that the introduction of biobased monomers generally leads to softer materials but it doesn't affect significantly other physical properties like wettability, adhesion and hydrolytic stability. Afterwards, the total impact of greenhouse gas emissions (GHG) and the total non-renewable energy use (NREU) are evaluated by a Life Cycle Assessment (LCA) study, following a cradle-to-factory gate approach. The ecoprofile of bio-based polyester binder is compared with other two fossil-based conventional polyesters. The results suggest that the use of bio-based monomers allows a significant reduction of the total GHG emissions of around 75% less and a reduction of around 35% less of the total NREU.

Contents

1. Introduction

Polyurethanes (PUs) are one of the most versatile protective coating materials and they are extensively used in many

* Corresponding author.
E-mail address: marianelly.garcia@polimi.it (M.N. Garcia Gonzalez).

http://dx.doi.org/10.1016/j.jclepro.2017.06.190
0959-6526/

manufacturing sectors such as in automotive, furniture, and heavy duty industries (Pfister et al., 2011; Szycher, 2013). Their excellent durability and mechanical properties are the main reasons that led to a successful industrial development (Zia et al., 2007). PU coatings are obtained by a stoichiometrically balanced mixture of polyols and polyisocyanates (Zhang et al., 2014) (Fig. 1). Among the polyols, mostly polyester oligomers (binders) are used, which contain both aliphatic and aromatic monomers and hydroxyl functional groups.

Currently, a large part of raw monomers for PU production is still based on petroleum sources. However, due to the foreseen decline of non-renewable feedstock, there is a growing interest in the development of monomers and macromers from renewable resources such as carbohydrates, vegetable oils, or microalgae (Pfister et al., 2011). Over the last few years, bio-based PU coatings have been proposed as sustainable alternatives due to their lower environmental impact, easy availability, biodegradability and acceptable cost (Mohanty et al., 2005; Ragauskas et al., 2006). Many works have appeared in literature about how to use these materials in a wide range of applications (Noreen et al., 2016).

The development of polyesters from renewable resources is an important topic in modern green chemistry (Vilela et al., 2014). These materials are certainly one of the most promising polymers which can be developed through biorefinery. Bio-based polyester oligomers can be used as components of paints and adhesives formulations, while high molecular weight polyester thermoplastics are promising packaging materials. There has been a certain ease of availability to obtain bio-based polyester precursors from biorefineries (Islam et al., 2014) where soybean oil-based is taking on a leading role (Miao et al., 2013; Pan and Webster, 2012), compared to, for example, isocyanates and diamines. More recently, bio-based phosgene-free routes for diisocyanate production have been described (More et al., 2013; Rajput et al., 2014). A polyisocyanate partially based on renewable carbon has been launched in the market (Bayer, 2015).

Renewable raw materials may reduce the environmental impacts compared with petroleum based counterparts. These effects can be quantified by the Life Cycle Assessment (LCA) method whose aim is to determine the environmental impacts of products and processes by the evaluation of the entire life cycle. There has been a growing use of this method since it is necessary to take measures against global climate change, and to become less dependent on petroleum sources. An example case is the study of LCA applied to the bio-based polyester polylactic acid (PLA) (Vink and Davies, 2015). In addition, an extensive number of studies have been reported where the assessment on a life-cycle basis of the different impacts of bio-based products has been compared to conventional fossil-derived products (Adom et al., 2014; Urban and Bakshi, 2009) or to other bio-based products (Cok et al., 2014).

However, bio-based resources could be involved in other environmental burdens, which can be assessed by the LCA, as it is the case of acidification, ozone depletion, land-use change, biodiversity, soil degradation, air pollution and social impacts among others.

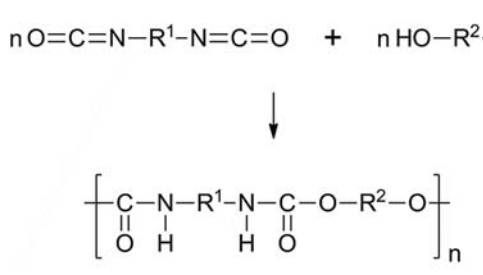

Fig. 1. Reaction of a diisocyanate with a diol to form a polyurethane.

In spite of the large number of papers describing polyurethane coatings, no specific study is reported in the literature concerning a cradle-to-gate LCA of polyester binders, which represent the larger component of the coating material. Nowadays, although the possibility of using bio-based monomers to synthesise polyester was already demonstrated, no specific evaluation of their ecoprofiles is available, being LCA studies predominantly focused on bio-based polyester as packaging materials. In the light of the above considerations, the aim of this work is to fill this specific gap in the literature. A new polyester binder for polyurethane coating was indeed re-designed through the selection of monomers derived from biorefinery. Polyester binders for coatings are complex copolymer systems made of at least 4–5 different monomers. The technological validation of the new bio-based polyester binders in comparison to fossil-based polyesters in bicomponent PU formulations was made through some preliminary experimental tests, including pull-off adhesion, indentation hardness, contact angle, and hydrolytic stability tests. The characterization of materials included the evaluation of the total impact of greenhouse gas emissions (GHG) and the total non-renewable energy use (NREU) by the Life Cycle Assessment (LCA) on the basis of a cradle-to-gate approach and considering the separated contributions of the monomer mixture composition, and of the production process of the copolyester (copolymerization).

2. Coating material

2.1. Monomer selection process

Suitable monomers were selected according to their functional role in the binder design and primary data availability in the Ecoinvent database version 3.2, and in the open literature. All the relevant information is summarized in Table 1. The data concerning succinic acid (SA) production came from the direct crystallization (SA-DC) process described by Cok et al. (2014).

2.2. Polyester binder composition

Table 2 shows the composition of the three 4-monomers copolyester binders synthesized and considered in the present study for the evaluation of their ecoprofiles, and tested experimentally in PU coating formulations. Polyesters 1 and 2 (PE1 and PE2) were designed and developed considering that all monomers are derived from fossil-based resources. The only difference between them is the change from 1,4-butanediol monomer to 1,2-propanediol monomer respectively. The latter presents a methyl side group and a secondary hydroxyl; this normally leads to a lower reactivity but at the same time it leads to the formation of sterically hindered ester groups in the polyester, which may be more stable towards hydrolysis. As for the polyester 3 (PE3), the composition was mainly based on monomers from renewable resources with the exception of the phthalic anhydride monomer. With regard to the aliphatic acids, the adipic acid has not yet a direct sustainable alternative so far. Therefore, the succinic acid was introduced as a renewable monomer (Cok et al., 2014). As the molecular structures of the two diacids are different, it is supposed that some differences between polymer Tg and hydrolytic stability may occur.

The polymerization process was the same for all the three polyesters, and consisted in a bulk polycondensation at high temperature (from 150° to 210 °C) under dry nitrogen flow to remove water as by-product. The progress of reaction was monitored by end group titration which monitored the residual acidity of

Table 1
Characteristics and functions of monomers for polyester binders.

Name of the monomer (acronym)	Family	The function in the material	Bio or fossil based	Reference for background data
Glycerine (Gly)	Polyols	Give residual –OH functions to the final polyester binder, allowing the crosslinking reaction with isocyanates	Bio-based (Palm Oil)	Ecoinvent 3.2 (Jungbluth et al., 2007)
Glycerine (Gly)			Fossil-based	
Phthalic Anhydride (Pht)	Aromatic diacids	Increase the coating glass transition temperature Tg	Fossil-based	Ecoinvent 3.2 (Althaus et al., 2007)
Adipic acid (AA)	Aliphatic diacids	Increase coating flexibility and outdoor durability	Fossil-based	Ecoinvent 3.2 (Althaus et al., 2007)
Succinic acid (SA)			Bio-based (Corn starch)	Cok et al., 2014
1,4-butanediol (1,4-BD)	Aliphatic diols	Increase polymer molecular weight	Fossil-based	Ecoinvent 3.2 (Sutter, 2007)
1,2-propanediol (1,2-PD)			Fossil-based	Ecoinvent 3.2 (Althaus et al., 2007)
1,3-propanediol (1,3-PD)			Bio-based (Corn sugar)	DT&L, 2009

Table 2
Polyester compositions of the three synthesized polyester binders.

PE1 monomers	Composition (% w/w)	PE2 monomers	Composition (% w/w)	PE3 monomers	Composition (% w/w)
Gly	6.4	Gly	6.7	Gly	7.0
1,4-BD	37.4	1,2-PD	33.2	1,3-PD	34.7
Pht	36.5	Pht	39.1	Pht	37.9
AA	19.7	AA	21.0	SA	20.4

polyesters, and stopped the polymerization when the acid number was <10 mgKOH/g.

2.3. Coating production and testing

The use of bio-based monomers into a polyester binder may improve its ecoprofile. Since not all the monomers commonly used have an identical corresponding bio-based counterpart, some changes in the composition of the copolyester were done, and some impacts on the properties of the final coating cannot be excluded. In particular, passing to binders with SA and 1,3-PD in PE3, polymers with a higher concentration of main chain ester groups and without methyl side groups will be produced. This may lead to an enhanced water sensitivity and possibly lower Tg, which are effects to be evaluated.

Therefore, the three model polyester binders were synthesized on lab-scale, and tested in standard bicomponent polyurethane (PU) formulations after formulation with a commercial polyisocyanate crosslinker (namely Vestanat, 1800). The binder reactivity was checked by monitoring the progressive disappearance of the NCO band through IR spectroscopy (stretching at 2260 cm-1). Coatings with a thickness of 40–50 mm were bar-applied onto glass or metal substrates after dilution with butyl acetate to reduce viscosity (solid content 50% w/w). All the binders considered gave fully crosslinked and transparent PU films.

The characterization of the PU films included thermal analysis by differential scanning calorimetry (DSC), surface wettability by a static optical contact angle (OCA) against water (10 determinations for each sample), mechanical properties by pull-off adhesion tests (ASTM D4541-09) (3 determinations of each sample) and indentation hardness (ISO 2815) (3 determinations of each sample). Finally, hydrolytic stability was tested by exposing the coatings at 60 °C, 100% humidity for a period of 30 days. The stability test was repeated in 3 different samples for each composition. The samples were periodically monitored through visual inspection, contact angle and indentation hardness tests.

3. LCA methodology

3.1. Data and methodological developments

The comparative analysis of the ecoprofiles of the different polyesters was done following the LCA methodology which is standardized in the ISO 14040–14044 series by the International Organization of Standardization. This study only covers the impact categories of NREU and GHG despite the other categories like eutrophication are also relevant in biomass derived products. This limitation is due to the fact that the data used for calculation derive from different literature sources, and only the NREU and GHG categories were common for all of them. Characterization factors were taken from Impact methods “Cumulative Energy Demand” (v1.09) and “Greenhouse Gas Protocol” (v1.01), respectively. The data were incorporated into SimaPro LCA software, and the Ecoinvent database version 3.2, attributional system model, was used as a background source. The foreground data were then evaluated. The geographical coverage is based on the European Union (EU) for all monomers except for the glycerine as it is global product. Fig. 2 shows the system boundaries for the different polyester binders analysed.

The functional unit is one kg of polyester binder, the basis for comparison of bio-based polyester versus fossil-based polyester. The system boundary was set up following a cradle-to-factory gate approach, comprising resource extraction, transportation to the monomer factory, production of raw monomers/macromers and polyester production (before it was transported to the end user, that is the paint producer in the specific instance) as shown in Fig. 2. Within the system boundary, the contributions of different monomers and the contribution of the polymerization process were analysed separately up to the step of binder production. A sensitivity analysis was also done with the aim of estimating the effects of choices made regarding methods and data on the outcome of the present study (ISO 14044). Finally, Table 3 reports schematically the inventory analysis with relevant figures.

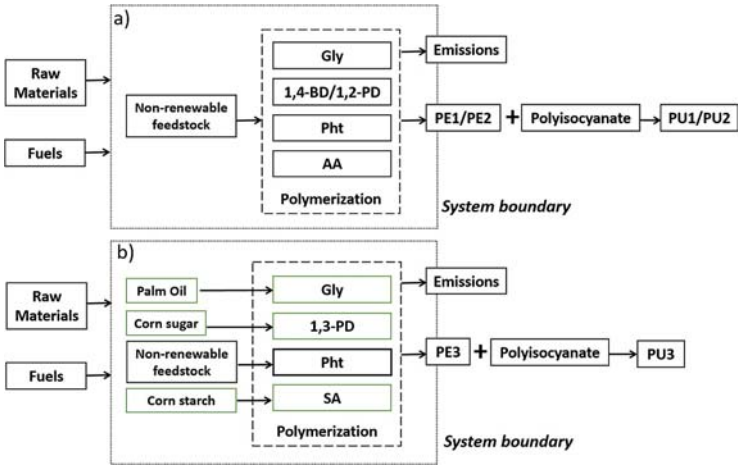

Fig. 2. The system boundary of the different polyesters: a) Fossil-based PE1 and PE2 b) Bio-based PE3.

4. Comparison of the processing data with other sources from literature

Data concerning monomers selected for the bio-based polyester binder (PE3) were compared with other literature sources (Fig. 3). Bio-based glycerine production (from palm oil) was compared with other glycerine production processes based on different biological feedstocks such as rape oil and soybean oil, taken from Ecoinvent (Jungbluth et al., 2007; Omni Tech International, 2010). All of them are based on global geographical coverage. The 1,3-PD production was compared with another 1,3-PD bio-based production taken from Urban and Bakshi's work (2009), where both processes came from corn-derived glucose. The geographical coverage is based on U.S.A (Urban and Bakshi, 2009) and Europe for DuPont's study (2009). The process which was chosen to be compared in Urban and Bakshi's study was the bio-based 1,3-PD production with mass allocation in the process LCA study (Urban and Bakshi, 2009). For SA production, a comparative of three different processes was also analysed according to the data from Cok's study. The three processes are direct crystallization (present study, SA-DC), electrodialysis (SA-ED) and ammonium sulphate (SA-AS) process. More recently (Gnansounou and Kenthorai Raman, 2016) SA from algae feedstocks with a complete LCA analysis was described. However, SA is only a co-product in this process and the extrapolation of GHG and NREU data is not straightforward. Therefore, we decided not to include it in the following comparison.

In the case of Gly production the effect of different biological feedstock was noticed. A significant decrease of GHG emissions and NREU was observed by passing from palm oil feedstock to rape oil feedstock. The reduction of the NREU was around 25%, and the decrease of the total GHG emissions were around 157%. This large difference is due to the fact that the CO_2 coming from land transformation is negligible, hence its value is really low (9.89^{-5} kg $CO_{2\ eq}$/kg PE3 for the Gly production with rape oil with respect to 0.220 and 0.223 kg $CO_{2\ eq}$/kg PE3 for the Gly production with palm oil and soybean oil respectively). In the case of the Gly production from soybean oil feedstock a higher NREU value by around 24% for palm oil and 43% for rape oil was observed. Regarding GHG emissions, a reduction was observed by around 58% compared to Gly production from palm oil feedstock. This fact can be explained considering that biogenic CO_2 is lower for the Gly production from soybean oil feedstock by around 0.003 kg $CO_{2\ eq}$/kg PE3 than for Gly production from palm oil feedstock by around 0.13 kg $CO_{2\ eq}$/kg PE3. When comparing the two alternative routes for 1,3-PD production, an increase of GHG emissions by around 22% and a reduction of non-renewable energy total use by around 30% was observed in comparison to Urban's study. However, the reason for this discrepancy is not clear because both studies do not reveal the specific data used. As for SA (present study, SA-DC) production, a significant reduction was observed with respect to the other alternatives in terms of GHG emissions and NREU.

This comparison shows the different-case scenarios of each bio monomer in terms of GHG emissions and NREU. For SA production, the direct crystallization process (SA-DC) was chosen as base case in our study because it has more benefits than the other methods (Cok et al., 2014). In the glycerine case, notwithstanding rape oil feedstock presented better results, we decided to work with palm

Table 3
Inventory analysis. Data not been reported in the table are from Ecoinvent.

Polyester binder	Input			Output		
PE 1	**Materials**		**Unit**	**Materials**		**Unit**
Fossil-based	Gly	0.06	kg	PE 1	1.00	Kg
	1,4-BD	0.37	kg			
	Pht	0.36	kg			
	AA	0.18	kg			
	Energy	–		**Emissions to air**	–	
PE 2	**Materials**		**Unit**	**Materials**		**Unit**
Fossil-based	Gly	0.07	kg	PE 2	1.00	Kg
	1,2-PD	0.33	kg			
	Pht	0.36	kg			
	AA	0.18	kg			
	Energy	–		**Emissions to air**	–	
PE 3	**Materials**		**Unit**	**Materials**		**Unit**
Bio-based	Gly Bio	0.07	kg	PE 3	1.00	kg
	1,3-PD	0.35	kg			
	Pht	0.38	kg			
	SA	0.20	kg			
	Energy			**Emissions to air**		
	Gly Bio	–		Gly Bio	–	
	1,3-PD	22.17	MJ	1,3-PD	7.57	kg CO_2eq
	Pht	–		Pht	–	
	SA	6.67	MJ	SA	0.18	kg CO_2eq

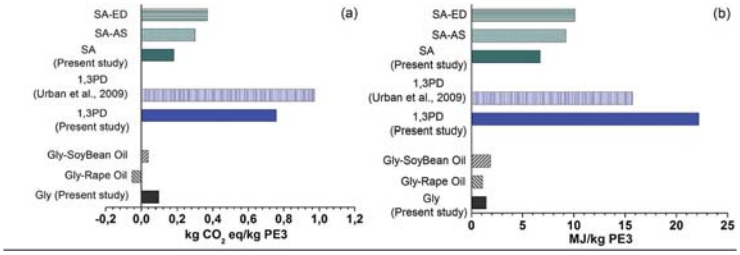

Fig. 3. Comparison of the processing data with other sources from literature in bio-based glycerine, SA and 1,3-PD monomers: a) $kgCO_{2eq}$/kg PE3 in terms of GHG emissions and b) MJ/kg PE3 in terms of non-renewable energy use.

oil since it is one of the oil grades with higher production volume together with the soybean oil. As for 1,3-PD production, DuPont's study (2009) was chosen due to the fact that it presents a geographical coverage based on the European Union (EU).

5. Results and discussion

5.1. Coating material characterization

The thermal transitions of the crosslinked PU coatings are shown in Table 4. It can be shown that the highest Tg is around +35 °C, corresponding to the fossil-based PU2 coating, containing 1,2-PD as a chain extender. PU1 and PU3 coatings only contain linear chain extenders like 1,4 BD and 1,3 PD (without methyl side groups) and therefore more flexible polymer structures are formed, showing a Tg value of 2.2 and 2.7 °C respectively. As far as surface wettability is concerned, the contact angle data reported in Table 4 show a good hydrophobic character in all PU coatings considered, without an apparent effect of polyester composition. The adhesion was evaluated for coatings supported onto glass and chromated aluminium. As shown in Table 4, all PU coatings applied onto glass substrates showed an excellent adhesion with the highest bonding strength observed on fossil-based PU2 coating at 7.3 MPa. The measurements of PUs on aluminium substrate showed moderately good adhesion with the highest adhesion strength (around 1.8 MPa) found in PU1. As far the indentation behaviour is concerned, the highest hardness is shown by the fossil-based PU2 coating, and this result is in agreement with its higher Tg value. PU1 and PU3 coatings show a much lower hardness, being the bio-based coating also the softest.

The different physical properties of the coatings suggest potentially differentiated applications. Actually, the harder PU2 coating is more scratch resistant and could be proposed as a mechanically protective coating in the automotive or furniture sector. However, softer PU1 and PU3 materials are more suitable as candidates for metal coil coatings, where an excellent post-cure flexibility and formability of the painted metal strip is needed (Wicks et al., 2007).

Finally, the hydrolytic stability of the PU coatings was investigated. Hydrolytic stability in polyester-based polyurethanes is known to be better in binders containing glycols with low concentration of ester groups, therefore glycols with longer hydrocarbon chains (Furukawa et al., 1999). The hydrolytic stability in PU films was monitored over 30 days of continuous exposure to water at +60 °C. A detailed visual inspection excluded the formation of blisters, which is an indication of high adhesion onto the substrate and overall stability of the polymer network in the tested conditions. A more quantitative evaluation was made through contact angle and hardness measurements, and results are shown in Figs. 4 and 5. Results are expressed as percentage retention of the property over the time. As it is shown in Fig. 4, a constant decrease of hydrophobicity is observed in all PU films throughout the 10th days of testing. After the 10th day, the superficial changes are more marked as shown by the large standard deviations. It is interesting to observe (Fig. 5) that there is an increase of the hardness especially in PU2 and PU3 coatings, while PU1 seems more stable. After one month of exposure, all the PU coatings retain more than 90% of

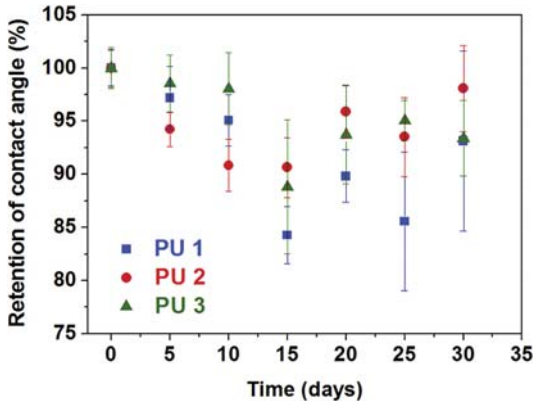

Fig. 4. Hydrolytic Stability monitoring by Contact Angle Test.

Table 4
Material characterization.

PU Coatings	Tg (°C)	OCA Test (°)	Adhesion Test (MPa)		Hardness Test (ἀb)
			Glass	Al Chromed	
1 FOSSIL-BASED **(PU1)**	2.2	89.0 ± 2.6	5.9 ± 2.1	1.8 ± 0.2	64.6 ± 0.2
2 FOSSIL-BASED **(PU2)**	34.8	82.5 ± 1.8	7.3 ± 2.3	1.1 ± 0.4	90.9 ± 0.4
3 BIO-BASED **(PU3)**	2.7	87.8 ± 3.4	6.4 ± 1.2	1.0 ± 0.2	54.1 ± 0.2

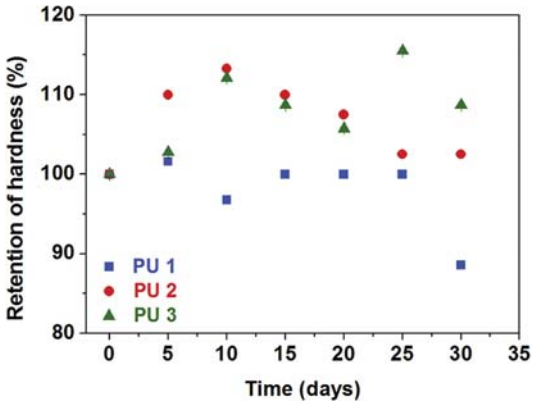

Fig. 5. Hydrolytic Stability monitoring by Hardness Test.

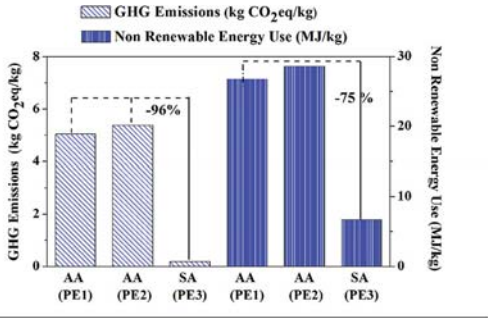

Fig. 7. Comparison between Adipic Acid and Succinic Acid monomers in terms of GHG emissions and NREU.

their initial hardness; it is worth underlining that the bio-based PU3 coating is remarkably stable and it even tends to increase slightly its hardness upon ageing. The reason of this latter effect is unclear, possibly it is due to some morphological changes of the polyurethane induced by ageing (like a microphase segregation with formation of harder urethane domains). In any case, hydrolytic degradation can be excluded, because it would have involved a dramatic decrease of molecular weight and consequently, a strong hardness decrease. This is particularly positive in view of potential application of bio-based PUs as protective coatings.

5.2. LCA analysis

Contributions from different monomers of polyesters 1–3 in terms of non-renewable energy total use (NREU) and total greenhouse gas emissions (GHG) were evaluated for the functional unit of 1.0 kg polyester.

Fig. 6 shows the total impact of GHG emissions and NREU for the three polyesters studied, including the contribution of the choice of the monomer and the contribution of the polymerization process to produce the binder, which is the same for all polyesters considered. It can be noticed that the use of 60–65% of bio-based monomers in polyester 3 reduced significantly the total GHG emissions by around 75%, and around 36% for the total NREU. The polymerization process shows a very low contribution to the total cradle-to-factory gate emissions. Consequently, the next part of the study is focused on the analysis of the monomer mixture contributions showing which monomers have a bigger impact in terms of GHG and NREU.

Concerning aromatic diacids, phthalic anhydride showed a low impact on the total non-renewable energy use, and a remarkable low impact on the total GHG emissions between fossil-based polyesters. Accordingly, a marked decrease of GHG emissions and NREU was observed by changing the fossil-based aliphatic diacid with succinic acid obtained from renewable sources. The reduction of the total GHG emissions were around 96%, and the decrease of NREU was around 75% (Fig. 7).

As for bio-based glycerine (from palm oil), it showed a significant reduction on the total GHG emissions by around 64% and non-renewable energy use by around 63% was shown with respect to glycerine from epichlorohydrin (Fig. 8).

Finally, it can be observed that the passing from fossil-based 1,4-BD to fossil-based 1,2-PD produced only a slightly effect in terms of GHG emissions (−12%), but almost the same total NREU (−6%). By contrast, it can be noticed that the change of fossil-based aliphatic diols to chemically similar bio-based aliphatic diols such as 1,3-PD caused a remarkable lower impact for GHG emissions and NREU, namely 1,3-PD is featured with around −30% with respect to 1,4-BD/1,2-PD on non-renewable energy consumption, and −53% compared to 1,4-BD/1,2-PD as far as GHG emissions are concerned (Fig. 9).

5.2.1. Sensitivity analysis

A sensitivity analysis was performed with the aim of assessing the reliability of the results and conclusions of the present work. Modifications on the calculation of category indicator results were introduced with the purpose of observing how much they were

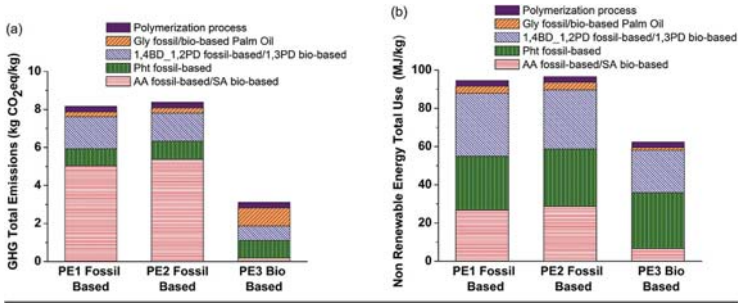

Fig. 6. Overview of the total impact of a) GHG emissions and b) NREU for the three polyesters studied.

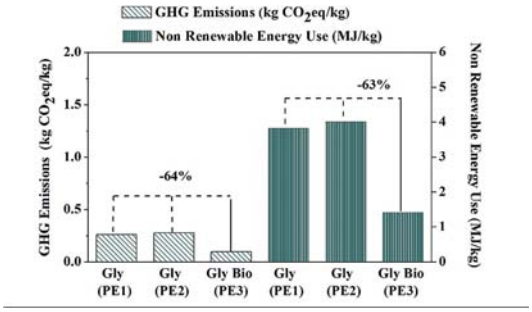

Fig. 8. Comparison between bio-based glycerine (from palm oil) and fossil-based glycerine monomers in terms of GHG emissions and NREU.

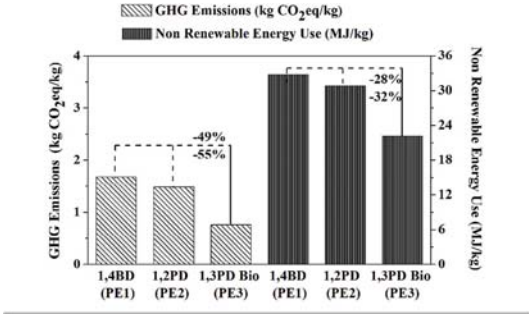

Fig. 9. Comparison between diol monomers in terms of GHG emissions and NREU.

affected. These assumptions were based on the calculation methodology whose aim was to compare the Greenhouse Gas Protocol (GHG protocol) method (IPCC Fourth Assessment ReportIPCC Fifth Assessment Report IPCC Fifth Assessment Report) to the IPCC 2013 Global Warming Potential with a timeframe of 100 years (100a) (v1.0) method (IPCC Fifth Assessment ReportIPCC Fifth Assessment Report) for the case of GHG emissions. In relation to NREU, the aim was to compare the Cumulative Energy Demand (CED) method (Frischknecht et al., 2007) to the IMPACT 2002+ (v2.12) method (Jolliet et al., 2003) taking the impact of the non-renewable energy in the case of the last method. A deviation was calculated between the different methods by subtracting the total impacts values of each monomer.

In Table 5, the calculation methodology between the GHG protocol and IPCC 2013 GWP 100a methods in all three 4-monomers polyester showed small differences. All the deviations were less than 0.42. As far as aliphatic diols and aromatic diacid are concerned, calculation of the total GHG emissions resulted less affected by the chosen methodology. In the case of bio-based glycerine, there was a significant increase in the total GHG emissions by around 65% with the IPCC 2013 GWP 100a method. This is due to the fact that the IPCC method does not take into account the CO_2 uptake in its calculation. The bio-based monomer glycerine has a greater impact on the cultivation process than the others. In the case of AA with the IPCC 2013 GWP 100a method, a small decrease in the total GHG emissions was present (around 8%). This is because the IPCC 2013 GWP 100a method characterization factor for the dinitrogen monoxide emission is lower than the GHG protocol method characterization factor. Then, the total GHG emission is slightly lower in IPCC 2013 GWP 100a method with respect to the GHG protocol method.

In Table 6, the comparison between the CED and IMPACT 2002 + methods in all the three 4-monomers polyester showed some differences. Deviations showed a maximum value of 0.88 among all of them. Aliphatic diols, aliphatic diacids and the aromatic diacid showed similar values with regards to the calculation methodology in the NREU. By comparison, for the bio-based glycerine (according to the IMPACT, 2002 + method) the total NREU decreased by over 62%. This is because in the IMPACT 2002 + method, the non-renewable biomass value is not taken into account.

Table 5
Sensitivity Analysis (GHG protocol- IPCC, 2013 GWP 100a).

kg CO_2 eq/kg PE	PE 1 fossil-based			PE 2 fossil-based			PE 3 bio-based		
	GHG protocol	IPCC 100a	Deviation	GHG protocol	IPCC 100a	Deviation	GHG protocol	IPCC 100a	Deviation
AA	5.03	4.63	0.40	5.37	4.95	0.42	0.18	0.18	0.00
SA									
Pht	0.90	0.92	−0.02	0.96	0.98	−0.02	0.93	0.95	−0.02
1,4BD	1.68	1.70	−0.02	1.48	1.50	−0.02	0.76	0.75	0.01
1,2PD									
1,3PD									
Gly	0.26	0.26	0.00	0.27	0.28	−0.01	0.09	0.26	−0.17

Table 6
Sensitivity analysis (CED- IMPACT, 2002+).

MJ/kg PE	PE 1 fossil-based			PE 2 fossil-based			PE 3 bio-based		
	CED	IMPACT 2002+	Deviation	CED	IMPACT 2002+	Deviation	CED	IMPACT 2002+	Deviation
AA	26.78	26.80	−0.02	28.61	28.60	0.01	6.67	6.67	0.00
SA									
Pht	28.14	28.10	0.04	30.03	30.00	0.03	29.19	29.10	0.09
1,4BD	32.83	32.80	0.03	30.84	30.90	−0.06	22.18	22.18	0.00
1,2PD									
1,3PD									
Gly	3.82	3.81	0.01	4.01	4.01	0.00	1.42	0.54	0.88

6. Conclusive remarks

Different polyester binders suitable as intermediates for the production of polyurethane coatings were designed, synthesized and technologically characterized. Monomers derived from both conventional (oil based) and renewable sources were used. It resulted that the introduction of bio-based monomers up to a level of 60% by weight does not impact many physical properties like adhesion, surface wettability or hydrolytic stability. However, softer polymer coatings are generally obtained.

The LCA methodology was applied for the evaluation of environmental impacts related to the production of polyester binders. The introduction of a fraction of monomers from renewable sources (60% by weight) may reduce the total GHG emissions by around 75% and the total NREU by 35%. Most of the environmental advantages are related to the replacement of adipic acid (a C6 aliphatic diacid) with the relatively similar succinic acid (a C4 aliphatic diacid), (the total GHG emissions by around −96% and the total NREU by around −75%) whereas the presence of aromatic monomers (phthalic acid in the specific instance) seems to show a minor contribution (11% of the total GHG emissions and 31% of the total NREU). However, the results are preliminary, as other environmental burdens are not covered in this study. A further improvement of environmental benefits in this sector is related to the future industrial availability of sustainable alternatives for the replacement of aromatic diacids, which is to date a difficult monomer to replace with a bio-based alternative. Moreover, further work on primary data is needed to refine LCA calculations including other impact categories like eutrophication, which are relevant for all products derived by biomasses and biorefinery processes.

Acknowledgments

The authors would like to acknowledge the financial support of project “Sustainable Manufacturing” (CTNO1_00163_148175) and gratefully acknowledge Gigliola Clerici for support with thermal analysis in the research.

References

Adom, F., Dunn, J.B., Han, J., Sather, N., 2014. Life-cycle fossil energy consumption and greenhouse gas emissions of bioderived chemicals and their conventional counterparts. Environ. Sci. Technol. 48, 14624–14631. http://dx.doi.org/10.1021/es503766e.

Althaus, H.-J., Chudacoff, M., Hischier, R., Jungbluth, N., Osses, M., Primas, A., 2007. Life Cycle Inventories of Chemicals. Ecoinvent report No. 8, v2.0. Swiss Centre for LCI, Dübendorf, CH. www.ecoinvent.org.

Bayer MaterialScience, 2015. New Milestones in Polyurethanes. http://press.covestro.com/news.nsf/id/9SSDPM-New-milestones-in-polyurethanes?Open&parent=Home_EN&ccm=001&presskit=1 (Accessed 29 May 2017).

Cok, B., Tsiropoulos, I., Roes, A.L., Patel, M.K., 2014. Succinic acid production derived from carbohydrates: an energy and greenhouse gas assessment of a platform chemical toward a bio-based economy. Biofuels, Bioprod. Biorefining 8, 16–29. http://dx.doi.org/10.1002/bbb.1427.

Dupont Tale and Lyle Bio Products (DT&L), 2009. Life Cycle Analysis Overview-Susterra/Propanediol. http://www.dupontstateandlyle.com/sites/default/files/Susterra%20LCA.pdf (Accessed 12 June 2017).

Furukawa, M., Shiiba, T., Murata, S., 1999. Mechanical properties and hydrolytic stability of polyesterurethane elastomers with alkyl side groups. Polymer 40, 1791–1798. http://dx.doi.org/10.1016/S0032-3861(98)00262-6.

Frischknecht, R., Jungbluth, N., Althaus, H.-J., Doka, G., Heck, T., Hellweg, S., Hischier, R., Nemecek, T., Rebitzer, G., Spielmann, M., Wernet, G., 2007. Overview and Methodology. Ecoinvent report No. 1, v2.0. Swiss Centre for LCI, Dübendorf, CH. www.ecoinvent.org.

Gnansounou, E., Kenthorai Raman, J., 2016. Life cycle assessment of algae biodiesel and its co-products. Appl. Energy 161, 300–308. http://dx.doi.org/10.1016/j.apenergy.2015.10.043.

Islam, M.R., Beg, M.D.H., Jamari, S.S., 2014. Development of vegetable-oil-based polymers. J. Appl. Polym. Sci. 131, 40787. http://dx.doi.org/10.1002/app.40787.

ISO 14040, 2006. Environmental Management – Life Cycle Assessment – Principles and Framework, Geneva, Switzerland.

ISO 14044, 2006. Environmental Management – Life Cycle Assessment – Requirements and Guidelines, Geneva, Switzerland.

Jolliet, O., Margni, M., Charles, R., Humbert, S., Payet, J., Rebitzer, G., Rosenbaum, R.K., 2003. IMPACT 2002+: a new life cycle impact assessment methodology. Int. J. Life Cycle Assess. 8, 324–330. http://dx.doi.org/10.1007/BF02978505.

Jungbluth, N., Chudacoff, M., Dauriat, A., Dinkel, F., Doka, G., Faist Emmenegger, M., Gnansounou, E., Kljun, N., Spielmann, M., Stettler, C., Sutter, J., 2007. Life Cycle Inventories of Bioenergy. Ecoinvent report No. 17, v2.0. Swiss Centre for LCI, Dübendorf, CH. www.ecoinvent.org.

Miao, S., Callow, N., Wang, P., Liu, Y., Su, Z., Zhang, S., 2013. Soybean oil-based polyurethane networks: shape-memory effects and surface morphologies. J. Am. Oil Chem. Soc. 90, 1415–1421. http://dx.doi.org/10.1007/s11746-013-2273-5.

Mohanty, A.K., Misra, M., Drzal, L.T., 2005. Natural Fibers, Biopolymers, and Biocomposites. CRC Press LLC, Florida.

More, A.S., Lebarbé, T., Maisonneuve, L., Gadenne, B., Alfos, C., Cramail, H., 2013. Novel fatty acid based di-isocyanates towards the synthesis of thermoplastic polyurethanes. Eur. Polym. J. 49, 823–833. http://dx.doi.org/10.1016/j.eurpolymj.2012.12.013.

Noreen, A., Zia, K.M., Zuber, M., Tabasum, S., Zahoor, A.F., 2016. Bio-based polyurethane: an efficient and environment friendly coating systems: a review. Prog. Org. Coat 91, 25–32. http://dx.doi.org/10.1016/j.porgcoat.2015.11.018.

Omni Tech International, The United Soybean Board, 2010. Life Cycle Impact of Soybean Production and Soy Industrial Products. http://biodiesel.org/reports/20100201_gen-422.pdf (Accessed 07 June 2017).

Pan, X., Webster, D.C., 2012. New biobased high functionality polyols and their use in polyurethane coatings. ChemSusChem. 5, 419–429. http://dx.doi.org/10.1002/cssc.201100415.

Pfister, D.P., Xia, Y., Larock, R.C., 2011. Recent advances in vegetable oil-based polyurethanes. ChemSusChem. 4, 703–717. http://dx.doi.org/10.1002/cssc.201000378.

Ragauskas, A.J., Williams, C.K., Davison, B.H., Britovsek, G., Cairney, J., Eckert, C.A., Frederick Jr., W.J., Hallett, J.P., Leak, D.J., Liotta, C.L., Mielenz, J.R., Murphy, R., Templer, R., Tschaplinski, T., 2006. The path forward for biofuels and biomaterials. Science 311, 484–489. http://dx.doi.org/10.1126/science.1114736.

Rajput, S.D., Mahulikar, P.P., Gite, V.V., 2014. Biobased dimer fatty acid containing two pack polyurethane for wood finished coatings. Prog. Org. Coat 77, 38–46. http://dx.doi.org/10.1016/j.porgcoat.2013.07.020.

Sutter, J., 2007. Life Cycle Inventories of Petrochemical Solvents. Ecoinvent final report No. 22, v2.0. Swiss Centre for LCI, Dübendorf, CH. www.ecoinvent.org.

Szycher, M., 2013. Szycher's Handbook of Polyurethanes, second ed. CRC Press LLC, Florida. http://dx.doi.org/10.1038/142853a0.

Urban, R.A., Bakshi, B.R., 2009. 1,3-Propanediol from fossils versus biomass: a life cycle evaluation of emissions and ecological resources. Ind. Eng. Chem. Res. 48, 8068–8082. http://dx.doi.org/10.1021/ie801612p.

Vilela, C., Sousa, A.F., Fonseca, A.C., Serra, A.C., Coelho, J.F.J., Freire, C.S.R., Silvestre, A.J.D., 2014. The quest for sustainable polyesters- insights into the future. Polym. Chem. 5, 3119–3141. http://dx.doi.org/10.1039/C3PY01213A.

Vink, E.T.H., Davies, S., 2015. Life cycle inventory and impact assessment data for 2014 ingeo polylactide production. Ind. Biotechnol. 11, 167–180. http://dx.doi.org/10.1089/ind.2015.0003.

Wicks, Z.W., Jones, F.N., Pappas, S.P., Wicks, D.A., 2007. Organic Coatings: Science and Technology, third ed. John Wiley & Sons, Inc., Jersey http://dx.doi.org/10.1021/ie50282a005.

Zhang, C., Ding, R., Kessler, M.R., 2014. Reduction of epoxidized vegetable oils: a novel method to prepare bio-based polyols for polyurethanes. Macromol. Rapid Commun. 35, 1068–1074. http://dx.doi.org/10.1002/marc.201400039.

Zia, K.M., Bhatti, H.N., Bhatti, I.A., 2007. Methods for polyurethane and polyurethane composites, recycling and recovery: a review. React. Funct. Polym. 67, 675–692. http://dx.doi.org/10.1016/j.reactfunctpolym.2007.05.004.

Journal of Applied Polymer Science

Lignin nanoparticles by ultrasonication and their incorporation in waterborne polymer nanocomposites

Maria Nelly Garcia Gonzalez, Marinella Levi, Stefano Turri, Gianmarco Griffini
Department of Chemistry, Materials and Chemical Engineering "Giulio Natta,", Politecnico di Milano, Piazza Leonardo da Vinci 32, Milano 20133, Italy
Correspondence to: G. Griffini (E-mail: gianmarco.griffini@polimi.it)

ABSTRACT: Lignin nanoparticles (nanolignin, NL) were prepared in this work by ultrasonic treatment of softwood kraft lignin to obtain lignin-water dispersions with excellent colloidal stability. A thorough characterization of the chemical, physical, and morphological properties of the new NL particles allowed for direct comparisons with the untreated parent material. Such NL particles were incorporated into a waterborne thermoplastic polyurethane matrix at different concentrations to yield bio-based nanocomposite materials. The effect of the bio-filler type (NL vs. untreated lignin) and loading on the chemical, physical, thermal, and morphological characteristics of the resulting nanocomposites was extensively investigated. In addition, tensile tests carried out on these systems highlighted the superior mechanical properties of NL-based nanocomposites compared to composite materials incorporating untreated lignin. The results of this study provide a direct demonstration of an easy and environmentally friendly approach to obtain waterborne polyurethane-based nanocomposites reinforced with NL in a relatively straightforward and accessible way and clearly evidence the potential of lignin nanoparticles as fully bioderived fillers for advanced nanocomposite applications. © 2017 Wiley Periodicals, Inc. J. Appl. Polym. Sci. **2017**, *134*, 45318.

KEYWORDS: biopolymers and renewable polymers; cellulose and other wood products; structure-property relationships; thermoplastics

Received 20 February 2017; accepted 22 May 2017
DOI: 10.1002/app.45318

INTRODUCTION

Lignin is a natural aromatic polymer found in the wall of cellular plants, where it accounts for about 15% to 25% of the wooden matter.[1] At present, several million tons per year of lignin are recovered in the waste streams of pulp and paper factories and in biorefineries fed with lignocellulosic biomass.[2,3] Such large abundance, second only to cellulose and hemicellulose, makes lignin particularly interesting as valuable renewable source of aromatics for the development of high performance and environmentally friendly polymer-based materials. However, despite such great potential, lignin is still enormously underutilized at industrial scale, as its fate is typically to be burnt as low-cost fuel for energy generation. Indeed, only a restricted fraction of the lignin produced annually is currently recovered for higher value-added applications, that typically include its incorporation in formulations for additives, fillers, and dispersants for composites, plastics, and rubbers.[4,5] This relatively limited range of commercial applications is largely related to the vast chemical heterogeneity, poor reactivity, and difficult processability of the available lignins, the latter aspect being closely associated with the highly branched and hydrogen-bonded three-dimensional structure of such amorphous material.[6–8]

In the attempt to tackle some of these limitations, several chemical and chemical–physical strategies have been proposed in the last few years to enhance the exploitability of lignin as macromonomer for the production of polymeric materials. To this end, different fractionation approaches (pH-induced precipitation, membrane-assisted ultrafiltration, and solvent extraction) have been used to improve the miscibility of lignin in common solvents while better controlling its chemical, structural, and physical properties.[9–19] In addition, highly specific chemical functionalization reactions have been applied to lignin to improve its reactivity, add functionalities to its structure, and allow easier incorporation as reactive material into bio-based thermoplastic and thermosetting polymers, including polyurethanes, (PUs) polyesters, phenolics, and epoxies.[20–28]

The large number of functional groups present in lignin (e.g., aliphatic and aromatic hydroxyls, carbonyls, carboxyls) makes this material particularly attractive as reinforcing filler for the

Additional Supporting Information may be found in the online version of this article.

preparation of polymer-based composites, due to the potentially favorable covalent and noncovalent interactions that may arise between such highly-functional filler and the polymeric matrix. In this respect, different attempts have been made involving the incorporation of lignin particles (generally in the 10–100 μm range) into plastics and rubbers.[29–31] Typically, it was shown that straightforward addition of lignin into the target matrix yielded little or no effect on the mechanical properties of the corresponding composite. Therefore, appropriate chemical modification strategies were required to improve filler/matrix compatibility by introducing new functional groups on the lignin particle surface via nitration,[32] esterification,[33–35] silanization,[36] butyration, or urethane-bond formation.[37]

An alternative strategy to achieve enhanced dispersion level of the lignin filler within the polymer matrix is the preparation and use of lignin-based nanoparticles. With respect to their micrometer-sized (or larger) counterpart, nanolignin (NL) particles are characterized by a larger surface-to-volume ratio that is expected to lead to a more efficient interaction with the polymer matrix. As a result, improved dispersion and matrix-to-filler interfacial load transfer may be anticipated, thus prospecting improved mechanical properties of the NL-based polymer composite.[38] To obtain lignin-based nanoparticles, different approaches have been adopted so far, that include the formation of NL colloids by self-assembly[39] and the application of chemical,[40,41] mechanical,[42] or ultrasonic[43,44] treatments to the pristine material. Contingent upon the process employed, particle dimensions of few tens to few hundreds of nanometers can be achieved. In particular, ultrasonication appears to be especially interesting as it allows to obtain stable colloidal suspensions of NL particles as small as 10 to 50 nm by simple physical treatment (viz., cavitation), thus avoiding the need of (hazardous) chemical pre- or post-treatments on the material (typically, no solvent fractionation is required) and potentially leading to a more environmentally favorable overall process (as water is the typically employed dispersing medium).

Despite the clear scientific and technological impact of NL as fully bio-based reinforcing filler with enhanced water-dispersion stability, only surprisingly few examples of its application in polymer-based nanocomposite materials have recently appeared in the literature.[42,45–47] In particular, it was shown that lignin nanoparticles obtained by high-shear mechanical treatment could be completely homogenized to diameters in the 100 nm range and readily dispersed within the polymer matrix poly (vinyl alcohol). This led to improved thermal stability of NL-based composite systems compared to materials incorporating untreated lignin.[42] On the other hand, natural rubber-based nanocomposites were obtained by addition of colloidal polyelectrolyte complexes (100 nm average size) obtained from lignin and poly(diallyldimethylammonium chloride). The resulting materials were shown to exhibit enhanced thermal stability and mechanical properties thanks to the strong filler-to-matrix adhesion.[45] Finally, lignin nanoparticles obtained by acidolysis were employed to improve the thermal, mechanical, and wettability properties of bioderived polymeric matrices such as poly (lactic acid) and wheat gluten.[46,47] Based on these recent results, it is evident that no demonstrations of polymer-based nanocomposites reinforced with NL obtained by ultrasonic treatment have been reported to date, notwithstanding the great potential of this approach in view of the development of more environmentally sustainable lignin treatment processes. Indeed, the few reports on ultrasonication of lignin mainly focused on the characterization of the effects of this treatment on the chemical, physical, and morphological properties of lignin,[43,48–50] with no detailed investigation on the use of such ultrasonically treated lignin nanoparticles in nanocomposite systems.

Accordingly, in this work NL particles were prepared by ultrasonically treating a commercially available softwood kraft lignin to obtain stable colloidal water dispersions. A thorough chemical, physical, and morphological characterization of the NL systems was carried out and compared with the parent untreated material. The obtained lignin nanoparticles were incorporated into a waterborne thermoplastic PU to form nanocomposite materials with increasing bio-filler concentration. Such polymeric matrix was chosen because of the wide industrial applicability of PUs that find use in a large variety of technological fields.[51] The effect of filler type (NL vs. untreated lignin) and concentration on the chemical–physical, thermal, and morphological characteristics of the resulting nanocomposites was investigated and the reinforcing effect was discussed based on mechanical tests.

The results of this study give a clear demonstration of a viable environmentally friendly strategy to obtain waterborne PU-based nanocomposites reinforced with NL in a straightforward manner and provide further evidence of the potential of lignin nanoparticles as fully bioderived fillers for advanced nanocomposite applications.

EXPERIMENTAL

Materials

All materials used in this study are commercially available. Softwood kraft lignin (Indulin AT) was supplied by MeadWestvaco. The PU used as matrix material for the nanocomposites was supplied by ICAP-SIRA Chemicals and Polymers S.p.A. in the form of aqueous dispersion (Idrocap 954). It was based on hexamethylene diisocyanate and on a macrodiol obtained from adipate of mixed glycols and polypropylene glycol, the latter derived from renewable sources.

Preparation of NL

NL was prepared via an ultrasonication treatment using a Sonic & Materials VCX130 sonicator tip at a frequency of 20 kHz, 130 W power, and 95% oscillation amplitude. The parent kraft lignin (from here on referred to as IND, 10 mg) was dispersed in deionized water (10 mL) and treated for 2, 4, and 6 h. The resulting dispersions (0.1 wt % lignin in water) were named NL-2 h, NL-4 h, and NL-6 h, respectively. An ice bath was used to avoid excessive heating of the dispersion due to the exothermicity of the ultrasonication process.

Preparation of Waterborne PU-Based (Nano)Composites

The aqueous PU solution (35% w/w) and the appropriate IND or NL suspensions were thoroughly mixed by stirring. The mass amount of IND and NL in the PU was 5%, 10%, and 20%. Water in each mixture was allowed to evaporate for 2 days at

room temperature under a fume-hood and for 1 day in a vacuum oven at 50 °C, until constant weight was reached. Solid samples used for characterization were obtained by hot-press moulding. An example of molded PU-based (nano)composite samples is shown in Figure S1 in the Supporting Information.

Materials Characterization

Transmission Electron Microscopy (TEM). TEM micrographs were acquired on NL fractions at increasing times of ultrasonic treatment using a Philips CM 200 electron microscope operating at 200 kV equipped with a Field Emission Gun filament. For sample preparation, few drops of lignin (IND or NL) suspension in water were deposited on a 200 mesh carbon-coated copper grid and air-dried for several hours before analysis. A Gatan U.S. 1000 CCD camera was used and 2048 × 2048 pixels images with 256 gray levels were recorded.

UV–Vis Spectroscopy. UV–vis spectroscopy was carried out on solid IND and NL samples dissolved in dimethyl sulfoxide at room temperature using an Evolution 600 UV−vis spectrophotometer (Thermo Scientific) in the 250 to 600 nm wavelength range with a scan speed of 100 nm/min and a bandwidth of 5 nm. A liquid cell of 1 cm path length with quartz window was used. The use of dimethyl sulfoxide enables complete solubilization of the IND and NL powders but limits the absorption spectral range to wavelengths longer than 260 nm.

Fourier Transform Infrared (FTIR) Spectroscopy. FTIR spectra were collected on a Nicolet 760-FTIR spectrophotometer on IND and NL solid samples (powder). Spectra were obtained from 64 accumulated scans performed from 4000 to 700 cm^{-1} at 2 cm^{-1} resolution.

Differential Scanning Calorimetry (DSC). DSC analyses were carried out on 10 ± 1 mg solid state lignin samples using a Mettler-Toledo DSC/823e instrument at a scan rate of 20 °C min^{-1} under nitrogen flux. The measurements consisted of three runs (heating/cooling/heating) from 25 to 200 °C. The glass transition temperature (T_g) of the materials was evaluated as inflection point in the second heating run.

Scanning Electron Microscopy (SEM). SEM analyses were performed on cryofractured IND and NL-PU composites using a Carl Zeiss EVO 50 Extended Pressure scanning electron microscope (acceleration voltage of 15.00–17.50 kV) to evaluate the filler particle distribution in the polymer matrix.

Thermogravimetric Analysis (TGA). TGA measurements were obtained on solid state samples (approximate weight 15 mg) by means of a Q500 TGA system (TA Instruments). The samples were heated from ambient temperature to 800 °C at a scan rate of 20 °C min^{-1} both in air and nitrogen atmosphere.

Tensile Tests. Tensile properties were determined at room temperature by means of a Zwick/Roell Z010 (Zwick Roell Italy) equipped with a 10 kN load cell and a longstroke extensometer. All specimens were tested according to the standard test method ASTM D638 (Type I specimen, dimensions down-scaled to 30%, namely 15 mm gage length, 4 mm width of narrow section, 2 mm thickness). At least five samples were tested for each experimental condition to obtain average values.

RESULTS AND DISCUSSION

Morphology and Water-Suspension Stability of Lignin (Nano)Particles

TEM analysis was used to investigate the morphology and dimensions of lignin particles before and after ultrasound treatment for different processing times (2, 4, and 6 h). As shown in Figure 1 where the corresponding TEM images are presented, the morphology of lignin nanoparticles was found to be irregular in shape throughout the entire sonication process. Concurrently, a notable decrease in particle size accompanied by a reduction of interparticle aggregation was observed for increasing ultrasonication times. Pristine untreated lignin (IND) was characterized by the presence of large agglomerates with dimensions in the 1 to 3 μm range [Figure 1(a)], likely arising from the strong intermolecular forces (typically, hydrogen bonds) acting between macromolecular lignin chains combined with the high insolubility of kraft lignin in water. By increasing ultrasonic treatment time, such agglomerates are found to progressively disaggregate and the average particle dimension to decrease by several orders of magnitude. In particular, after 6 h of ultrasound treatment, a water dispersion of submicrometric lignin particles could be obtained, with minimum size in the 10 to 50 nm range [Figure 1(d) and Supporting Information]. This clearly indicates that successful formation of NL could be achieved. These results are in good agreement with recent literature reports where comparable particle dimensions were obtained on wheat straw and Sarkanda grass lignins.[43] In order to evaluate the effect of ultrasonication time on the further particle size reduction, lignin was also treated for 9 h. However, no significant size modifications were observed for longer treatment times (see Supporting Information), likely due to a less efficient cavitation effect on nanoparticle dimension in the range of a few tens of nanometers. As a result, the characterizations that will be presented in the following will be based on NL-6 h.

To assess the stability of the NL dispersion in water, settling experiments were performed on ultrasound-treated (NL-6 h) and pristine (IND) systems. As shown in Figure 1(e), the as-obtained water dispersion containing NL-6 h exhibits a dark brown tint resulting from the presence of homogeneously distributed lignin nanoparticles successfully suspended within the entire liquid volume. The same dispersion was found to maintain such homogeneous tint for over 5 months without any noticeable formation of solid precipitate [Figure 1(f)], clearly indicating the excellent water-dispersion stability of the ultrasonically treated NL-based system. Conversely, the as-prepared untreated IND water suspension (obtained by magnetically stirring a 1 mg/mL dispersion of pristine lignin in water for 12 h) evidenced poor homogeneity immediately after interruption of the stirring process. In particular, all lignin material was found to settle down as solid precipitate already after 5 min at rest, as a result of the highly hydrophobic character of pristine kraft lignin that preferentially forms agglomerates and aggregates in water ultimately resulting in solid/liquid phase segregation.

UV−Vis Spectroscopy on Lignin (Nano)Particles

UV–vis spectroscopy was used to qualitatively investigate the compositional evolution of lignin as a result of the ultrasonic treatment. In this respect, possible changes in the type and

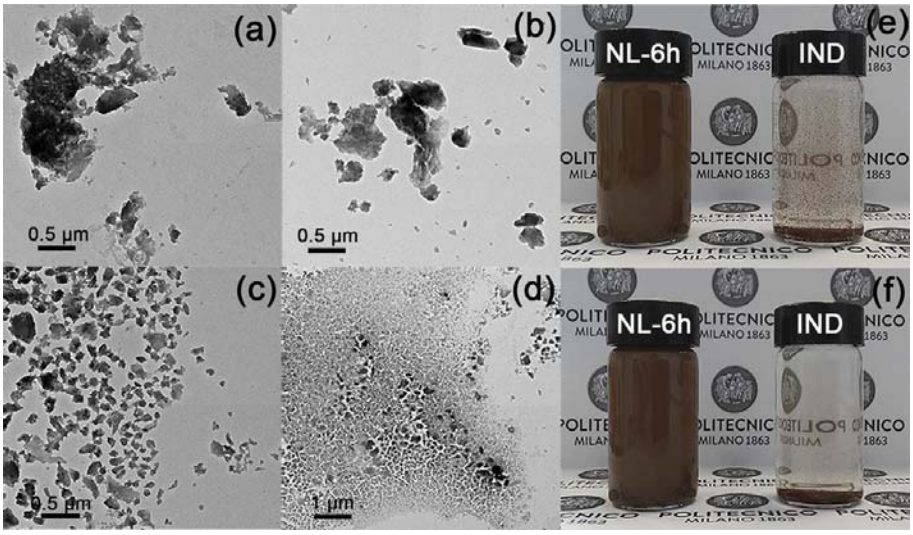

Figure 1. TEM images of kraft lignin particles at increasing ultrasound treatment times: (a) pristine material (0 h), (b) 2 h, (c) 4 h, and (d) 6 h. Photographic images of water dispersions of ultrasonically treated NL-6 h and pristine IND lignin (e) after dispersion process and (f) after 5 months at rest. [Color figure can be viewed at wileyonlinelibrary.com]

amount of conjugated moieties in lignin occurring during the ultrasonication process may lead to modifications of its UV–vis absorption response. Figure 2(a) presents the UV–vis absorption spectra of IND and NL-6 h samples. In both cases, a maximum is observed at 280 nm which is ascribable to the presence of noncondensed phenolic groups in guaiacyl units that are characteristic of softwood lignin.[19,52] In addition, a shoulder centered at 340 nm is present in the absorption spectra of both IND and NL-6 h, although with different relative intensities. This absorption feature is attributable to the presence of conjugated moieties such as α-carbonyl groups and esters of hydrocinnamic acids that are also present in softwood lignin.[53] This signal is found to exhibit a slight decrease in intensity in NL-6 h compared to pristine IND, likely suggesting that during the ultrasonication treatment partial loss of conjugation in lignin may occur due to the interaction of conjugated species with radical species forming as a result of the cavitation process.[48,49]

Fourier Transform Infrared Spectroscopy (FTIR) on Lignin (Nano)Particles

To investigate the chemical modifications potentially occurring to lignin during the ultrasonication process, FTIR spectra were collected on both IND and NL-6 h [Figure 2(b)]. The absorption intensities of the spectra were normalized with respect to the signal at 1515 cm^{-1}, corresponding to the C=C stretching vibrations of the aromatic ring.[48] The parent material exhibits a

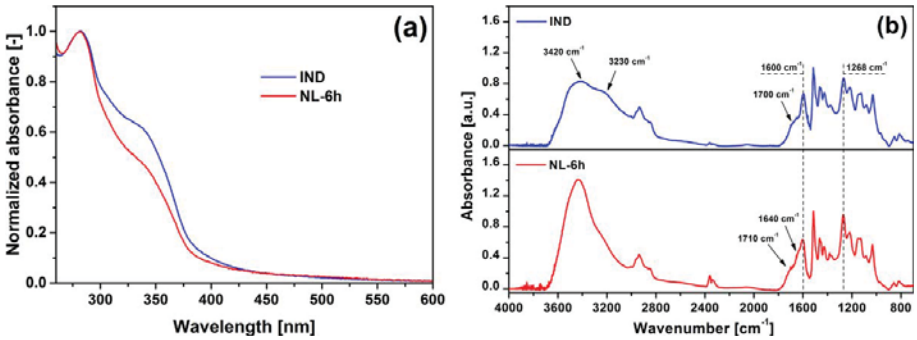

Figure 2. (a) UV–Vis spectra and (b) Fourier transform infrared (FTIR) spectra of untreated pristine lignin (IND) and lignin (nano)particles (NL-6 h). [Color figure can be viewed at wileyonlinelibrary.com]

wide absorption band in the 3700 to 3050 cm^{-1} range that is typically associated with stretching vibrations of —OH groups present in lignin. In particular, two main vibrational components can be distinguished in this region at 3420 cm^{-1} (peak) and 3230 cm^{-1} (weak shoulder), ascribable to stretching vibrations of intramolecular and intermolecular hydrogen bonded hydroxyl groups, respectively. As opposed to this, the treated NL-6 h material only exhibits a single sharp absorption peak centered at 3420 cm^{-1}, whose intensity is found to increase at increasing ultrasonic treatment times (see Supporting Information). These results indicate that the ultrasonication process may induce partial oxidation to lignin that results in the formation of a higher concentration of —OH moieties in the macromolecule as compared to the parent material, ultimately leading to increased polarity in the treated system. As evidenced by the FTIR analysis, these additional hydroxyl functionalities are more likely to establish intramolecular rather than intermolecular hydrogen bonding interactions, thus leading to lower interparticle attractions when dispersed into polar media. Consistently, markedly improved stability in water is observed for NL-6 h suspensions compared to pristine IND [see Figure 1(f)]. No significant modifications are observed in the characteristic signals attributed to C—H stretching vibrations in methyl and methylene groups, clearly detectable in the 3050 to 2800 cm^{-1} spectral region for both untreated and treated materials. In the C=O stretching region, IND only shows a very weak shoulder centered at 1700 cm^{-1}, ascribable to the relatively low concentration of carbonyl moieties (e.g., conjugated aldehydes and carboxylic acids) in the parent material, as also observed in previous studies on similar systems.[54] Upon ultrasonic treatment, a broader shoulder at around 1710 cm^{-1} is formed (C=O stretching in carbonyl and carboxyl groups), accompanied by the appearance of an additional sharp signal centered at 1640 cm^{-1}, whose intensity is found to increase with ultrasonic treatment time (see Supporting Information). This latter signal may be ascribed to C=O stretching vibrations resulting from the contribution of intramolecular hydrogen-bonded carboxylic acids that may form during the ultrasonication process. Interestingly, these observations are in good agreement with the modifications found in the 3700 to 3050 cm^{-1} range on —OH stretching vibrations, where the formation of oxidized species during the sonication process resulted in a sharp increase of the signal associated to the stretching vibrations of intramolecular hydrogen-bonded —OH groups in NL-6 h. Further evidence of the oxidative effect of ultrasounds on the lignin macromolecule may be inferred by considering the signal observed at 1268 cm^{-1} (C=O and C—O vibrations in guaiacyl units present in lignin) whose intensity is found to increase compared to the parent material as a result of the ultrasound treatment. The region characteristic of the aromatic skeletal C=C and C—C stretching vibrations in lignin does not appear to be affected by the ultrasonication process, as the strong signal found at 1600 cm^{-1} is observed with comparable intensities in both parent and treated materials. This observation indicates that in the conditions employed in the present study the sonication process does not affect the aromaticity of lignin. Similarly, no significant modifications due to the ultrasonic process are found in the 1480 to 1300 cm^{-1} (vibrations of phenolic O—H groups combined with aliphatic C—H in methyl groups) and 1250 to 800 cm^{-1} (C=O, C—H, and C—O in-plane and out-of-plane deformations in guaiacyl, syringyl, and *p*-hydroxyphenyl units) spectral ranges, where similar signals with comparable intensities are observed in both IND and NL-6 h.

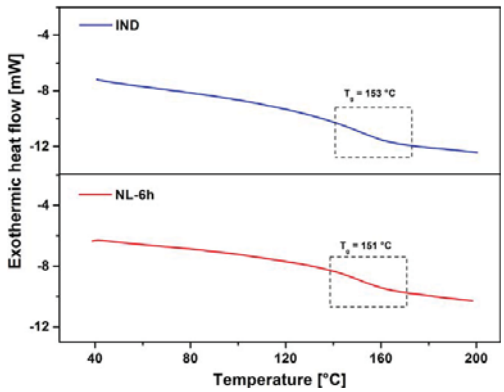

Figure 3. Differential scanning calorimetry (DSC) curves of untreated pristine lignin (IND) and lignin nanoparticles (NL-6 h). [Color figure can be viewed at wileyonlinelibrary.com]

DSC on Lignin (Nano)Particles

In order to assess the effect of ultrasonic treatment on the thermal behavior of lignin, DSC analysis was performed on both IND and NL-6 h samples. As shown in Figure 3, no significant variations were observed after ultrasonication, as comparable T_g were found in pristine and treated material, with values lying in the typical temperature ranges observed on softwood lignins (153 and 151 °C for IND and NL-6 h, respectively).[52] T_g is directly related to the mobility of the macromolecular chains, which may be affected by a complex interplay between several factors including the molecular weight of the material, the presence of chemical or physical crosslinks, and the presence of strong intermolecular interactions between the macromolecular chains such as intermolecular hydrogen bonds. As previously observed [Figure 2(b)], the ultrasonication process was found to reduce the extent of intermolecular hydrogen-bonded hydroxyl-mediated interactions. Considering these observation, a noticeable reduction of T_g may have been expected upon treatment. However, further analysis through gel permeation chromatography revealed a slight increase of M_n and M_w after the ultrasonication process accompanied by a broadening of the molecular weight distribution (see Supporting Information). These results may indicate that in the experimental conditions employed in this study cavitation may have occurred to some extent during the ultrasonic treatment.[50] Accordingly, partial oxidative coupling may have taken place leading to a higher degree of branching in lignin and ultimately yielding increased chain length, molecular weight, and thus prospective increased T_g. Based on these considerations, the negligible modifications in T_g observed via DSC prior to and after ultrasonic treatment may be the result of these two counteracting effects (decrease in

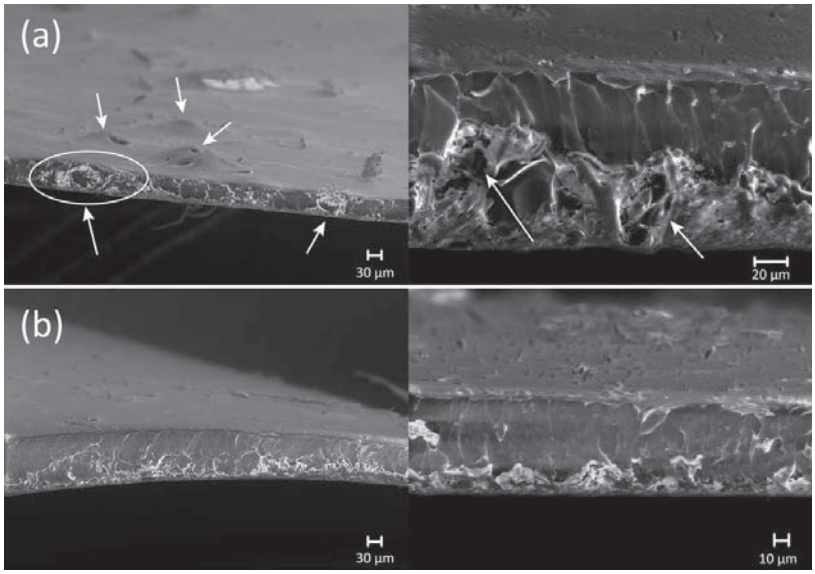

Figure 4. Scanning electron microscopy (SEM) images of (a) PU/IND composites and (b) PU/NL nanocomposites. In both samples 10 wt % filler loading was employed. White arrows indicate lignin agglomerates.

intermolecular hydrogen bonding vs. increase in molecular weight).

SEM of Composite Materials

To obtain lignin-based nanocomposite materials, NL-6 h particles were incorporated at varying concentrations into a thermoplastic PU matrix and the resulting composite materials were characterized in terms of thermal and mechanical properties. To qualitatively evaluate the level of dispersion of the fillers in the polymeric matrix, SEM analysis was employed on PU/NL-10 nanocomposites (10 wt % NL-6 h in PU) and compared with the corresponding PU/IND-10 composite material (10 wt % IND in PU). As shown in Figure 4(a), the introduction of micrometer-sized lignin particles into the PU matrix results in the formation of large agglomerates clearly visible as protruding features on the top surface of the sample. Similarly, the cryo-fractured section of PU/IND-10 systems highlights the poor level of dispersion of pristine lignin within the polymeric system, with the presence of large aggregates and defects randomly dispersed throughout the bulk of the material. As opposed to this, PU/NL-10 systems show an excellent level of dispersion and distribution of NL particles into the PU polymer matrix, as confirmed by the relatively smooth surface of these systems and the absence of any noticeable aggregate within the volume of the samples [Figure 4(b)] (SEM images of all investigated filler concentrations are presented in the Supporting Information). Given the importance of a high-quality dispersion of the reinforcing filler in the polymeric matrix for high-performance composite materials, these evidences may anticipate improved mechanical properties of PU/NL compared with PU/IND systems, as will be discussed in the following sections.

TGA of Composite Materials

The thermal stability of the obtained (nano)composite materials was investigated by means of TGA in nitrogen atmosphere. The results are presented in Figure 5, where TGA curves of PU/NL nanocomposites at increasing NL-6 h loading are compared with the corresponding systems based on pristine micrometer-sized lignin particles (PU/IND). All materials exhibit a three-step thermal degradation profile which reflects the thermolytic response of the unfilled PU matrix. In particular, a first weight loss (~8–10%) is found in the 200 to 300 °C temperature range that can be associated with cleavage of the urethane bonds in the polymeric matrix.[55] Between 300 and 400 °C another ~20% thermal degradation step is observed that may be ascribed to the decomposition of ether and ester linkages. Finally, a third major weight-loss region is observed above 400 °C as a result of the complete depolymerization and thermal degradation of the polymer. The addition of NL-6 h leads to a slight improvement of the thermolytic stability compared to the unfilled PU matrix at high temperatures (>400 °C), as indicated by the increase in the maximum mass loss derivative temperature (T_{DTGmax}) observed in PU/NL nanocomposites for increasing NL-6 h loading (Table I). Similarly, the char mass residue at 750 °C ($R_{750\,°C}$) is found to progressively increase in PU/NL systems with the addition of increasing amounts of NL-6 h ($R_{750\,°C} = 3\%$, 5%, 9% for PU/NL-5, PU/NL-10, and PU/NL-20, respectively) ultimately leading to improved stability compared with the unfilled PU matrix ($R_{750\,°C} = 1\%$). On the contrary, no clear trends are observed for PU/IND composites in this high temperature region at increasing filler loading, likely due to a relatively poorer stabilizing effect of IND at high temperatures. In the lower temperature region (<300 °C), no significant

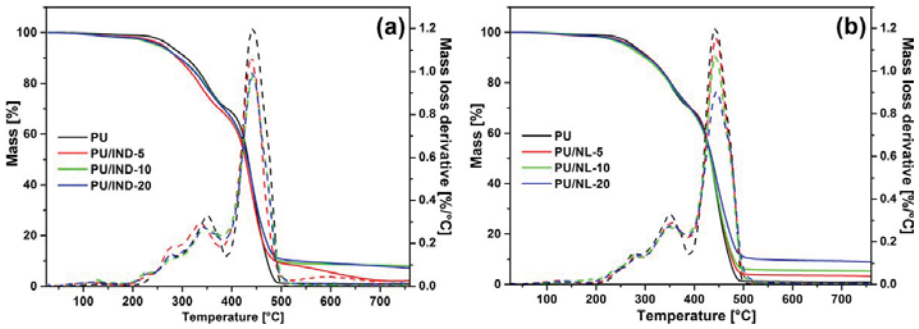

Figure 5. Thermogravimetric analysis (TGA) curves (under nitrogen atmosphere) for (a) PU/IND composite and (b) PU/NL nanocomposite materials at different filler loadings. [Color figure can be viewed at wileyonlinelibrary.com]

modifications with respect to the thermal response of unfilled PU are observed irrespective of the type of lignin-based filler employed (IND vs. NL-6 h), although a relatively more stable behavior is observed on PU/NL nanocomposites. Indeed, these systems exhibit higher thermal degradation temperatures at 10% ($T_{10\%}$) and 50% ($T_{50\%}$) mass loss as compared with the IND-based counterpart. In particular, slightly improved thermal stability is observed on PU/NL nanocomposites with respect to unfilled PU in terms of $T_{50\%}$ values (Table I). These trends may be associated with the higher thermal stability of NL-6 h compared with unfilled PU and with untreated IND at high temperatures (see Supporting Information), as also observed in recent reports on analogous systems.[42,48] The thermo-oxidative properties of the lignin-based composite materials were investigated by means of TGA under air flux (see Supporting Information). Similar trends as those observed under N_2 atmosphere were observed on all systems, further confirming the positive stabilizing effect of the addition of NL-6 h especially at high filler loadings.

Tensile Properties of Composite Materials

The mechanical properties of the composite materials at increasing filler loadings were investigated by means of tensile tests on dog-bone specimens (Figure 6). Figure 7 summarizes the trends observed on elastic modulus E, ultimate tensile strength σ_u, and elongation at break ε_{br} for all systems (the unfilled PU matrix was also included for reference). Representative stress–strain curves of PU/IND, PU/NL, and unfilled PU matrix are presented in Figure 7(a), where distinctive responses can be clearly observed depending on the nature of reinforcing filler employed. Compared to the unfilled PU matrix, PU/NL nanocomposite materials exhibit a progressive increase in elastic modulus for increasing NL-6 h loadings, leading to E values of 45.4, 52.5, and 65.6 MPa for PU/NL-5, PU/NL-10, and PU/NL-20 systems, respectively [Figure 7(b)]. As a result, a twofold increase in elastic modulus is observed in highly filled nanocomposites (20 wt % NL-6 h) with respect to the unfilled matrix material (33.0 MPa). This trend is in line with previous studies on the reinforcing effect of lignin nanoparticles in polymer-based nanocomposites[46,47] and may be correlated with the ability of NL to establish effective (noncovalent) interactions

Table I. Thermal Degradation Temperatures at 10% (T_{10}) and 50% (T_{50}) Mass Loss, Final Char Residue at 750 °C ($R_{750\,°C}$), and Maximum Mass Loss Derivative Temperature (T_{DTGmax}) for PU/inD and PU/NL Composites at Different Filler Loadings, as Obtained from TGA in Nitrogen atmosphere

	$T_{10\%}$ (°C)	$T_{50\%}$ (°C)	$R_{750\,°C}$ (%)	T_{DTGmax} (°C)
PU	308	433	1	442
PU/IND-5	290	428	2	442
PU/IND-10	294	431	8	443
PU/IND-20	294	431	7	442
PU/NL-5	307	434	3	445
PU/NL-10	300	433	5	443
PU/NL-20	305	436	9	445

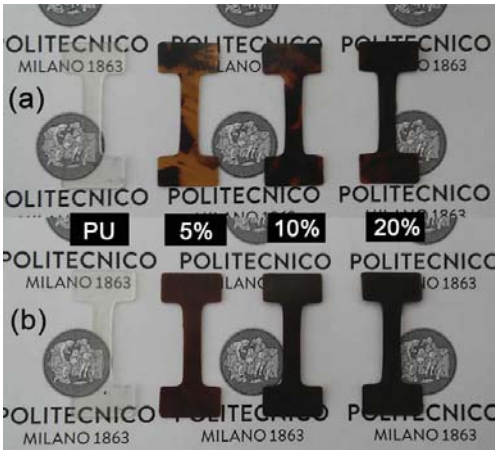

Figure 6. Photographic image of representative dog-bone samples of (a) PU/IND and (b) PU/NL composite systems at varying filler loading. For comparison, the unfilled PU matrix system is also presented (transparent samples). [Color figure can be viewed at wileyonlinelibrary.com]

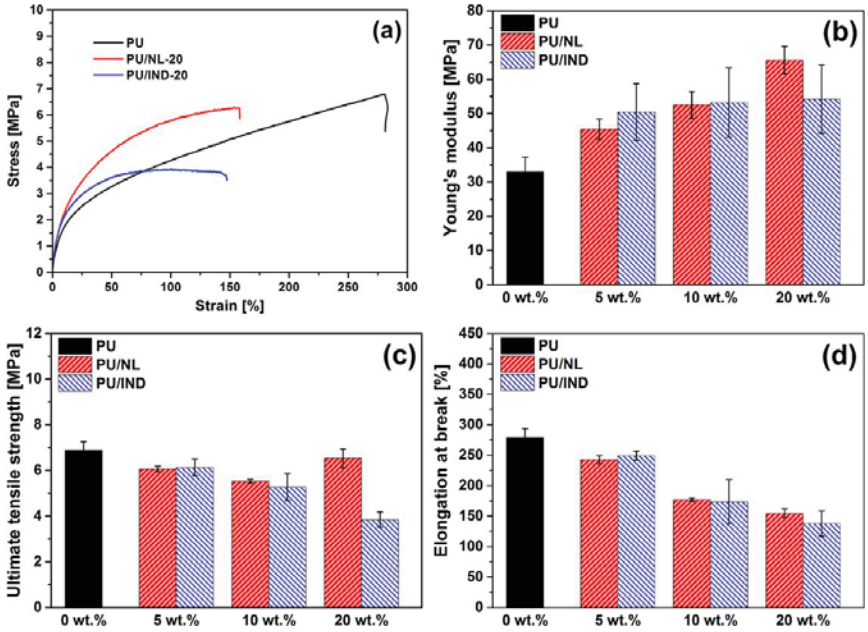

Figure 7. (a) Representative strain–stress curves of PU, PU/IND-20, and PU/NL-20 systems. Average values of (b) elastic modulus E, (c) ultimate tensile strength σ_{to} and (d) elongation at break ε_{br} for all (nano)composite systems at varying filler loading. The unfilled PU matrix is also included for reference. Error bars indicate the standard deviation out of at least five measurements on different specimens. [Color figure can be viewed at wileyonlinelibrary.com]

with the polymer matrix due to the high surface/volume ratio characteristic of the nanoscale dimensions resulting from the ultrasonication process. As opposed to the case of PU/NL, unclear trends are observed on the elastic modulus of composite materials based on untreated lignin. Indeed, E values in the 50 MPa range are found for all PU/IND systems irrespective of the amount of lignin present in the composite. This behavior may be explained by considering the poor level of dispersion of micrometer-sized untreated lignin particles in the PU matrix (SEM analysis, Figure 4) that may prevent efficient filler/matrix interactions, thus ultimately leading to limited mechanical reinforcing effect. Additionally, the large lignin aggregates observed both on the surface and in the bulk of PU/IND composite samples may act as defect sites that may induce the formation of cracks during the mechanical test, ultimately leading to limited reinforcing effect and relatively poor reproducibility of the results [as evidenced by the non-negligible magnitude of the error bars observed in Figure 7(b) for PU/IND composite systems]. Indeed, visual inspection of the dog-bone specimens employed for tensile tests clearly highlighted uneven distribution of the filler in PU/IND systems, which was not observed in PU/NL systems (Figure 6). When examining the ultimate tensile strength response of the composite materials as a function of filler loading [Figure 7(c)], a marked decrease of σ_u is found in the case of PU/IND systems, with values dropping from 6.1 MPa (PU/IND-5) to 3.8 MPa (PU/IND-20). On the contrary, a slight increase of σ_u is observed in NL-based nanocomposites especially for high filler content systems. In particular, in the case of PU/NL-20 systems, σ_u values (6.5 MPa) comparable to those found for the unfilled PU matrix (6.9 MPa) are observed. This behavior indicates that the addition of nanosized lignin particles allows to improve the stiffness of the polymeric matrix material without significantly affecting its fracture toughness, although a decrease of elongation at break is observed on both PU/IND and PU/NL composites at increasing filler loading [Figure 7(d)]. These mechanical characteristics (higher elastic modulus accompanied by preserved strength) may widen the use of such materials to low deformation applications where greater structural integrity is required, such as for instance in the automotive interior field or in the footwear field.[56,57]

CONCLUSIONS

A straightforward approach was presented in this work to obtain lignin nanoparticles suitable to be employed as bio-based fillers in polymer nanocomposites. Such approach consists in the ultrasonic treatment of a commercially available softwood kraft lignin to yield lignin/water dispersions characterized by excellent colloidal stability. By suitably tuning the ultrasonic treatment time, a remarkable decrease in lignin particle size

could be attained, leading to the formation of lignin nanoparticles of around 10 to 50 nm. UV–vis spectroscopy evidenced that partial loss of conjugated moieties (α-carbonyl groups and esters of hydrocinnamic acids) may occur upon treatment as a result of the interaction between lignin and the radical species forming during the ultrasonication process. In addition, FTIR spectroscopy showed that the ultrasonication treatment may impart some chemical modifications to lignin, resulting in increased oxidation in NL compared to the parent material. This gives rise to increased polarity in NL that well correlates with the markedly improved stability in water compared to pristine lignin. The obtained NL particles were incorporated at varying concentrations into a thermoplastic PU matrix and the morphological, thermal, and mechanical properties of the resulting composite materials were assessed. SEM analysis on NL-based nanocomposites evidenced an excellent level of dispersion and distribution of NL particles into the PU matrix as opposed to untreated lignin. In addition, a slight improvement of thermal stability was observed on NL-based nanocomposites compared with systems incorporating untreated lignin, especially at high temperatures (>400 °C), which was associated with the higher thermal stability of the nano-sized bio-based filler. Finally, tensile tests on the (nano)composites at increasing filler loading evidenced significantly improved mechanical properties of the systems incorporating NL particles compared to pristine lignin in terms of elastic modulus, ultimate tensile strength, and elongation at break. These trends were correlated with the ability of NL to establish effective noncovalent interactions with the polymer matrix due to the high surface/volume ratio characteristic of the nanoscale dimensions resulting from the ultrasonication process.

The results of this study provide a clear demonstration of a viable strategy to obtain lignin nanoparticles in an easily implementable and straightforward fashion and provide further evidence of the potential of NL as fully bioderived filler for advanced nanocomposite applications.

ACKNOWLEDGMENTS

This project was funded by the European Commission's Seventh Framework Programme for research, technological development and demonstration under grant agreement no. FP7-KBBE-2013–7–613802 (ValorPlus—Valorisation of biorefinery by-products leading to closed loop systems with improved economic and environmental performance). Authors gratefully acknowledge Gigliola Clerici for support with gel permeation chromatography and thermal analysis.

REFERENCES

1. Gellerstedt, G.; Henriksson, G. In Monomers, Polymers and Composites from Renewable Resources; Belgacem, M. N., Gandini, A., Eds.; Elsevier: Amsterdam, **2008**; Chapter 9; p 201.
2. Ragauskas, A. J.; Beckham, G. T.; Biddy, M. J.; Chandra, R.; Chen, F.; Davis, M. F.; Davison, B. H.; Dixon, R. A.; Gilna, P.; Keller, M.; Langan, P.; Naskar, A. K.; Saddler, J. N.; Tschaplinski, T. J.; Tuskan, G. A.; Wyman, C. E. *Science* **2014**, *344*, 1246843.
3. Tuck, C. O.; Pérez, E.; Horváth, I. T.; Sheldon, R. A.; Poliakoff, M. *Science* **2012**, *337*, 695.
4. Andrzej, V. A. K. *Bioresources* **2011**, *6*, 3547.
5. Lora, J. In Monomers, Polymers and Composites from Renewable Resources; Belgacem, M. N., Gandini, A., Eds.; Elsevier: Amsterdam, **2008**; Chapter 10, p 225.
6. Calvo-Flores, F. G.; Dobado, J. A.; Isac-Garcia, J.; Martin-Martinez, F. J. Lignin and Lignans as Renewable Raw Materials; John Wiley and Sons, Ltd.: Chichester, **2015**.
7. Doherty, W. O. S.; Mousavioun, P.; Fellows, C. M. *Ind. Crops Prod.* **2011**, *33*, 259.
8. Hatakeyama, H.; Hatakeyama, T. In Biopolymers; Abe, A., Dusek, K., Kobayashi S., Eds.; Springer: Berlin, **2010**; Vol. *232*, p 1.
9. Alekhina, M.; Ershova, O.; Ebert, A.; Heikkinen, S.; Sixta, H. *Ind. Crops Prod.* **2015**, *66*, 220.
10. Arshanitsa, A.; Ponomarenko, J.; Dizhbite, T.; Andersone, A.; Gosselink, R. J. A.; van der Putten, J.; Lauberts, M.; Telysheva, G. *J. Anal. Appl. Pyrolysis* **2013**, *103*, 78.
11. Boeriu, C. G.; Fiţigău, F. I.; Gosselink, R. J. A.; Frissen, A. E.; Stoutjesdijk, J.; Peter, F. *Ind. Crops Prod.* **2014**, *62*, 481.
12. Colyar, K. R.; Pellegrino, J.; Kadam, K. *Sep. Sci. Technol.* **2008**, *43*, 447.
13. Cui, C.; Sun, R.; Argyropoulos, D. S. *ACS Sustainable Chem. Eng.* **2014**, *2*, 959.
14. Dodd, A. P.; Kadla, J. F.; Straus, S. K. *ACS Sustainable Chem. Eng.* **2015**, *3*, 103.
15. Helander, M.; Theliander, H.; Lawoko, M.; Henriksson, G.; Zhang, L.; Lindström, M. E. *Bioresources* **2013**, *8*, 2270.
16. Li, H.; McDonald, A. G. *Ind. Crops Prod.* **2014**, *62*, 67.
17. Saito, T.; Perkins, J. H.; Vautard, F.; Meyer, H. M.; Messman, J. M.; Tolnai, B.; Naskar, A. K. *ChemSusChem* **2014**, *7*, 221.
18. Toledano, A.; Serrano, L.; Garcia, A.; Mondragon, I.; Labidi, J. *Chem. Eng. J.* **2010**, *157*, 93.
19. Passoni, V.; Scarica, C.; Levi, M.; Turri, S.; Griffini, G. *ACS Sustainable Chem. Eng.* **2016**, *4*, 2232.
20. Bonini, C.; D'Auria, M.; Emanuele, L.; Ferri, R.; Pucciariello, R.; Sabia, A. R. *J. Appl. Polym. Sci.* **2005**, *98*, 1451.
21. Cateto, C. A.; Barreiro, M. F.; Rodrigues, A. E.; Brochier-Salon, M. C.; Thielemans, W.; Belgacem, M. N. *J. Appl. Polym. Sci.* **2008**, *109*, 3008.
22. Duval, A.; Lawoko, M. *React. Funct. Polym.* **2014**, *85*, 78.
23. Gandini, A.; Belgacem, M. N. In Monomers, Polymers and Composites from Renewable Resources; Belgacem, M. N., Gandini A., Eds.; Elsevier: Amsterdam, **2008**; Chapter 11, p 243.
24. Isikgor, F. H.; Becer, C. R. *Polym. Chem.* **2015**, *6*, 4497.
25. Laurichesse, S.; Avérous, L. *Prog. Polym. Sci.* **2014**, *39*, 1266.
26. Saito, T.; Perkins, J. H.; Jackson, D. C.; Trammel, N. E.; Hunt, M. A.; Naskar, A. K. *RSC Adv.* **2013**, *3*, 21832.

27. Thanh Binh, N. T.; Luong, N. D.; Kim, D. O.; Lee, S. H.; Kim, B. J.; Lee, Y. S.; Nam, J. D. *Compos. Interfaces* **2009**, *16*, 923.
28. Griffini, G.; Passoni, V.; Suriano, R.; Levi, M.; Turri, S. *ACS Sustainable Chem. Eng.* **2015**, *3*, 1145.
29. Kaewtatip, K.; Thongmee, J. *Mater. Des.* **2013**, *49*, 701.
30. Thakur, V. K.; Thakur, M. K.; Raghavan, P.; Kessler, M. R. *ACS Sustainable Chem. Eng.* **2014**, *2*, 1072.
31. Luo, X.; Mohanty, A.; Misra, M. *Ind. Crops Prod.* **2013**, *47*, 13.
32. Zhang, L.; Huang, J. *J. Appl. Polym. Sci.* **2001**, *80*, 1213.
33. Sailaja, R. R. N.; Deepthi, M. V. *Mater. Des.* **2010**, *31*, 4369.
34. Maldhure, A. V.; Chaudhari, A. R.; Ekhe, J. D. *J. Therm. Anal. Calorimetry* **2011**, *103*, 625.
35. Dehne, L.; Vila Babarro, C.; Saake, B.; Schwarz, K. U. *Ind. Crops Prod.* **2016**, *86*, 320.
36. Yeo, J.-S.; Seong, D.-W.; Hwang, S.-H. *J. Ind. Eng. Chem.* **2015**, *31*, 80.
37. Zhang, C.; Wu, H.; Kessler, M. R. *Polymer* **2015**, *69*, 52.
38. Schaefer, D. W.; Justice, R. S. *Macromolecules* **2007**, *40*, 8501.
39. Qian, Y.; Deng, Y.; Qiu, X.; Li, H.; Yang, D. *Green Chem.* **2014**, *16*, 2156.
40. Lievonen, M.; Valle-Delgado, J. J.; Mattinen, M.-L.; Hult, E.-L.; Lintinen, K.; Kostiainen, M. A.; Paananen, A.; Szilvay, G. R.; Setala, H.; Osterberg, M. *Green Chem.* **2016**, *18*, 1416.
41. Frangville, C.; Rutkevičius, M.; Richter, A. P.; Velev, O. D.; Stoyanov, S. D.; Paunov, V. N. *Chem Phys Chem* **2012**, *13*, 4235.
42. Nair, S. S.; Sharma, S.; Pu, Y.; Sun, Q.; Pan, S.; Zhu, J. Y.; Deng, Y.; Ragauskas, A. J. *ChemSusChem* **2014**, *7*, 3513.
43. Gilca, I. A.; Popa, V. I.; Crestini, C. *Ultrason. Sonochem.* **2015**, *23*, 369.
44. Zimniewska, M.; Kozłowski, R.; Batog, J. *Mol. Cryst. Liq. Cryst.* **2010**, *484*, 43.
45. Jiang, C. *eXPRESS Polym. Lett.* **2013**, *7*, 480.
46. Yang, W.; Kenny, J. M.; Puglia, D. *Ind. Crops Prod.* **2015**, *74*, 348.
47. Yang, W.; Fortunati, E.; Dominici, F.; Kenny, J. M.; Puglia, D. *Eur. Polym. J.* **2015**, *71*, 126.
48. García, A.; Erdocia, X.; González Alriols, M.; Labidi, J. *Chem. Eng. Process* **2012**, *62*, 150.
49. Seino, T.; Yoshioka, A.; Fujiwara, M.; Chen, K.-L.; Erata, T.; Tabata, M.; Takai, M. *Wood Sci. Technol.* **2001**, *35*, 97.
50. Wells, T., Jr.; Kosa, M.; Ragauskas, A. *J. Ultrason. Sonochem.* **2013**, *20*, 1463.
51. Engels, H. W.; Pirkl, H. G.; Albers, R.; Albach, R. W.; Krause, J.; Hoffmann, A.; Casselmann, H.; Dormish, J. *Angew. Chem. Int. Ed.* **2013**, *52*, 9422.
52. Gellerstedt, G. *Ind. Crops Prod.* **2015**, *77*, 845.
53. Gärtner, A.; Gellerstedt, G.; Tamminen, T. *Nord. Pulp Pap. Res. J.* **1999**, *14*, 163.
54. Faix, O. In Methods in Lignin Chemistry; Lin, S. Y., Dence C. W., Eds.; Springer-Verlag: Heidelberg, **1992**; Chapter 5, p 233.
55. Chattopadhyay, D. K.; Webster, D. C. *Prog. Polym. Sci.* **2009**, *34*, 1068.
56. Abdeen, Z. I. In Rubber Nano Blends—Preparation, Characterization and Applications; Markovic, G., Visak, P. M., Eds.; Springer International Publishing: Cham, **2017**; Chapter 4, p 89.
57. Smart, S. K.; Edwards, G. A.; Martin, D. J. In Rubber Nanocomposites—Preparation, Properties and Applications; Thomas, S., Stephen, R., Eds.; John Wiley & Sons (Asia) Pte Ltd: Singapore, **2010**; Chapter 10, p 239.